THE BREAKDOWN VOLTAGE-TIME CHARACTERISTICS OF SF_6 AND ITS MIXTURES IN COAXIAL CYLINDER GAPS WITH SPECIAL REFERENCE TO STEEP-FRONTED IMPULSE VOLTAGES WITH TIME TO CHOPPING DOWN TO 100 ns

By

Ziqin Li

A thesis
presented to the University of Manitoba
in fulfillment of the
thesis requirement for the degree of
Doctor of Philosophy
in
the Department of Electrical Engineering

Winnipeg, Manitoba

ISBN 0-315-51579-1

THE BREAKDOWN VOLTAGE-TIME CHARACTERISTICS OF SF_6 AND ITS MIXTURES IN COAXIAL CYLINDER GAPS WITH SPECIAL REFERENCE TO STEEP-FRONTED IMPULSE VOLTAGES WITH TIME TO CHOPPING DOWN TO 100 ns

BY

ZIQIN LI

A thesis submitted to the Faculty of Graduate Studies of the University of Manitoba in partial fulfillment of the requirements of the degree of

DOCTOR OF PHILOSOPHY

I hereby declare that I am the sole author of this publication.

I authorize the University of Manitoba to lend this publication to other institution or individuals for the purpose of scholarly research.

full name of author

I further authorize the University of Manitoba to reproduce this publication by photocopying or by other means, in total or in part, at the request of other institution or individuals for the purpose of scholarly research.

full name of author

The University of Manitoba requires the signatures of all persons using or photocopying this publication. Please sign below, and give address and date.

ACKNOWLEDGEMENTS

The author wishes to express his deep gratitude to Dr. E. Kuffel, Dean of the Engineering Faculty, his dissertation supervisor, for his valuable guidance and encouragement during the course of this investigation.

The author also wishes to thank Dr. J. R. Cahoon for proofreading the manuscript and making suggestions prior to submitting the thesis in its final form to the Examining Committee and to thank Mrs. L. Philip for her help in the English editing of this dissertation and Mr. G. Toole for his cooperation and help in constructing the apparatus.

The financial support from the National Science and Engineering Research Council and Manitoba Hydro which made this investigation possible was also greatly appreciated.

Abstract

The breakdown voltage characteristics for SF_6 and SF_6 mixtures with N_2, CO, CO_2 and dry air as buffer gases were investigated experimentally in a coaxial cylinder gap in the pressure range from 100 to 600 kPa with *dc* and impulse voltages. The influence of adding small amounts of $c - C_4F_8$ gas to the mixtures was also studied. In the experiment, emphasis was placed on the breakdown voltage time characteristics of the gas or gaseous mixtures under steep-fronted impulse voltages chopped on the wave-front with time to breakdown down to 100 ns. In breakdown voltage-pressure characteristics, an apparent discontinuity was observed at a pressure of about 300 kPa for both SF_6/N_2 and $SF_6/N_2/c - C_4F_8$ mixtures under negative lightning impulses. Moreover, the breakdown values were found to be insensitive to replacement of a small amount of SF_6 by $(c - C_4F_8)$ gas. Measurement of the impulse breakdown voltage-time characteristics under steep-fronted voltages showed that abnormal breakdown took place within the gap in pure SF_6 gas and $1\%SF_6$/dry air mixture. The phenomenon was attributed to the so called "sweeping action" on the electrons, or negative ions, in the gas or gaseous mixture under rapidly rising impulse voltages. Experimental data indicated that the "sweeping effect" was controlled by many other factors such as polarity, gas pressure and content of component gases in a gas mixture.

To reliably measure the steep-fronted impulse voltages with a commercial type resistor divider, an analog compensating network was developed. It

was found that the response time of a commercial resistor divider measuring system compensated in this way can be profoundly reduced and hence used for the steep-fronted impulse voltage measurement.

Finally, a theoretical treatment of breakdown voltage-time characteristics by applying the "streamer theory" is presented with some assumptions. Experimental results are then compared with the theoretical values. The agreement between measured results and computed values is considered satisfactory, although the parameters used in the computation still need refinement.

Contents

List of Figures

Chapter 1

Introduction

1.1 Advantages and disadvantages of SF_6 as an insulating gas

Owing to an increasing demand for electrical power, the limited space in densely populated areas, the rising cost of land, etc., engineers have to design compact, efficient, economical, operationally safe, esthetically acceptable and reliable distribution systems. These requirement have led to the development of compact substations or cable systems insulated with compressed gas.

The selection of an insulating gas for electrical use depends on many factors such as high dielectric strength, low condensation temperature, chemical inertness, nontoxicity, nonflammability and good heat transfer ability.

Several decades of research revealed that Sulphur Hexafluoride (SF_6) is a very suitable gas with the required properties. SF_6 is a compound of polyatomic molecules, combining sulphur and fluorine, which was first discovered in 1900 by Moissan and Lebeau [1]. It is colourless, odorless, tasteless, uncombustible, nonflammable, quite inert and nontoxic. SF_6 remains stable when heated to about $500^{o}C$ [2] in a closed system in the absence of O_2 or H_2O. Its electrical breakdown strength is substantially higher than that of traditional gaseous dielectrics such as air, nitrogen or carbon dioxide, and is about 2.5 times that of air at 1 atm. [3]. SF_6 has better heat transfer ability than either air or nitrogen because its lower viscosity, combined with its greater density, lead to more extensive gas circulation than otherwise could be obtained with nitrogen or air under the same thermal conditions. Moreover, its strong tendency for the capture of free electrons to form relatively immobile negative ions makes it an exceptional arc-quenching and insulating medium for circuit breakers. Hence, SF_6 has been widely used as an insulating medium in H. V. apparatus to reduce the size and to improve the reliability of a system.

Despite its many important advantages, SF_6 possesses some disadvantages. Its decomposition under electrical discharges forms lower fluorides of sulphur such as SOF_2, SO_2F, SF_4, SOF_4 etc., which are toxic and corrosive to many insulating and conducting materials. It liquifies at higher pressures and its cost is comparatively high. Moreover, the dielectric strength of SF_6 is very sensitive to field nonuniformity. Hence, in practice, the electrical breakdown strength of compressed SF_6 is often governed by local field enhancement due to protrusions, surface roughness and presence of conducting particles in a system. A number of publications [4,5,6,7,8] has shown that the dielectric strength of compressed SF_6 can be greatly reduced due to the presence of contamination by particles.

1.2 The search for replacement gases

The disadvantages of pure SF_6 as a dielectric and the need for more efficient, economical electrical power transmission and distribution, have given impetus to the investigation of new insulating gases. Since no single gas can meet all of the multiple needs and operation conditions that exist in power apparatus, mixtures have been studied with the objective of tailoring the dielectric for a specific application.

It was concluded that the most effective way of preventing electrons from initiating a breakdown is to remove them by electron attachment to the gas molecules thus forming stable negative ions. SF_6 has good dielectric strength because it is an electronegative gas. However, SF_6 molecules can only capture electrons with low energies since the electron attachment cross section, a measure of the electron attaching ability of a gas (which is a function of electron energy), becomes small for electron energies above 0.4 eV. Hence, high energy electrons associated with the enhanced field at a rough surface or at a particle will escape the capture and initiate a breakdown.

Although the electron attachment cross sections for some other electronegative gases are substantially higher than that for SF_6 for electron energies above 0.4 eV, this becomes insignificant when the electron energies are above 1.2 eV. Therefore, for a good dielectric, not only must its electron attachment cross section be as large as possible over as wide energy range as possible, but the ability to reduce electron energies is also of paramount significance. Based on the above mentioned concept, a great number of gas mixtures have been studied in the past two decades.

1.2.1 Binary gaseous mixtures

Binary gaseous mixtures comprise either an electronegative gas and a non-electronegative gas (buffer) or two different electronegative gases. For a electronegative/buffer gaseous mixture the electronegative gas provides the ability of capturing free electrons in the mixture while the buffer gas scatters electrons into an energy range in which the electronegative gas attaches them more efficiently. For example, H_2, N_2, CO, and CO_2 can slow down electrons efficiently via their strong, low-lying negative ion states [9]. Therefore, the mixtures show substantial positive synergistic effects. (Synergism is defined here as the difference in the measured breakdown voltages of the mixture and the partial-pressure-weighted breakdown voltage of the component gases). However, for an electronegative/electronegative gaseous mixture the synergism may be positive, negative or practically zero depending on the constituent gases used [9,10].

As early as 1955, Cobine [11] studied some electrical and thermal characteristics of a SF_6-He mixture to explore if potentially hazardous H_2 could be replaced, as a cooling medium in electrical machines, by a mixture of chemically inert He and SF_6. Later Moruzzi and Craggs carried out uniform field breakdown measurement in SF_6-H_2 and SF_6-Ar mixtures [12]. They found that the limiting breakdown value for both SF_6-H_2 and SF_6-Ar mixtures with 10% SF_6 additive increases by a factor of three above those of the pure gas values. They also measured ionization and attachment coefficients for SF_6-H_2 mixtures containing up to 20% SF_6. Their results showed that the addition of SF_6 to H_2 causes a large change in the electron energy distribution function of H_2 and thus affects the values of ionization and electron attachment coefficients.

Impulse breakdown measurements for both positive and negative standard voltages using 12.5 mm square rod-plane gaps in hydrogen-SF_6 mixtures were conducted by Farish and co-workers [13,14] in 1976 and 1978 respectively. The striking feature of their results is that under positive polarity, the effect of addition of SF_6 depends on both the gas pressure and the gap length. For pressures in the range from 60 to 200 kPa the 50% breakdown voltages for all gap lengths increased by 100% for a SF_6 concentration of 0.2%. At a pressure of 300 kPa, the 50% breakdown voltages increased with increasing SF_6 content only for gap lengths less than 10 cm but were unaffected for a gap length of 15 cm and decreased with the addition of SF_6 for larger gap lengths. For negative rod-plane gaps in SF_6/hydrogen mixtures the improvement in impulse strength related to hydrogen was much smaller than for positive polarity. For longer gaps and higher pressures, the 50%

breakdown voltages were lower in the mixture than in pure hydrogen. However, the 50% breakdown voltages for negative polarity were still equal or higher than that for positive polarity for a given pressure in the range from 50 to 300 kPa. In 1978, Cookson and Wootton [15] observed that corona and breakdown in SF_6-H_2 mixtures having SF_6>50% can cause an explosive reaction.

The studies of static breakdown voltage of SF_6-N_2O mixtures containing 1% to 50% of SF_6 by volume for values of pd, where p is gas pressure and d is gap length, within the range $40 < pd < 400\ kPa \cdot cm$ showed that in those mixtures deviations from Paschen's law are much reduced as the concentration of SF_6 in the mixtures is increased to 10% [16,17]. In a mixture of N_2O with 6% SF_6 or more this deviation is hardly detectable. The relative dielectric strength of a N_2O mixture containing 50% SF_6 is about 90% that for pure SF_6 [17].

Other binary mixtures have been investigated [18,19,20,21]. However, the most detailed studied binary mixtures were SF_6 mixtures with other common gases, ie. N_2, air, CO, and CO_2. Among these, SF_6-N_2 mixtures received special attention because N_2 is one of the most stable, inert and abundantly available gas. Moreover, although N_2 does not capture electrons itself, it is a good buffer gas because it possesses a negative ion resonance at about 2.3 eV which is very effective in slowing down electrons in this energy range [22]. A 50%SF_6-50%N_2 mixture at 15% higher total pressure than pure

SF_6 exhibits the same dielectric strength as pure SF_6 at about 35% lower cost [23]. This mixture also has many other advantages (e.g. with respect to condensation temperature, nonuniform field behaviors and particle effects) which make it the strongest candidate yet to replace pure SF_6 in practical equipment.

1.2.2 Ternary and multicomponent gaseous mixtures

Ternary and multicomponent gaseous mixtures were also investigated with the same goal to meet a multiplicity of needs and operating conditions in high voltage insulation.

To make the electron attachment process more effective, it is important to choose electronegative gas components having a high attachment cross section over as wide an electron energy range as possible. Knowledge of the electron-attaching, electron-slowing-down and the electron-impact-ionization properties of gases allows one to choose and tailor gaseous dielectrics. While the electron attachment cross section for SF_6 is large at very low energies and thus only electrons with energies in the very low-energy range can be removed efficiently by electron attachment, those for perfluorocarbons (PFCs) are substantially higher than that for SF_6 in the energy range from 0.4 to 1.2 eV.

Basic physics dictates that electron attachment can be effected only at lower energies < 2 eV. Therefore, if breakdown is to be controlled by electron attachment, either the electrons must be captured before the electric field accelerates them above the energy range from 0.0 to 2.0 eV. or gases must be added to effectively slow down electrons which reach higher energies thus returning them to the energy range where they are likely to be captured [26]. SF_6-PFC-buffer gaseous mixtures are therefore chosen for these studies.

The studies of mixtures of SF_6 and various PFCs such as 2-C_4F_8, c-C_4F_8 and 2-C_4F_6 with N_2 and other buffer gases in a cylindrical gap with grooves on the center conductor to simulate surface roughness showed that these PFC gases add some control to electrons at energies higher than those subject to SF_6 control, thus forming a "team" of two gases which control electrons better to reduce ionization at localities of very high stress. For example, ternary mixtures of 30%SF_6-30%PFC-40%buffer give dielectric strengths from 3-15% higher than SF_6 at 410 kPa [24].

1.3 Objective of present investigation

From the above it can be seen that SF_6-N_2 binary mixtures and SF_6-N_2-(c-C_4F_8) ternary mixtures are promising gaseous mixtures for industrial applications. It was, therefore, the objective of this investigation to explore further the breakdown properties of these gaseous mixtures.

Chapter 2

Literature Review

2.1 Previous investigations

2.1.1 Binary gaseous mixtures

Breakdown voltage characteristics under dc applied voltages

The breakdown and prebreakdown characteristics of SF_6-N_2, SF_6-air, and SF_6-CO_2 mixtures in nonuniform fields under dc applied voltages have been the subjects of several studies [25 − 41]. In 1956, Cohen studied the breakdown characteristics of SF_6/N_2 and SF_6/air mixtures using a 1 mm uniform field gap under direct applied voltages [25]. He investigated the breakdown voltage pressure characteristics with a fixed content of SF_6 in the mixtures. Therefore, little information was given on the effect of the SF_6 content on the mixtures.

Pace and co-workers later conducted dc breakdown voltage measurements on SF_6/N_2 mixtures in a very uniform electric field [26]. The electrodes used comprised 2 parallel discs 14 cm in diameter polished to approximately 0.1 μm surface roughness. They found that the addition of a small amount (a few percent by volume) of SF_6 to N_2 results in an appreciable increase in the breakdown strength of N_2 . However, a further increase of the SF_6 content in the mixture does not result in such a rapid increase in the breakdown strength and the beneficial influence of adding SF_6 on the breakdown properties of N_2 seems to saturate. It appears that this may be due to the very high electron attachment cross section of SF_6 at low electron energies. Thus, a modest amount of added SF_6 could attach almost all of the low energy electrons causing an appreciable increase in the breakdown strength and the further addition of SF_6 has relatively little effect on the dielectric strength of the mixture [26].

Malik and co-workers proposed a method based on the streamer criterion to calculate the discharge inception voltages for SF_6-N_2, SF_6-air, and SF_6-CO_2 mixtures [27,30]. To estimate the effective ionization coefficients used in the calculation, they carried out measurements using polished stainless steel uniform field electrodes and dc applied voltages at total pressures up to 500 kPa for 5 and 10 mm gaps [30]. They showed that whereas the measured and the calculated values agree reasonably well for pressures up to about 300 kPa, the difference between these values becomes significant at higher pressures. The difference is especially significant for mixtures containing 50% or more SF_6.

The behavior of SF_6 and its mixtures in a highly nonuniform field under positive polarity, typically a rod-plane gap, is characterized by the existence of a pressure range over which the breakdown takes place considerably in excess of the corona threshold, while at higher pressures the breakdown and corona onset levels coincide. The positive corona onset voltage increased continuously with the pressure and SF_6 content. The breakdown voltage increased with pressure to a certain value P_{max}. At this pressure, the breakdown voltage reaches a maximum (relative). For pressure higher than P_{max} the breakdown voltage decreased to a minimum level corresponding to the pressure of P_{min} and then started to increase again. For pressures higher than P_c, known as the critical pressure, the breakdown voltage coincides with the positive corona onset curves. In the lower pressure range the high breakdown voltages are due to the stabilization of the field near the highly stressed electrode by the space charges of the same polarity generated as a result of corona discharges, Thus, the voltage-pressure characteristics exhibit a peak in this range.

Similar to SF_6 gas [30,31], there is a discontinuity in the voltage-pressure characteristics for SF_6 mixtures with air, N_2 and CO_2 [30,36] in the transition region in which the breakdown transition from corona stabilized breakdown to nonstablized breakdown takes place. However the pressure at which the discontinuity was observed was higher in the mixtures than in pure SF_6 and appeared to depend on the mixture ratio [30].

In visual appearance, the positive corona discharge at low pressures was in the form of a stable glow (a diffuse glow-type discharge) around the highly stressed electrode, while at higher pressure (corresponding to the rising part of the V-P curve) it comprised many short streamer filaments. At still higher pressure, corresponding to the pressure region in which the V-P curve has a negative slope, the glow/streamer stabilization corona continues to exist and appears to be confined to the vicinity of the highly stressed electrode. It is accompanied by the appearance of long filamental discharges which develops out of the streamer corona. As the pressure is further increased only leader type corona exists.

In nonuniform field gaps, where the highly stressed electrode is the cathode, the breakdown voltage-pressure curves show a similar feature as in the case of positive polarity. However, the values of the critical pressure are higher for the negative rod than for positive rod. Hence, for a rod-plane gap of 1.59 mm rod cathode in SF_6 mixtures with air, N_2, or CO_2, the breakdown are corona stabilized over the entire pressure range from 50 to 500 kPa [36]. Generally the breakdown voltages increase linearly and have similar values as in the case of positive polarity for low pressures. However at higher pressures the negative breakdown voltages tend to saturate but are still significantly higher than the positive ones. Therefore, at such pressures positive values are more critical from a practical point of view.

Similar to the case of positive polarity, the corona inception voltages for negative rod-plane gaps increase with SF_6 content and gaseous pressure. However, the inception voltages for negative polarity are significantly lower than the corresponding values for positive polarity.

Malik and co-workers studied spark channels of a 20 mm negative rod-plane gap in SF_6-N_2 mixtures [30]. They found that the spark channels were affected by the total gas pressure and attributed the effect to negative ion space charges. They argued that the negative ion space charge inhibits the propagation of streamers along the shortest interelectrode path available. This effect increases with pressure because of increasing space charge density and reduced diffusion at higher pressures. The result is that at higher pressures, the breakdown streamers are more curved.

Breakdown voltage characteristics under ac applied voltages

As early as 1956, Howard studied power frequency breakdown voltage characteristics of SF_6-N_2 mixtures using sphere-sphere and point-sphere gaps [34]. The spheres used were 50 mm diameter and the point electrode was a hemisphere capped tungsten cylinder of 1.98 mm diameter. As in the cases of uniform field [26], the breakdown strength of the mixture increases substantially even with a very small addition of SF_6 to N_2. For sphere-sphere gaps of 2 mm and 5 mm the SF_6-N_2 mixture with 10% SF_6 reached about 80% of the electric strength of pure SF_6. The substantial positively synergistic effects of the SF_6-N_2 mixture with a small amount of SF_6 additive under ac applied voltages were further confirmed by Ermel's measurement with uniform field electrodes in the mixture [40]. However, the ac breakdown characteristics for the point-sphere gap in the mixture as a function of mixture ratio exhibits a peak for a given pressure and gap length [34]. Hence, one could optimize by monitoring the three parameters if such a gap is encountered in practice.

In an effort to assess their potential use in compressed gas insulated transmission lines, Cookson and Pederson [42] investigated the breakown voltage characteristics of mixtures of SF_6 with N_2, air, and CO_2 under 60 Hz ac voltage using two concentric cylindrical aluminum electrode systems. Little difference was found among the mixtures in ac breakdown voltage as a function of SF_6 content in the mixtures.

Breakdown voltage characteristics under impulse applied voltages

Impulse breakdown voltage characteristics have been studied for SF_6-N_2 [42 − 61], SF_6-air [42,48,53,54,58] and SF_6-CO_2 [42,54,58] mixtures. The impulse breakdown voltages in the SF_6 mixtures depend markedly on the field configuration, the polarity, the front duration of the applied voltage and the gas pressure used. For wavefronts of the order of 100 μs, there is time for corona shielding to develop and the breakdown curve is similar in shape to the dc characteristics. For short rise time, the influence of the corona space charges is much reduced. In this case the breakdown voltage is strongly dependent on the statistics of discharge initiation [43,44]. In a wire cylinder geometry, for example, where statistical time lag is insignificant, the impulse breakdown voltage is much lower than the dc value and the breakdown characteristic is almost flat in the neighborhood of the corona stabilized peak [37]. In point-plane geometry, however, the 50% breakdown probability can be relatively high [43] but the minimum impulse breakdown voltage is again found to be independent of the pressure in that pressure region. Hence, for impulse voltage with a short rise time, the corona onset voltage increased continuously with the pressure, while the breakdown voltage, starting from low pressure, increased almost linearly to a certain pressure P_1, at which the transition of the breakdown mode from streamer breakdown to leader breakdown begins. In the pressure range from P_1 to P_c the impulse breakdown voltage is subjected to statistical variation depending on the field nonuniformity and pulse wavefront but the minimum impulse breakdown voltages remain nearly constant [33]. For pressures higher than P_c the breakdown voltage coincides with the corona onset characteristics.

In 1978, Cookson and Pederson [42] investigated the negative impulse breakdown voltage as a function of SF_6 content for a coaxial cylinder gap in SF_6 mixtures with N_2, air or CO_2 using both negative lightning (1.2/40 μs) and negative switching (250/3000 μs) impulses. Their results showed that in all these mixtures the negative impulse breakdown voltage increases with increasing SF_6 content.

In 1965 Skipper and McNeall [45] measured the impulse strength (1.0/50

μs) of SF_6-N_2 mixtures at 1400 kPa using uniform field electrodes of parallel brass planes with a Bruce profile. They found that the breakdown voltage increases rapidly with increasing SF_6 content up to 20%, similar to that observed with dc and ac applied voltages. However, further increase in the percentage of SF_6 in the mixtures increased the impulse breakdown voltage nearly linearly but with a smaller increment.

In highly nonuniform field gaps, Kuffel and Yializis [49] observed that for a positive 1.59 mm rod-plane gap of 50mm length the breakdown values under impulse voltages (1.5/50 μs) for pure N_2 exceeded the corresponding values of the mixture composed of 90% N_2 and 10% SF_6 at pressures above 200 kPa. As the SF_6 content was reduced below 5% the breakdown strength of the mixture started increasing reaching a strength well in excess of that of pure SF_6. The highest strength was observed in a mixture of 99.8% N_2 and 0.2% SF_6. Further decrease of SF_6 content lowered the peak breakdown values. No breakdown value for SF_6-N_2 mixtures was lower than that of pure N_2 at a pressure of 100 kPa.

Contrary to the results of Kuffel and Yializis, Watanabe and Takuma [48] observed that a small addition of SF_6 to N_2, or air, results in a decrease in the breakdown voltages under a 3.07/46 μs impulse. They also observed that the breakdown voltages of N_2 and air were even higher than those for pure SF_6. These observations suggested that electrode configuration plays very important role in the breakdown characteristics of a gas mixture, since the experimental conditions in their studies were 10 mm diameter rod and gaps were 300 and 500 mm at a pressure of 100 kPa, quite different from those employed by Kuffel and Yializis.

The impulse breakdown characteristics for rod-plane gaps in SF_6-N_2 with less than 1% of SF_6 mixtures were investigated in further detail by Yializis and Kuffel using 1.8/50 and 310/3500 μs impulse voltages [50]. They reported that under positive polarity, the addition of a small trace of SF_6 to N_2 enhance the effect of the stabilization process resulting in a substantial increase in the breakdown voltage of N_2 at lower pressures. The stabilization effect decreases as the pressure becomes higher, leading to a drop in the breakdown voltages producing a breakdown voltage peak. The peak is associated with movements of the initiation point of the discharges away from the spherical tip of the rod electrode. The movement of the spark away from the anode tip exhibited a definite dependence on both the total pressure of the mixture as well as the partial pressure of SF_6. This behavior is more pronounced when the field configuration is highly nonuniform and/or the gas pressure is high.

The negative impulse breakdown voltage-pressure characteristics of rod-plane gaps insulated with SF_6-N_2, SF_6-air, and SF_6-CO_2 mixtures with low SF_6 content did not exhibit a peak. Moreover, while Kuffel and Yializis reported that the breakdown voltages increased continuously with increasing SF_6 content [49] at pressures up to 500 kPa, Safar and co-workers [58] reported a pressure range in which a small addition of SF_6 to the gases can decrease the breakdown voltages of the gases under a 2.0/50 μs negative impulse. In general, the negative impulse breakdown levels in the pressure range from 100 to 500 kPa were substantially higher than positive ones and therefore are less significant from a practical point of view.

It was found that breakdown levels for SF_6-N_2 and SF_6-air mixtures were similar. None of these mixtures exhibited a breakdown voltage higher than the corresponding value for pure SF_6 in a 50 mm rod-plane gap with 1.59 mm rod diameter. However, SF_6-CO_2 mixtures gave breakdown voltages similar to or even slightly higher than pure SF_6 at high pressure. SF_6-CO_2 mixtures with 10 to 20% SF_6 showed the highest negative impulse breakdown voltages [58]. The studies showed that the visual appearance of corona was strongly affected by the total gas pressure [37,53,58]. For a negative 1.55 mm diameter rod-plane gap with 50 mm gap length in SF_6 mixtures with N_2, air and CO_2, Safar observed leader-type corona in almost all of these mixtures at gas pressures of 100 kPa and above [58]. Moreover, when the gas pressure and SF_6 content of the mixture were high, leader discharge extended into the gap in a stepped manner.

2.1.2 Ternary and multicomponent gaseous mixtures

Information on dielectric strength of some multicomponent gaseous insulations can be found in many articles [26,62 – 69]. Based on the knowledge of the electron attachment and the inelastic electron scattering cross section, James and co-workers [26,62] studied a number of multicomponent mixtures containing C_4F_6. They found C_4F_6 to be an excellent additive. For example, a mixture of $20\%C_4F_6/20\%SF_6/60\%N_2$ had a dc breakdown strength approximately 7% higher than that of pure SF_6, while a $30\%C_4F_6/20\%SF_6/50\%N_2$ mixture had 33% higher dielectric strength than pure SF_6 for a plane-plane uniform field gap.

A systematic study of ternary gas mixtures, of which SF_6 -N_2 - perfluorocarbon mixtures received special attention, was conducted by a group of scientists in Oak Ridge National Laboratory [26,62,63,65,66,68]. Pai and co-workers [68] measured the impulse breakdown voltage (1.2/50 μs) for a point-plane gap (9.5 mm diameter rod with a 30° cone terminated by a 2 mm diameter hemisphere) in SF_6-(2-C_4F_8)-N_2 mixtures. They observed a large effect on the breakdown voltages of SF_6 mixtures with $60\%N_2$ for both positive and negative polarities when a small amount of $(2 - C_4F_8)$ was initially substituted for SF_6. Under positive polarity, the striking feature of their data was the immediate loss of corona stabilization for a 5% substitution of SF_6 by 2-C_4F_8 and the absence of any further significant change thereafter even for complete replacement of SF_6 by (2-C_4F_8). While under negative polarity a 5% replacement of SF_6 by $(2 - C_4F_8)$ increased the 50% impulse breakdown voltage profoundly. They attributed this effect to increased positive and negative ion production which led to enhanced space charge effects, since the ionization onset of (2-C_4F_8) (12.8 eV) [69] is substantially lower than the ionization onset of either N_2 (15.6 eV) or SF_6 (16 eV) [69]. Similar voltage-pressure characteristics were found for the point-plane gaps in SF_6-$(c-C_4F_8)$-N_2 mixtures for lightning impulse waveforms [63]. For positive dc point-plane geometry a $10\%(c-C_4F_8)$-$20\%SF_6$-$70\%N_2$ mixture had practically the same voltage-pressure characteristics as $1\%(c-C_4F_8)$-$29\%SF_6$-$70\%N_2$ mixture and the replacement of 5% of SF_6 by $(c-C_4F_8)$ in the SF_6 mixture with $70\%N_2$ enhanced the breakdown voltages in the corona stabilization region. They reasoned that this effect was again caused by space-charge shielding of the point electrode which tended to decrease the degree of field nonuniformity in that region. The substitution of as little as $1\%(c-C_4F_8)$ for SF_6 enhanced corona stabilization in the mixture apparently by increasing the production of space charges. Furthermore, the corona stabilization region was broadened and the critical pressure was increased for all $(c-C_4F_8)$ containing SF_6-N_2 mixtures.

A number of SF_6 gas mixtures have been identified as good candidates for industrial testing and adoption [23] of which SF_6-N_2 binary mixtures and SF_6-N_2-$(c-C_4F_8)$ ternary mixtures are of particular interest

2.1.3 Breakdown voltage-time characteristics for gaseous mixtures

Data for breakdown voltage-time characteristics for SF_6 mixtures are very limited. Rizk and Eteiba [70] measured impulse breakdown voltage—time curves for SF_6-N_2 in coaxial cylinder gaps. Their data showed a pronounced rise in the breakdown voltage for times to breakdown below 1 μs. Since the unit step response of the voltage measuring system they used was 30 ns, corrections were necessary for breakdown occurring at the impulse front.

Okabe and Kuffel [71] studied the volt-time characteristics of rod-sphere gaps in gas mixtures comprising 59% SF_6-1%($c-C_4F_8$)-40% CO and 99% dry air - 1%SF_6 under lightning and switching impulse applied voltage conditions. They observed a significant reduction in breakdown voltages for the fast rising impulses under certain experimental conditions.

2.2 Present investigation

Review of previous work shows that while SF_6-N_2 and SF_6-N_2-($c-C_4F_8$) mixtures were identified as potential dielectric gas mixtures for industrial applications and were subjected to extensive testing from many aspects, investigations on the volt-time characteristics of the mixtures were very limited especially with steep-fronted impulse applied voltages. It was therefore suggested [66] that studies of gaseous dielectrics with steep-fronted voltage pulses would be desirable.

The main objective of this investigation is to gain additional information on the mixtures. Since N_2, air, CO_2 have similar dielectric characteristics in many aspects, it is unwise to limit this study to only SF_6-N_2 and SF_6-N_2-($c-C_4F_8$) mixtures. Hence mixtures with air and CO_2 as buffer gases were also included in the studies under otherwise the same experimental conditions for purposes of comparison.

The details of this investigation are given in the following chapters. Chapter III describes the equipment and experimental techniques employed in the study and experimental procedures. Chapter IV presents the experimental results. The impulse voltage breakdown characteristics and the volt-time curves are treated in this chapter. The theoretical consideration is presented in Chapter V with a comparison between experimental results and theoretical values. The following chapter, Chapter VI, deals with the interpretation and includes a discussion of the significance of the results. In the final section, conclusions are drawn and some suggestions for further work are made.

Chapter 3

Test equipment and experimental techniques

3.1 Test Equipment

The studies were carried out using coaxial cylinder electrodes housed in a pressure chamber. The cross section of the arrangement is shown in Figure 3.1.

3.1.1 Pressure chamber

The test chamber consisted of a fiberglass reinforced cylinder 82.5 cm high and 35 cm diameter, which had a permissible maximum pressure limit of 700 kPa. Both ends of the chamber were covered with brass plates. The bottom end was fitted with inlet and outlet tubes and valves for gas filling and releasing. The pressures or partial pressures were measured using two mechanical pressure gauges both having an accuracy of 0.25%.

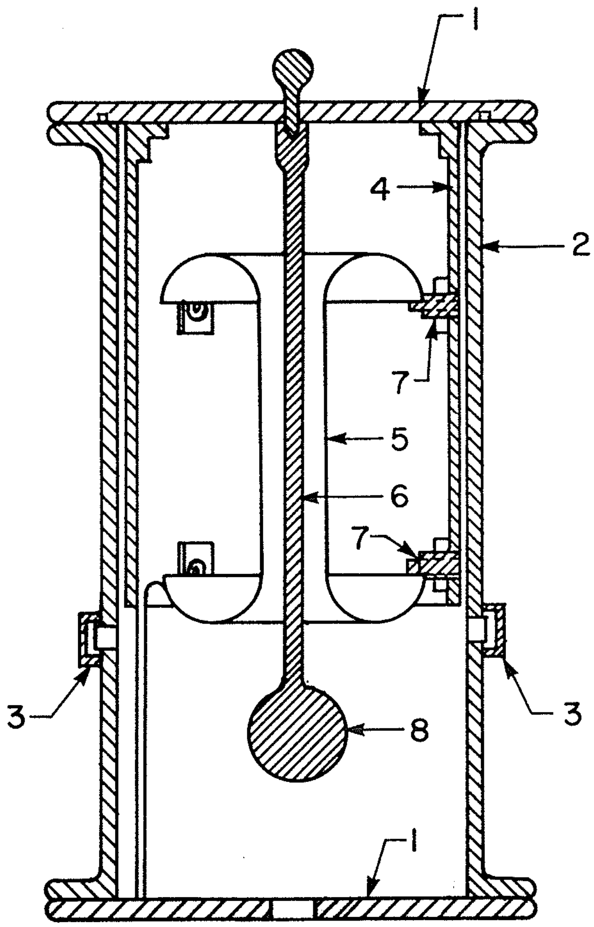

Figure 3.1: Cross section of the test chamber: 1. Brass endplates; 2. Fiberglass cylinder; 3. Observation windows; 4. Polyvinyl chloride support; 5. Outer electrode (brass) 6. Inner electrode (brass rod); 7. Adjustable supports for setting center position; 8. Stress controlling sphere.

3.1.2 Electrode configurations

From a practical point of view, most compressed gas insulated high voltage equipment are contructed in the form of concentric spheres or coaxial cylinders. Therefore, the cylindrical configuration was chosen for the present experiment. The coaxial cylinder gaps were 1.27/5.2, 1.86/5.2 cm diameter respectively and 30 cm in length. The electrodes were equiped with appropriate terminations to eliminate end effects and were mounted vertically inside the pressure chamber. The electrodes were polished with 600 grit sand paper and then cleaned with methanol to remove any grease. The surface roughness of the inner electrodes of the coaxial cylinder gaps was estimated to be 0.2 μm.

3.2 Experimental techniques

3.2.1 Switching and lightning impulse sources and measurement

Both the switching surge and lightning impulse voltages were generated by an 800 kV, 10 kJ impulse generator with appropriate waveshapping resistors. For switching surge voltages, 15/1200, 275/2500 μs waveshapes were used. The breakdown voltages and times to breakdown were measured using a capacitor divider in connection with a storage oscilloscope (type 466 Tektronix). The breakdown voltages measured were the actual values and not the anticipated peak values.

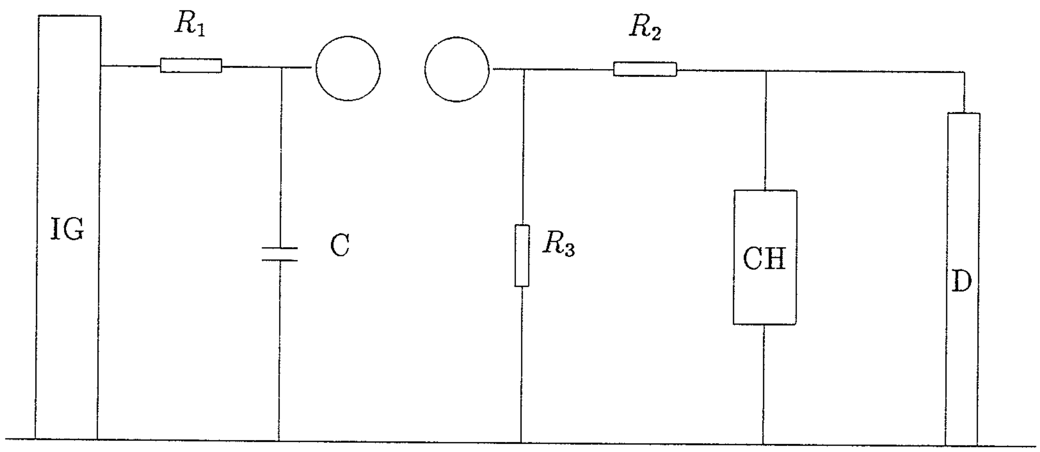

Figure 3.2: Steep-fronted impulse generating circuit. IG-impulse generator; CH-gas filled chamber; D-voltage divider; $R_1, R_2, R3$- resistors; C-capacitor.

3.2.2 Circuit to generate steep-fronted impulses

The circuit used to generate the steep-fronted impulse is shown in Figure 3.2. The impulse generator described in 3.2.1 was used as a power supply for the circuit. As shown in the figure, in order to lessen the effect of the impulse generator on the steep-fronted impulse waveshape a large value resistor was chosen for R_1. The desired impulse waveshape was obtained by choosing adequate resistances for R_2 and R_3 in the circuit. With this circuit arrangement a steep-fronted impulse of 0.2/50 μs can obtained.

3.2.3 Steep-fronted impulse voltage measurement

With the front time range to be used in this investigation, it was immediately realized that measurement would be a problem since the impulse voltage dividers available in the laboratory were not suitable for the steep-fronted impulse measurement because of their slow unit step responses. Therefore, the search for an adequate measuring system constituted part of this investigation.

Steep-fronted impulse measured by compensated resistor divider

After analyzing the circuit representation of a resistor divider, it was concluded that an analog compensation technique could be used to improve the unit step response of the resistor divider. It was, therefore, decided to design and build an electronic circuit to compensate the resistor divider in our laboratory. The unit step response of the measuring system was reduced from about 78 ns to 13 ns after compensation. Hence, with this system, the measuring error can be greatly reduced. The detailed description of the compensation will be given in the next chapter.

Steep-fronted impulse measured by compact resistor divider

Another way to obtain a resistor divider with a fast step response is to use a compact structure for the divider [72]. To check the performance of the compensated resistor divider and for comparison purposes, a compact oil immersed resistor divider with about a 500 kV voltage rating was built and tested. The unit step response of the compact resistor divider was 8 ns. It was used as an alternative method for the steep-fronted impulse voltage measurement.

3.2.4 Gas filling and pressure measurement

Before filling the chamber with a gas or gaseous mixture it was evacuated to a pressure of about 6.7 Pa and then flushed with the gas or the cheapest component gas of the mixture to be tested. Subsequently a predetermined amount of $(c-C_4F_8)$ in the case of a ternary mixture, or SF_6 in the case of a binary mixture was introduced into the chamber. Finally, the chamber was filled with the other component gas/gases to the desired pressure. The total pressure as well as the partial pressures were measured by two mechanical pressure gauges. The gas/mixture was left for at least 16 hours before testing.

The purity of the gases used was as follows: SF_6 of C.P. grade (99.8%), dry air ($H_2O<$ 100ppm, $CO_2<$ 330ppm), prepurified N_2 (99.995%), CO of C.P. grade (99.5%), CO_2 of commercial grade (99.5%) and $(c-C_4F_8)$ (99.9%).

3.2.5 Test procedure

For the 50% impulse breakdown voltage tests, the *"up and down"* method was used.

For the volt-time characteristics measurements two slightly different methods were used. The first method was to determine the 50% breakdown voltage, then use this voltage as the first voltage level for the volt-time characteristics measurements. The applied voltage level was then increased stepwise until the desired measurements were obtained. For each voltage level, at least 10 voltage applications were made. The breakdown voltages and times to breakdown recorded. The breakdown times were recorded from the virtual origin, determined according to the IEEE standard [79], to the instant that the applied voltage collapsed.

The second method was restricted to the steep-fronted impulse voltage-time characteristics measurements. In this case, impulse waves of different front durations were used. For each of the impulse voltage waveshapes, the 50% breakdown voltage was obtained again using the *"up and down"* method. The applied voltage was then raised $10 - 20\%$ above the 50% breakdown level. In doing so, the breakdown of the cylinder gap always occured at or before the peak of the applied voltage. Thus, the volt-time curve and the comparison of the results among the different waveshapes were meaningful. The breakdown voltages and times to breakdown were recorded in the same manner as mentioned previously. In all cases, the time interval between successive impulses was at least 1 minute to allow complete recovery of the gap.

Chapter 4

Experimental results

4.1 The development and application of analog compensation in impulse resistor voltage dividers

As described in section 3.2.3, the most difficult part of a volt-time characteristics study under steep-fronted impulse voltages is its accurate measurement. Therefore, the search for an adequate measuring divider was an important part of this investigation and it is considered to be part of this thesis presentation.

To generate very steeply rising impulse voltages, it is essential to provide very small capacitive loading for the impulse circuit. The shielded resistor divider in which the shielding takes the form of grading rings at the high and low voltage ends of the resistor is an ideal divider in this aspect. It is simple in construction, light in weight and it presents only a very light loading to the impulse generator.

The divider is not, on the other hand, completely suitable for steep fronted impulse measurements since its response time is generally quite long and the capacitance of the connecting leads produces an oscillating response similar to a pure capacitor divider. Although the latter can be considerably improved by the addition of a series resistor to damp out oscillations in the divider circuit, it further slows the response of the measuring system.

There are many ways to improve the response of a divider. One possible way is to use a compensating network. Harada and co-workers suggested a compensation type divider with the element incorporated in the high voltage terminal of an impulse resistor divider [73]. Jiang Guoxiong and co-workers introduced a R-C compensating network in the low voltage side of the resistor divider [74]. However, the R-C compensation was basically an overshoot type compensation, and it did not reduce significantly the time taken for the response to settle at its steady state value. Therefore, a measuring system with a divider compensated by this method is not adequate for very steeply rising impulse voltage measurements, especially when the impulse voltage is chopped on the front after very short time, since the error caused by the measuring system is unpredictable.

Another possible way to reduce the measuring error caused by the response time is to use numerical correction techniques to reconstruct the measured input impulse voltage [75,76]. The numerical correction method however, over estimates the correction needed by 5 to 7% even when the time to chop is only slightly less than 1 μs [76]. Moreover, the effect of skip-coding of the A/D conversion for digitized recording on the accurate measurement is also pronounced when it is used for sampling steep fronted impulse voltages. With the increasing steepness of the recorded voltage more and more digital levels or points are skipped [77]. This means that a larger error is bound to occur when the method is used to reconstruct a chopped voltage with short time duration. Furthermore, the advent of storage oscilloscopes makes real time single impulse measurement possible. This is very convenient in terms of monitoring test processes. The numerical correction method mentioned, however, does not provide this convenience. While the numerical correction techniques are still in the developing stage there is no information available on reconstruction of input impulse distorted by a measuring system with a resistor divider by analog compensation techniques. Theoretically the analog compensating network is simply an analog computer with an oscilloscope as its output device. If it could be used in high voltage environment with adequate protection, it would be very convenient for this measurement. It was therefore considered that the analog compensation would be the best way to achieve the desired requirement.

4.1.1 Theory consideration of the compensation

It is well known that a shielded resistor divider can be represented approximately by the lumped equivalent circuit shown in Figure 4.1. [78]. In this circuit, L is the inductance of the lead from the test object to the divider, R_d

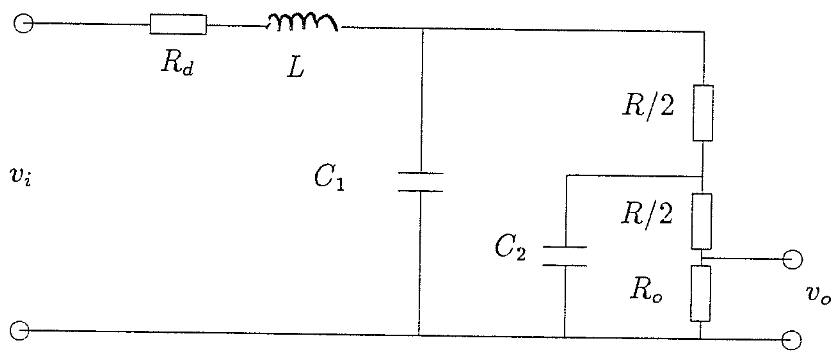

Figure 4.1: Equivalent circuit of a resistor divider.

is the damping resistance and C_1 is the shunt capacitance across the divider due to the grading rings. R is the high voltage resistor and C_2 represents the distributed capacitance across the high voltage resistor.

The Laplace transform circuit for the equivalent circuit of the divider is sketched in Figure 4.2. For this circuit, for $R/2 >> R_o$ one obtains

$$v_i(s) = \frac{R}{R_o}[(1+\frac{R_d}{R})v_o(s) + (R_dC_1 + \frac{R_dC_2}{2} + \frac{L}{R} + \frac{RC_2}{4})Sv_o(s)$$
$$+ (\frac{RR_dC_1C_2}{4} + LC1 + \frac{LC_2}{2})S^2v_o + \frac{RLC_1C_2}{4}S^3v_o(s)] \qquad (4.1)$$

Generally, R is within several tens of $k\Omega$, L is in the order of several μH depending on the dimension of the high voltage lead used, C_1 is in the order of several tens of pF and C_2 is only several pF for a shielded resistor divider. Therefore, the contribution of the fourth term in the reconstruction of the

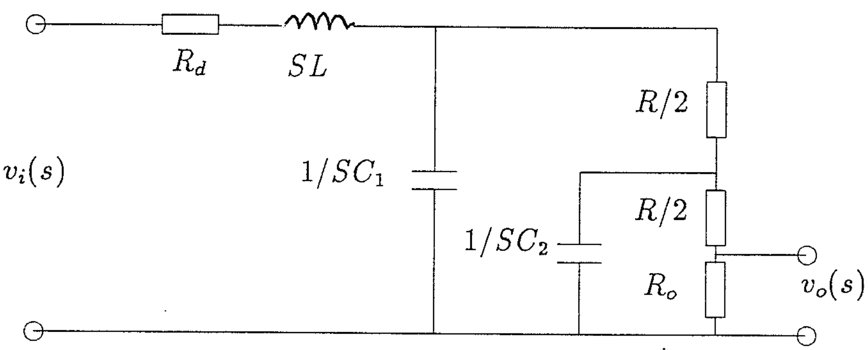

Figure 4.2: Transform circuit of the equivalent circuit.

input $v_i(s)$ is insignificant. Besides, the above equivalent circuit is only an approximation of a real resistor divider. Therefore, the omission of this term is considered not to cause significant error as far as the reconstruction is concerned. Thus:

$$\begin{aligned} v_i(s) &\doteq \frac{R}{R_o}[(1+\frac{R_d}{R})v_o(s) + (R_dC_1 + \frac{R_dC_2}{2} + \frac{L}{R} + \frac{RC_2}{4})Sv_o(s) \\ &+(\frac{RR_dC_1C_2}{4} + LC_1 + \frac{LC_2}{2})S^2v_o(s)] \\ &= \frac{R}{R_o}(1+\frac{R_d}{R})(1+AS+BS^2)v_o(s) \qquad (4.2) \\ where\ \ A &= (R_dC_1 + \frac{R_dC_2}{2} + \frac{L}{R} + \frac{RC_2}{4})/(1+\frac{R_d}{R}) \\ B &= (\frac{RR_dC_1C_2}{4} + LC_1 + \frac{LC_2}{2})/(1+\frac{R_d}{R}) \end{aligned}$$

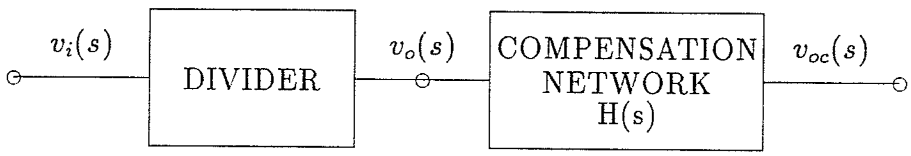

Figure 4.3: Principle of the compensation

If a compensation network with a transfer function

$$H(s) = \frac{v_{oc}(s)}{v_o(s)} = K(1 + AS + BS^2) \tag{4.3}$$

shown in Figure 4.3 is connected to the output of the divider, where $v_{oc}(s)$ being the output of the compensation network, then from equation (4.2) and (4.3), we obtain

$$\begin{aligned} v_i(s) &= \frac{R}{R_o}(1 + \frac{R_d}{R})(1 + AS + BS^2) \cdot \frac{1}{K}(1 + AS + BS^2)^{-1} v_{oc}(s) \\ &= \frac{R}{KR_o}(1 + \frac{R_d}{R}) v_{oc}(s) \end{aligned} \tag{4.4}$$

Therefore, the output of the compensation network is directly proportional to the input of the measuring system compensated.

4.1.2 The analog circuit

The complete analog circuit is sketched in Figure 4.4. It comprises two cascaded proportional differentiators. The operational amplifier used was

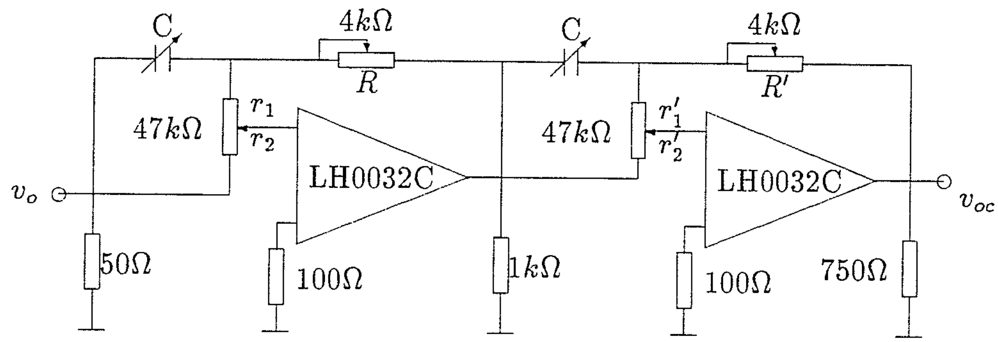

Figure 4.4: A sketch of the compensation circuit

a $LH0032c$ ultra fast FET with a $500v/\mu s$ slew rate, 70 MHz bandwidth and 10^{12} Ω input impedance. The values of the circuit parameters r_1, r_2 are relatively unimportant since they only affect the scale factor of the circuit. However, the values of the circuit parameters R, C should be adjustable to match the parameters of the measuring system to be compensated.

The whole circuit is placed inside a small metallic box and is supplied by rechargeable batteries. To obtain a suitable voltage input for the circuit, an attenuator with input impedance of 75 Ω to match the surge impedance of the signal cable was used. Since analog circuits are very vulnerable to interference, the metallic box to which the analog circuit is grounded is solidly connected to the cases of both the attenuator and the oscilloscope used for the measurement to reduce interference due to the discharges of the impulse generator.

4.1.3 The compensated measuring system and its step response

Figure 4.5 shows a block diagram of the compensated system. The damping resistor used was 300 Ω. The resistor divider, manufactured by Haefely Company, is rated at 600 kV. The height of the HV resistance column is about 1.7 m with resistance of 46.2 $k\Omega$. The maximum outside diameter and the diameter of the cross section of the toroids are about 0.96 and 0.1 m respectively. The response time of this system with 300 Ω damping resistor, 1.6 m horizontal and 2 m vertical leads, before compensation, is about 75 ns and the time taken for the response to settle down to its steady state value is about 300 ns. Figure 4.6 (a) shows an oscillogram of the step response of the measuring system before compensation and Figure 4.6 (b) shows that after compensation. The step response time of the compensated system, according to the $IEEE$ standard [79], is estimated to be 13 ns with the time taken to settle to its steady state value about 24 ns.

4.1.4 Comparison of impulse voltage measurements

To check the performance of the compensated measuring system under impulse voltages, a series of comparison tests was carried out. The comparison was made against an oil immersed compact resistor divider with a unit step response time of about 8 ns. The two measuring systems were connected in parallel so that impulse voltages could be measured by either of the two

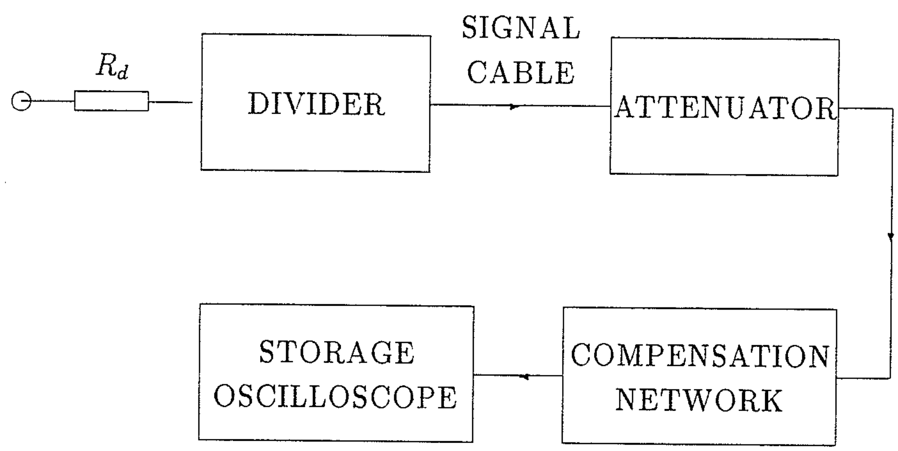

Figure 4.5: Block diagram of the compensated measuring system

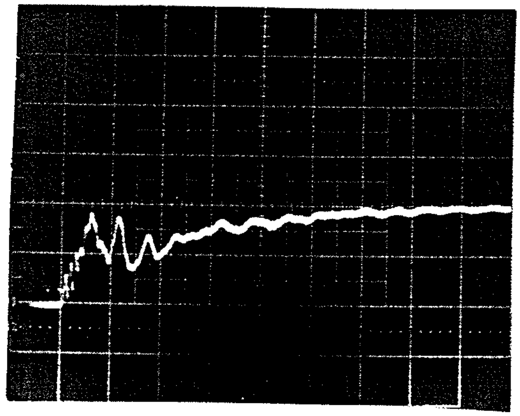

(a)

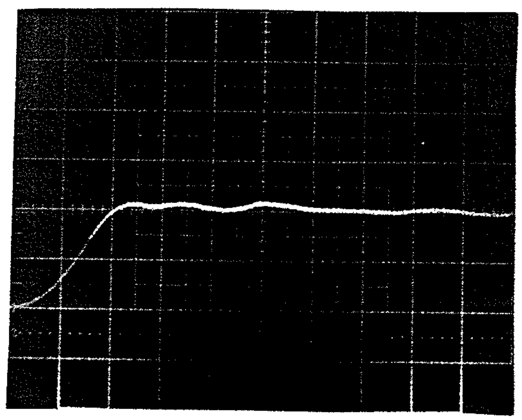

(b)

Figure 4.6: Step response of the resistor divider: (a) before compensation 50 ns/div; (b) after compensation, 20 ns/div.

systems. The planes of the two measuring systems were at right angles to minimize coupling. Figures 4.7, 4.8 and 4.9 show the full impulse wave oscillograms measured by the two systems for different front impulse voltages and Table 1 gives the results of the comparative measurements. As can be seen from these figures, the impulse voltage waves obtained by the two measuring systems with the same discharging circuit arrangement are almost identical except that the amplitude of the superimposed oscillation on the oscillogram obtained by the compensated measuring system is higher than that on the corresponding one obtained by the compact resistor divider measuring system. This was perhaps due to the larger physical size of the toroid divider which might pick up noise from the surroundings. Nevertheless, it is evident that the compensated measuring system works properly and hence can be used for the steep-front impulse voltage measurements.

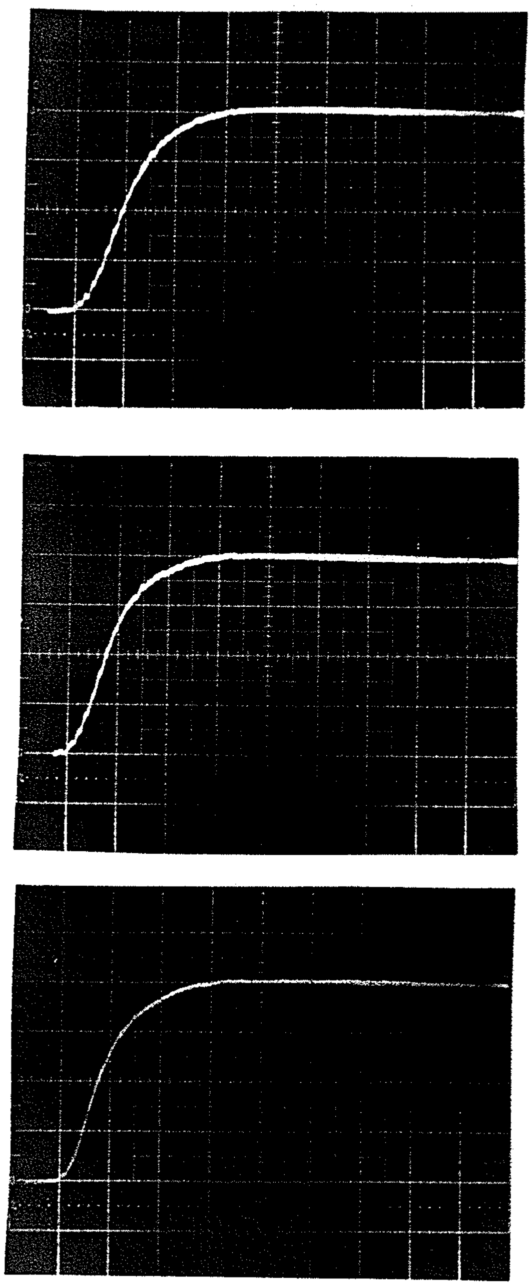

(a)

(b)

(c)

Figure 4.7: Full lightning impulse. 500 ns/div. : (a) resistor divider before compensation; (b) resistor divider after compensation; (c) compact resistor divider

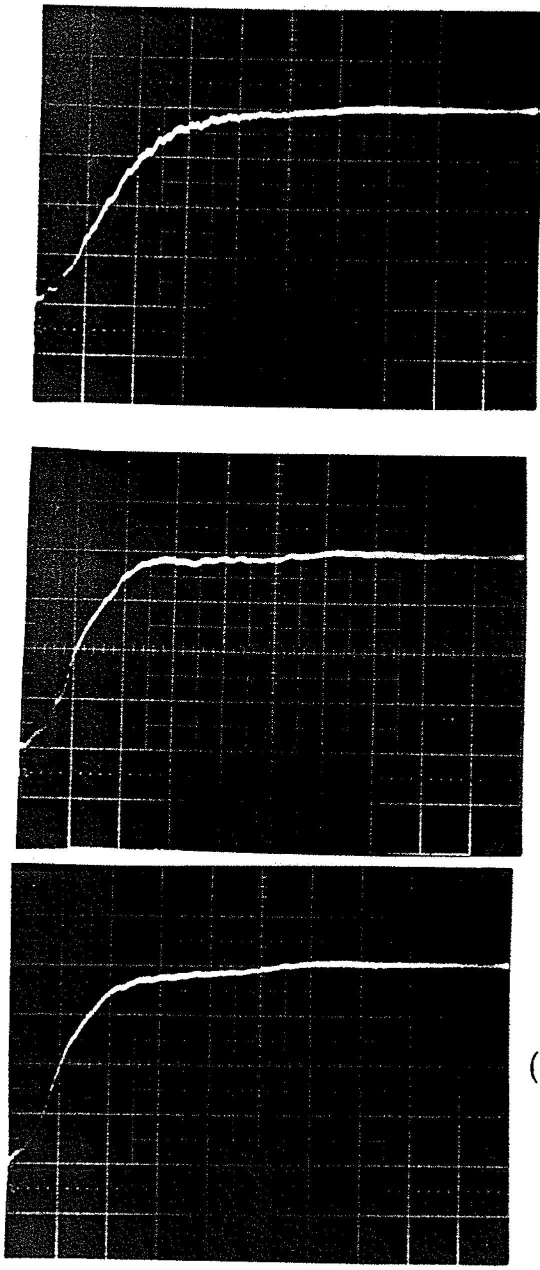

(a)

(b)

(c)

Figure 4.8: 0.45/50 μs impulse voltages, 200 ns/div. : (a) resistor divider before compensation; (b) resistor divider after compensation; (c) compact resistor divider

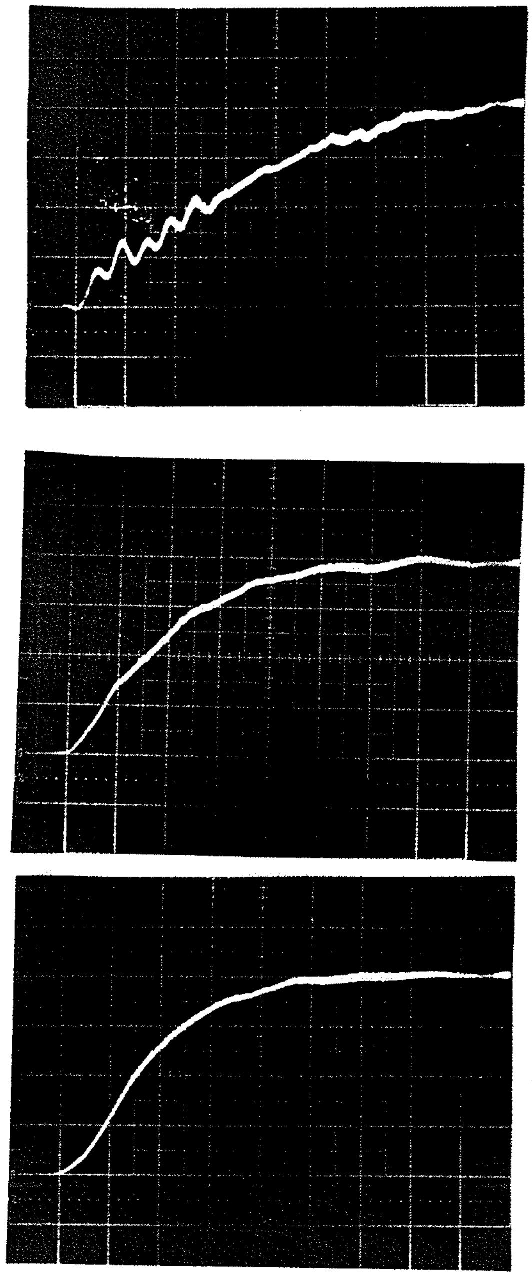

(a)

(b)

(c)

Figure 4.9: 0.22/50 μs impulse voltages, 50 ns/div. : (a) resistor divider before compensation; (b) resistor divider after compensation; (c) compact resistor divider

Table 1: Measured values of the peak voltages and front times of full impulses (same input for each group of measurements)

Divider		Compact	Compensated	Uncompensated
1	Front Time (μs)	1.1	1.13	1.13
	Peak Voltage (kV)	80.6	80.6	80.4
2	Front Time (μs)	0.47	0.45	0.7
	Peak Voltage (kV)	90.6	90.8	90.3
3	Front Time (μs)	0.22	0.25	0.39
	Peak Voltage (kV)	86.8	86.3	85.6

The characteristics of the compensated measuring system were further explored by measuring impulse voltages chopped on the front. The measuring system with the compact resistor divider was again used for the purpose of comparison. The circuit arrangement of the two measuring systems was the same as mentioned earlier. The chopping gap used for the comparison was a sphere-sphere gap of 10 cm diameter and 2 cm gap spacing. Since there was no second storage oscilloscope available, the comparative measurements were made on alternative impulses with the same voltage applications rather than simultaneous measurements on each impulse voltage. Hence, the comparison was made by comparing the average values of two groups of measurements obtained by the two measuring systems. 30 voltage applications were made for each measuring system for a particular circuit arrangement. Figures 4.10 and 4.11 show typical chopping wave shapes recorded and Table 2 gives both the average values and standard deviations of the data obtained in the test. It was concluded from the comparison measurements that the compensated measuring system can also function properly under chopping conditions with times to chop well below 1 μs.

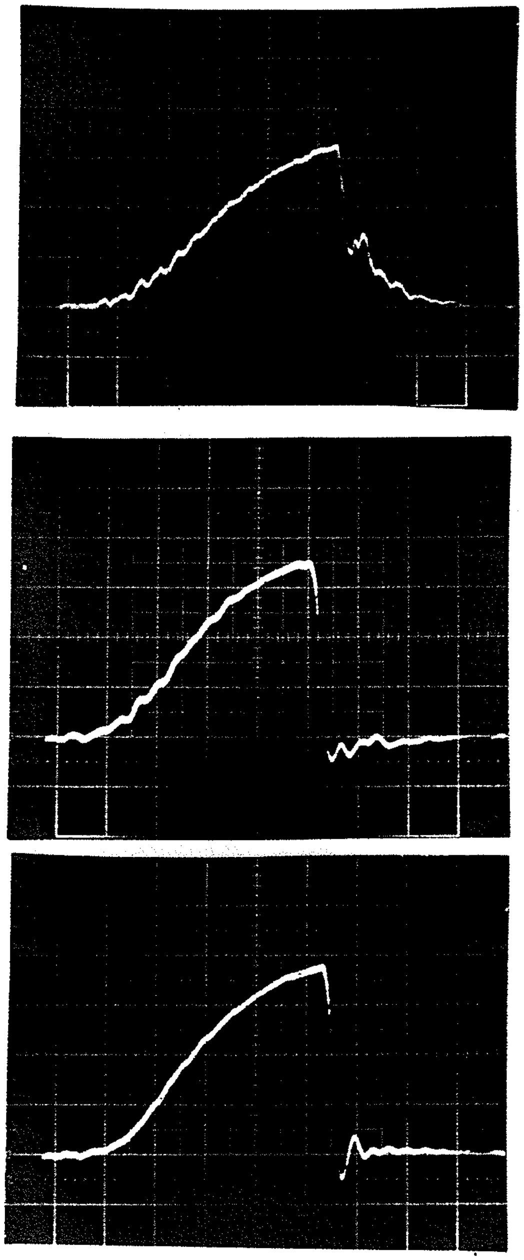

(a)

(b)

(c)

Figure 4.10: Chopped impulses, 200 ns/div. : (a) resistor divider before compensation; (b) resistor divider after compensation; (c) compact resistor divider

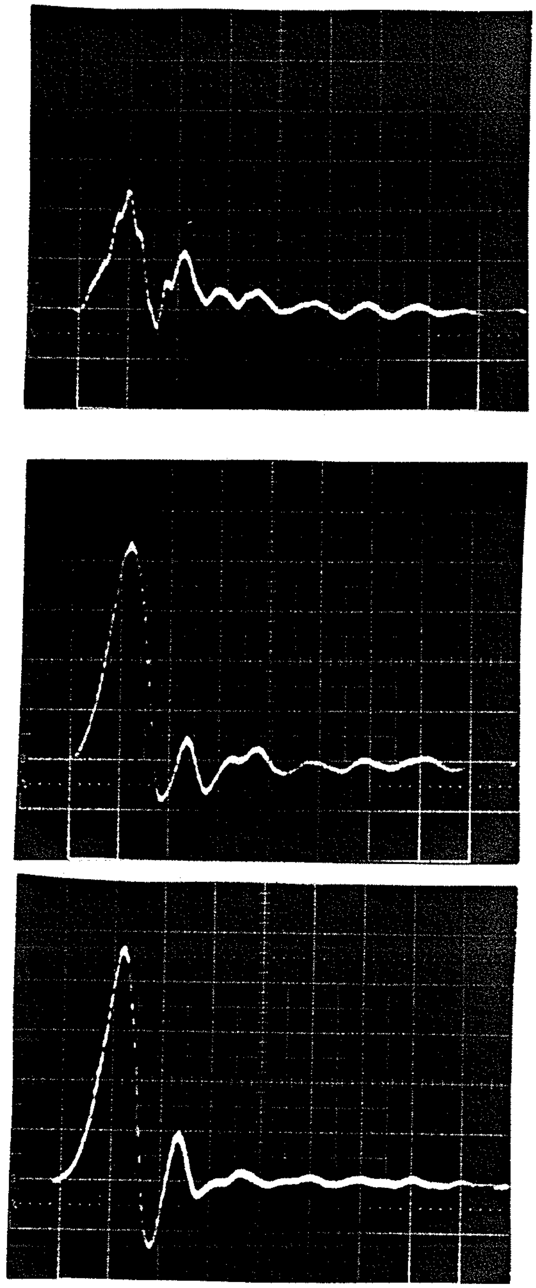

(a)

(b)

(c)

Figure 4.11: Chopped impulses, 100 ns/div. : (a) resistor divider before compensation; (b) resistor divider after compensation; (c) compact resistor divider

Table 2: Comparision of crest values of chopped voltages

Divider		Compact	Compensated	Uncompensated
1	Time to chop(μs)	0.62-0.83	0.65-0.84	0.68-0.94
	Crest Voltage (kV)	54.95-62.93	56.53-63.38	54.3-62.14
	$\overline{V}(kV)$	59.50	59.54	59.04
	σ_v	3.41	3.15	3.25
2	Time to chop(μs)	0.16-0.20	0.16-0.20	0.15-0.20
	Crest Voltage (kV)	60.44-67.90	59.95-68.52	46.7-52.4
	$\overline{V}(kV)$	64.66	66.10	49.58
	σ_v	3.16	3.89	3.14
3	Time to chop(μs)	0.07-0.09	0.07-0.09	0.07-0.09
	Crest Voltage (kV)	66.24-79.49	67.66-81.36	40.43-46.50
	$\overline{V}(kV)$	73.71	74.32	43.35
	σ_v	5.65	4.88	3.39

4.2 Impulse voltage breakdown characteristics of SF_6 mixtures in the coaxial cylinder gap

The selection of the gaseous dielectrics used in this experiment is based on the knowlege of the electron attaching, electron slowing down and electron impact ionization properties obtained by many investigations. As shown in Figure 4.12, in a gas, at a given number density (N), the free electrons obtain an equilibrium energy distribution $f(\varepsilon, E/N)$ which is a function of the gas and E/N, where ε and E are electron energy and field intensity respectively. When the value of E/N is low (e.g., 1.24×10^{-16} V cm^2 for N_2), $f(\varepsilon, E/N)$ lies at low energies, and the number of electrons capable of ionizing the gas is negligible. As the voltage is increased, however, $f(\varepsilon, E/N)$ shifts to higher energies, ε, and for sufficiently high E/N the number of electrons capable of ionizing the gas is such that the gas makes the transition from an insulator to a conductor. In figure 4.12 $f(\varepsilon, E/N)$ is shown for N_2 at the limiting value of E/N, $(E/N)_{lim}$ ($\simeq 1.3 \times 10^{-15}$ Vcm^2) (i.e., the value of E/N at which breakdown occurs). Even at this high E/N value only a small fraction of electrons possesses sufficient energy to induce ionization. This is designated in figure 4.12 by the shaded area α which is a measure of the ionization coefficient, α/N, expressed as

$$\frac{\alpha}{N} = (\frac{2}{m})^{1/2} w^{-1} \int_{I_o}^{\infty} \underbrace{f(\varepsilon, E/N)\varepsilon^{1/2}\sigma_i(\varepsilon)d\varepsilon}_{I} \tag{4.5}$$

where I_o is the ionization threshold energy, m is the electron mass, w is the electron drift velocity, and $\sigma_i(\varepsilon)$ is the electron-impact-ionization cross section.

The most effective way to prevent electrons from initiating breakdown is to remove them by attachment to the molecules forming stable negative ions as mentioned earlier. As can be seen from figure 4.12 $\sigma_a(\varepsilon)$ is large for SF_6 at very low energies, and thus only electrons with energies at the extreme low-energy range can be removed efficiently by electron attachment. The shaded area in figure 4.12 designated by η is a measure of the effective electron attachment coefficient, η/N_a, expressed as

$$\frac{\eta}{N_a} = (\frac{2}{m})^{1/2} w^{-1} \int_0^\infty \underbrace{f(\varepsilon, E/N)\varepsilon^{1/2}\sigma_a(\varepsilon)d\varepsilon}_{A} \tag{4.6}$$

where N_a is the attaching gas number density ($N = N_a$ for a unitary electronegative gas). Knowledge of α/N and η/N_a allows one to predict $(E/N)_{lim}$, which for a uniform field is defined as the value of E/N at which $\alpha = \eta$.

Considering eqn.(4.5) and (4.6) it is easy to understand that the gas dielectric can be optimized by maximizing the quantity A and by minimizing the quantity I. For this, not only must $\sigma_a(\varepsilon)$ be as large as possible and $\sigma_i(\varepsilon)$ as small as possible but also the reduction of the electron energies is of paramount significance because a lower-lying $f(\varepsilon, E/N)$ minimizes I and maximizes A [66].

A number of PFCs have excellent dielectric strength as compared to SF_6

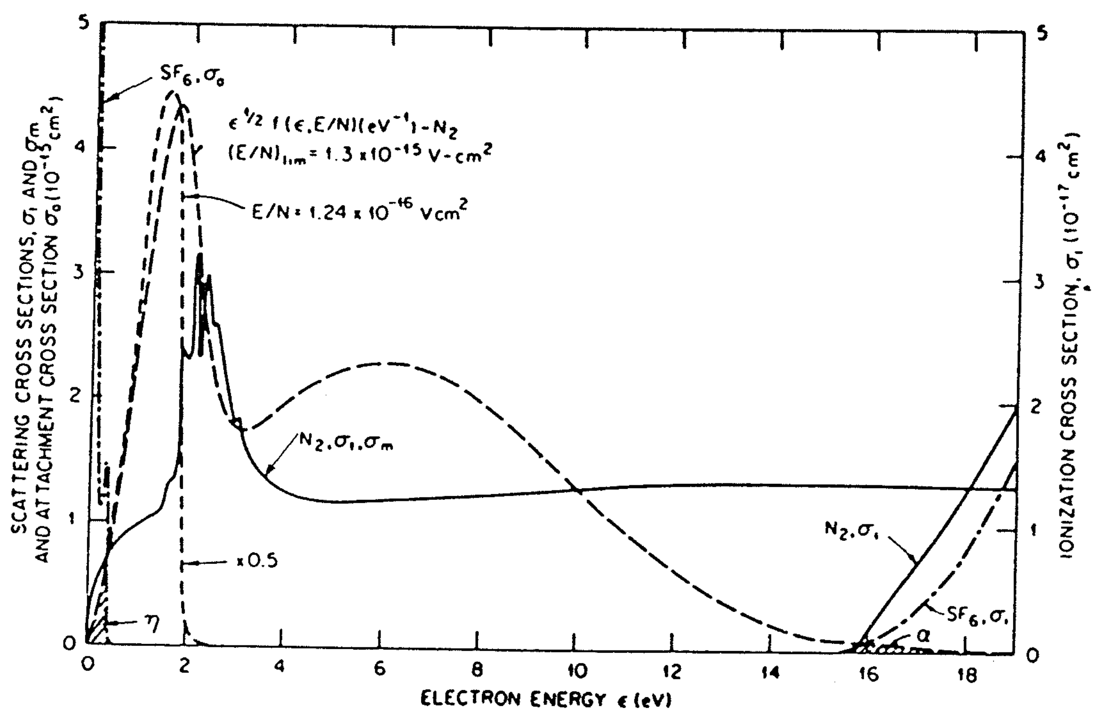

Figure 4.12: Ionization cross section $\sigma_i(\varepsilon)$ for N_2 and SF_6 close to the ionization onset. Electron scattering cross section as a function of ε for N_2 and electron attachment cross section σ_a for SF_6. Normalized electron energy distribution function $\varepsilon^{1/2}f(\varepsilon, E/N)$ as a function of ε for N_2 at two values of E/N [66]

due particularly to their exceedingly large electron attachment cross section below about 1.5 eV. The most desirable of the PFCs are, of course, those which capture efficiently not only thermal energy electrons but also higher energy electrons to complement the electron attachment properties of SF_6. As mentioned earlier, many PFC's attach electrons over a wider part of the free electron energy distribution as shown in figure 4.13 [26], thus increasing their proportion in a mixture provides additional attachment. However, such PFC gases may be expensive or toxic, or have a low vapor pressure, or may form copious quantities of elemental carbon when sparked by themselves. Hence, only small amounts of selected PFCs can be used in a mixture to alleviate or substantially suppress these problems.

The reduction of electron energies could be achieved by adding gas molecules which can slow down electrons that have obtained enough energy to escape the effective attachment energy range. In this regard CO, N_2 and H_2 have been identified to have the ability to slow down electrons through inelastic scattering via negative ion resonances [62]. As indicated in figure 4.14, although the cross section for vibrational excitation of N_2 is not as good as CO, N_2 is a good candidate for this purpose. It is cheap, abundant and inert. Its negative ion resonance at about 2.3 ev is very effective in slowing down electrons around this energy. Hence $SF_6 + N_2$ and SF_6 + PFC + N_2 mixtures have obtained special attention in the past 10 years.

It has long been known that a SF_6/N_2 mixture has a saturation effect,

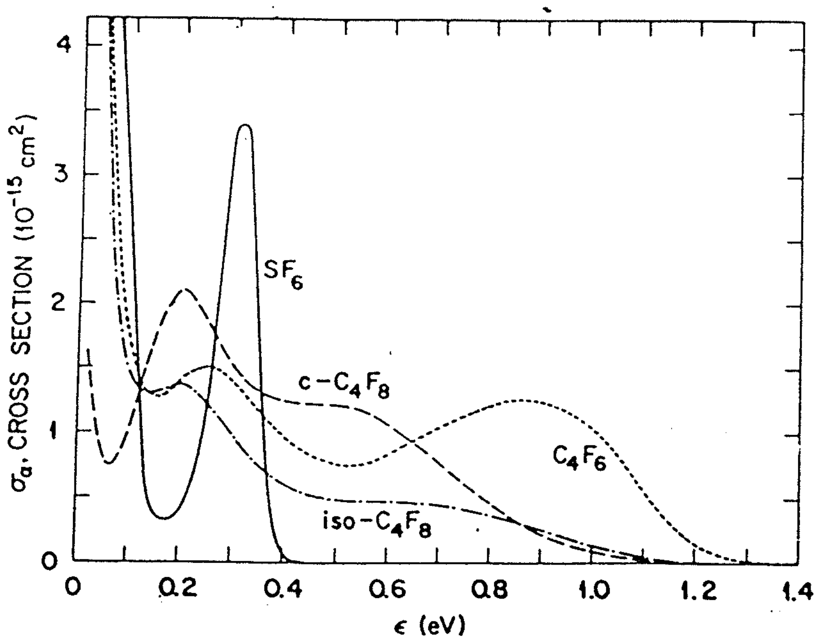

Figure 4.13: Electron attachment cross sections for SF_6 and some PFC's [26]

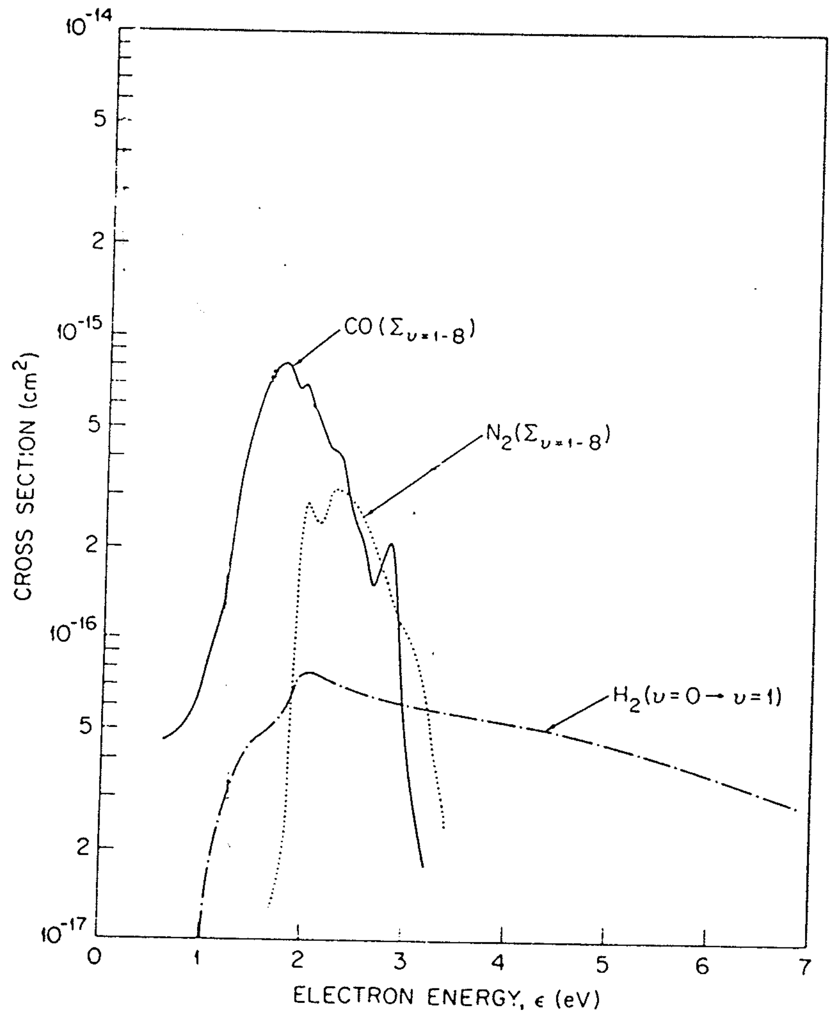

Figure 4.14: Cross section for vibrational excitation of CO, N_2 and H_2 via negative ion resonances [62]

although the causes for this are still not fully understood. As shown in figure 4.15, the breakdown strength of the mixture as a function of percentage of SF_6 content increases very rapidly with SF_6 content up to about 20% and then becomes gradually saturated. This can also be viewed in terms of synergistic effect as indicated in figure 4.16, where the vertical coordinate represents the ratio of the breakdown voltage to the calculated weighted breakdown voltage for a given mixture. As can be seen from the figure, the positive synergistic effect is strongest at a SF_6 content of around 10%. On the other hand, the relative insulating strength decreases more and more rapidly as the content of SF_6 decreases. From these data, it seems reasonable to use a SF_6 content of 40% to 60% to gain the desired benefits of lower total cost, and lower condensation temperature, better particle contamination control etc. . A $50\%SF_6/50\%N_2$ mixture at 15% higher total pressure has the same dielectric strength as pure SF_6 at about 35% lower cost with a $20^{\circ}C$ lower condensation temperature [23]. On the other hand, Pace and co-workers [82] found that the effect of particles depends not only on the total pressure but also on the partial pressure. Particle effects appear to be the least at a total pressure of about 6 atm. and $60\%SF_6/40\%N_2$ gas composition. Their results were obtained under negative *dc* apllied voltages from a concentric cylinder geometry (radii 0.75 and 2.0 cm) with rough surface grooves of 0.051 cm depth on the inner cylinder and free copper particles of 0.381 mm diameter and 3.175 mm length. In addition, this mixture exhibits the highest negative

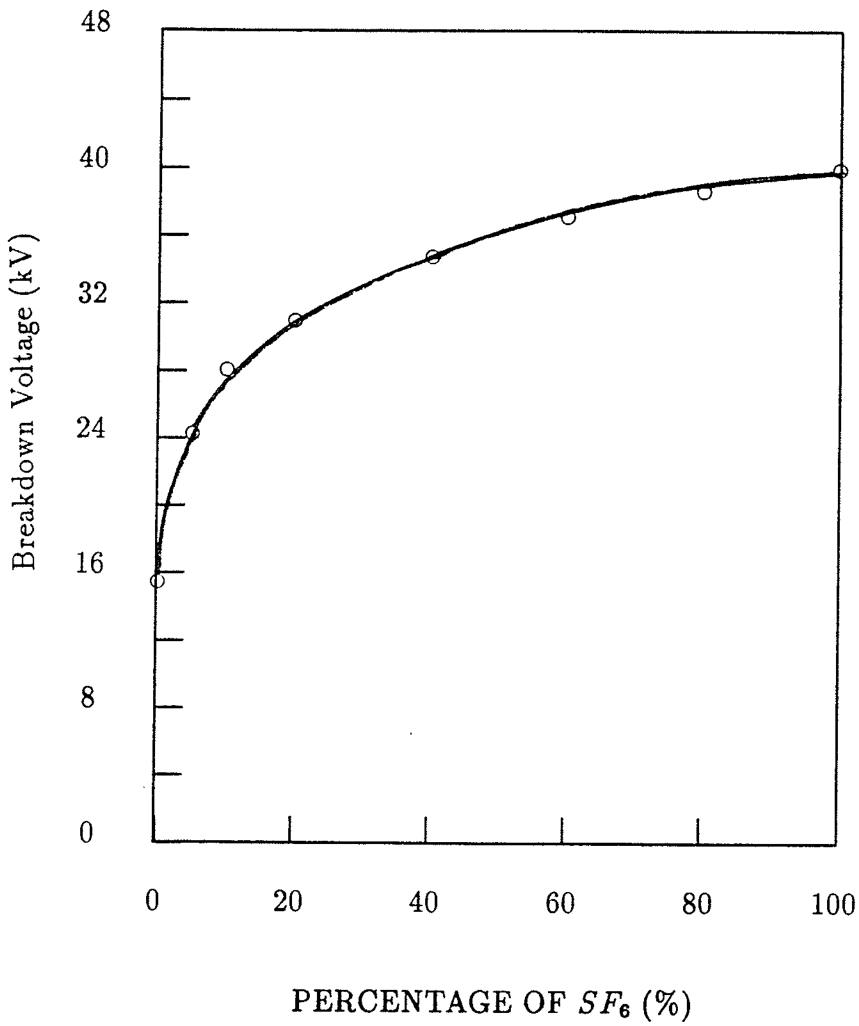

Figure 4.15: Breakdown strength of SF_6/N_2 mixtures in uniform field under *dc* applied voltages [26]

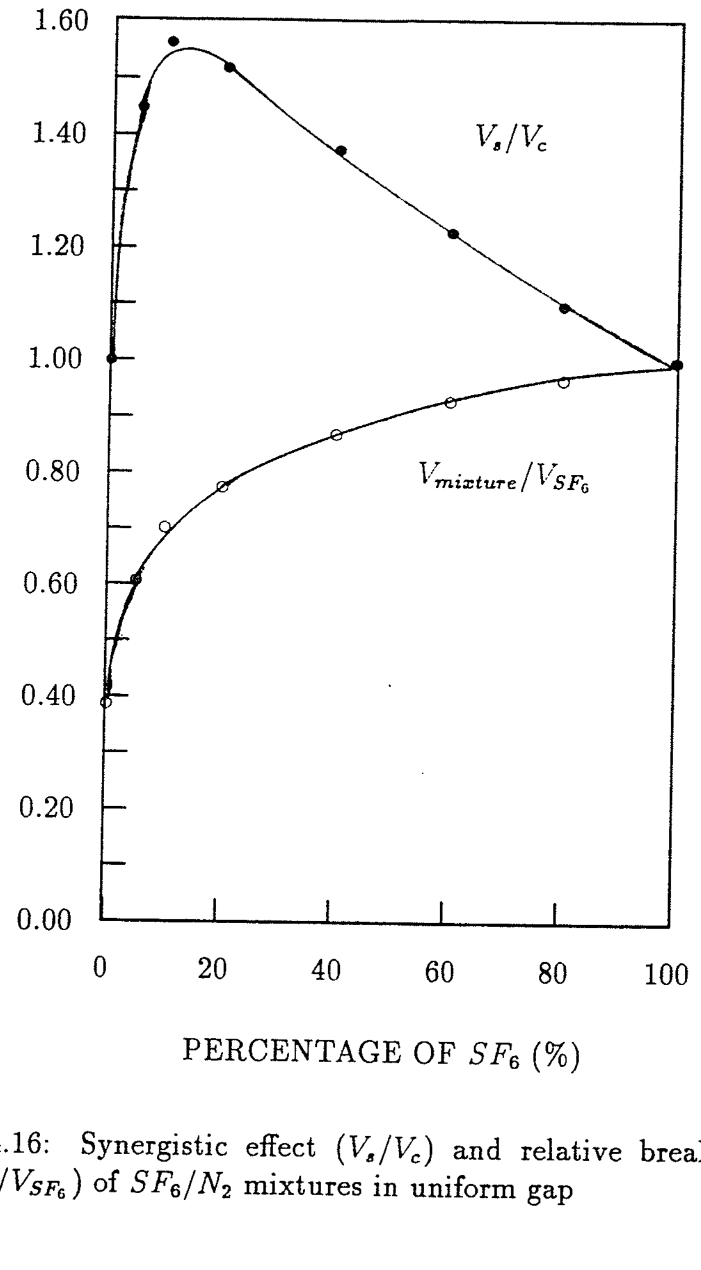

Figure 4.16: Synergistic effect (V_s/V_c) and relative breakdown strength ($V_{mixture}/V_{SF_6}$) of SF_6/N_2 mixtures in uniform gap

dc breakdown voltages at all pressures used.

For $SF_6 + N_2 + c - C_4F_8$ ternary mixtures in non-uniform gaps such as a point/plane gap under positive *dc* applied voltages, a small amount of $c - C_4F_8$ in the mixture enhances the corona stabilized breakdown voltages [63]. The corona stabilization region is broadened and the critical pressure is increased. Moreover, the experimental data show that increasing the $c-C_4F_8$ content from 1% to 10% while maintaining 30% electronegative gases in the mixture has little effective on its positive breakdown characteristic.

Optimization of the dielectric strength of ternary mixtures can be obtained by systematically changing the partial pressure of the component gases at fixed total pressure. From the dielectric strength point of view, an "optimum" mixture can be defined as that with the highest V_s/V_c, where V_s and V_c are the measured breakdown voltage for the mixture and the calculated value for the same mixture according to the partial-pressure weighted breakdown voltages of the individual components respectively. For this to occur, the basic properties of the components of the mixture must complement each other. However, from a practical point of view, the "optimum" mixture does not necessarily imply the highest increase in V_s by the addition of small amounts of PFC to SF_6/N_2, since a system insulated by the gaseous mixture must be also optimized in terms of other properties such as surface roughness and particle contamination control, dew point etc.

Christophorou and co-workers [63] identified a number of $SF_6 + N_2 +$

$c - C_4F_8$ mixtures to be good mixtures for practical applications. Under negative *dc* applied voltages, $60\%N_2 + 35\%SF_6 + 5\%(c - C_4F_8)$ and $40\%N_2 + 30\%SF_6 + 30\%(c - C_4F_8)$ have relative dielectric strengths of 0.93 and 1.08 respectively (compared to pure SF_6) in a cylindrical gap of 0.75/2.0 *cm* inner and outer diameters with a spiraling groove 0.051 *cm* deep on the inner electrode. Similar to the positive breakdown characteristics for a non-uniform field gap, their data showed that the replacement of $5\%(c - C_4F_8)$ by $10\%(c - C_4F_8)$ while maintaining 30% of electronegative gases had little effect on the breakdown strength. A $70\%N_2 + 25\%SF_6 + 5\%(c - C_4F_8)$ had a relative dielectric strength of 0.88 while the corresponding value for $70\%N_2 + 20\%SF_6 + 10\%(c - C_4F_8)$ is 0.89. On the other hand, the addition of $(c - C_4F_8)$ to the mixture affects the dew-point profoundly. For example, $60\%N_2 + 40\%SF_6$ lowers the condensation point by 19^oC [83], while $60\%N_2 + 35\%SF_6 + 5\%(c - C_4F_8)$ raises the condensation point by 6^oC compared with pure SF_6 at a pressure of 405 kPa.

Throughout the discussion, it is assumed that for a $SF_6 + N_2 + (c - C_4F_8)$ ternary mixture the content of electronegative gases should be chosen to be 40% to 60% with as small a content of $(c - C_4F_8)$ gas as possible to obtain the desired properties as a gaseous dielectric for industrial application. Therefore, 60% of buffer gas was chosen in the present experimental studies and the results were compared to mixtures of SF_6 with air, CO_2, and CO as a buffer gas under otherwise the same experimental conditions. In addition, the effect of adding $(c - C_4F_8)$ gas on the impulse breakdown voltages for the same electrode arrangement was examined. These results were published in IEEE Transaction on Electrical Insulation [80].

4.2.1 SF_6 mixtures with N_2 as a buffer gas

Figure 4.17 shows the impulse breakdown voltage-pressure characteristics under positive polarity voltages for SF_6 mixtures with $60\%N_2$ as buffer gas and Figure 4.18 shows the corresponding values for the 1.27/5.2 cm coaxial cylinder gap under negative impulses.

Under positive polarity voltages the breakdown voltage-pressure curves increase nearly linearly with increasing pressure up to about 400 kPa. Above 400 kPa, saturation of the voltage-pressure curve is noted. While increasing the $(c - C_4F_8)$ content in the mixture has little effect on the breakdown voltage for pressures up to 400 kPa, a slight reduction of the breakdown voltages was noted at pressures above 450 kPa.

Under negative polarity applied voltages, the V-P curves are not smooth, although the breakdown voltage increases continuously with increasing pressure. A discontinuity appears in the curves at a pressure of 300 kPa corresponding to the field intensity on the inner electrode of about 250 kV/cm. The discontinuity is also noted under positive polarity but at a higher pressure of about 450 kPa. The influence of the replacement of a small amount of SF_6 by $c - C_4F_8$ on the breakdown voltages is similar to that obtained in a highly non-uniform field under impulse applied voltages as reported by Pai

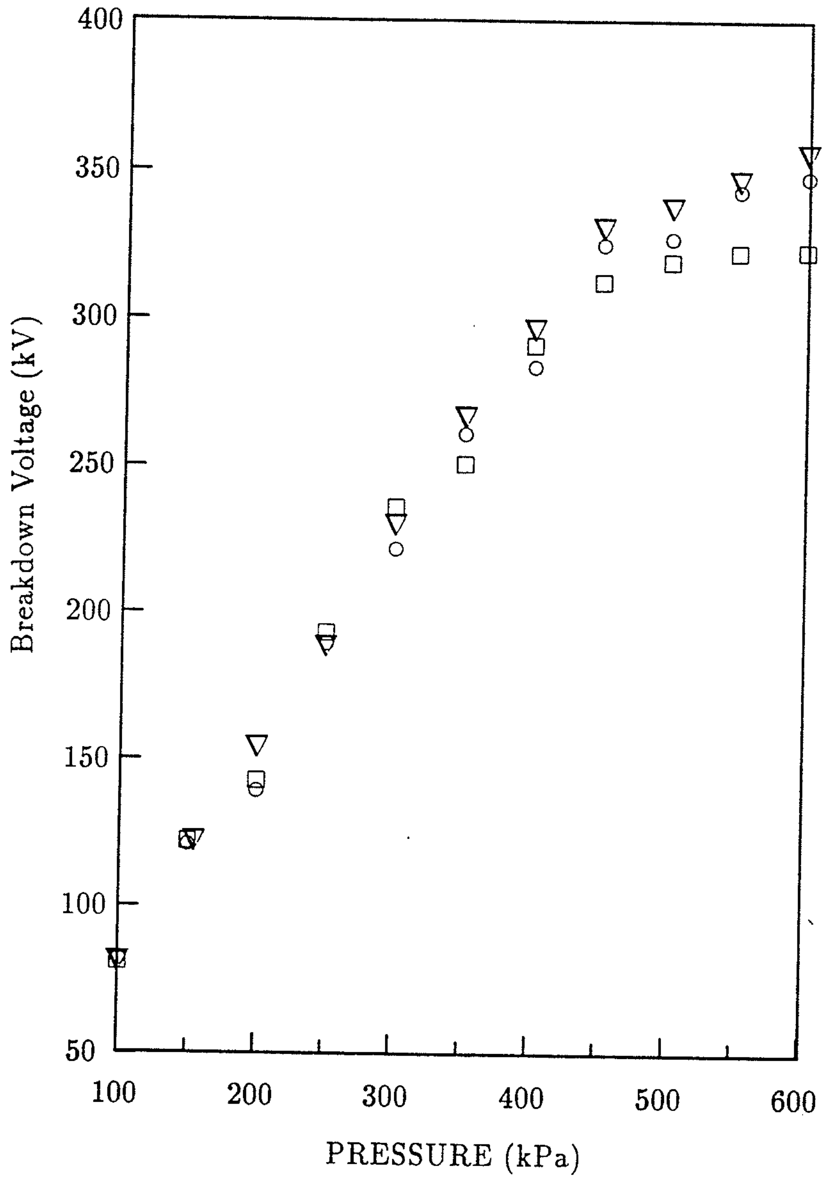

Figure 4.17: The impulse breakdown voltage *vs* total pressure in N_2 mixtures for the coaxial cylinder gap under *positive* polarity voltages: $60\%N_2+40\%SF_6$ (∇); $60\%N_2 + 39\%SF_6 + 1\%(c - C_4F_8)$ ($\bigcirc$); $60\%N_2 + 35\%SF_6 + 5\%(c - C_4F_8)$,($\square$).

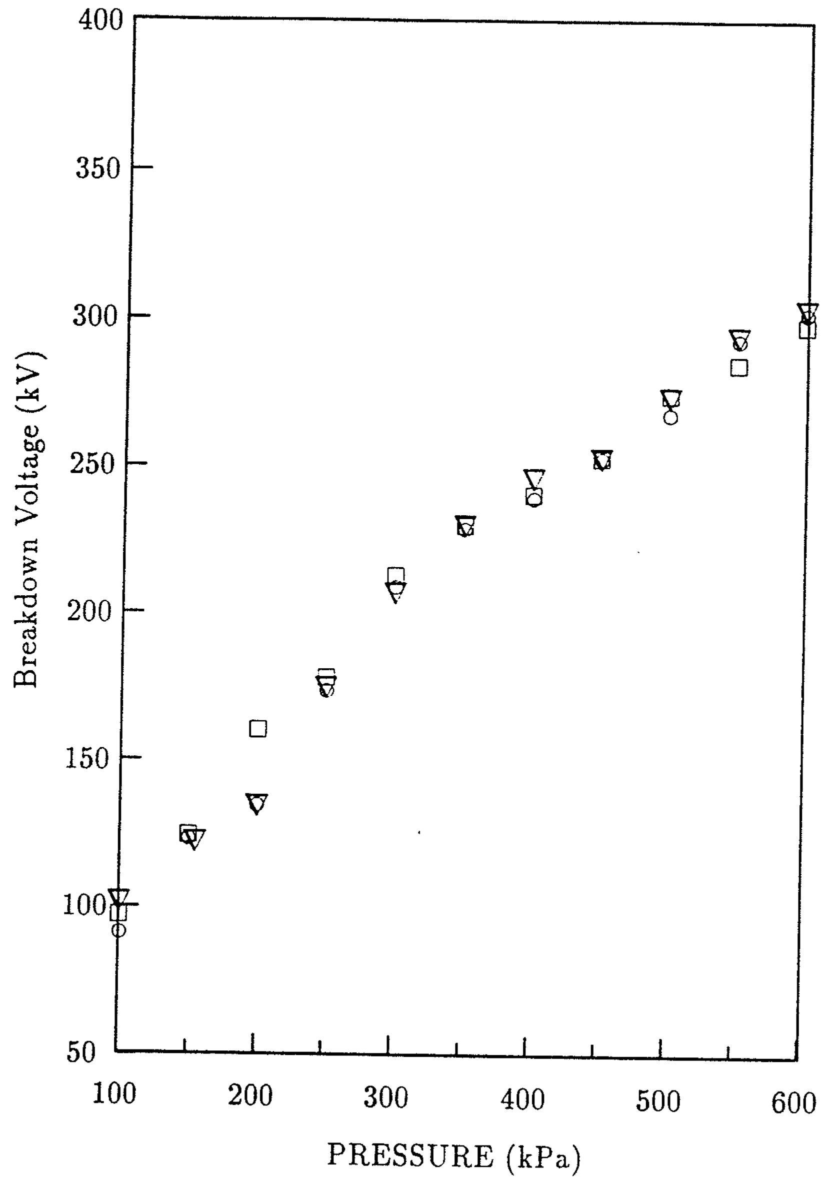

Figure 4.18: The impulse breakdown voltage *vs* total pressure in N_2 mixtures for the coaxial cylinder gap under *negative* polarity voltages: $60\%N_2 + 40\%SF_6$ (∇); $60\%N_2 + 39\%SF_6 + 1\%(c - C_4F_8)$ ($\bigcirc$); $60\%N_2 + 35\%SF_6 + 5\%(c - C_4F_8)$ ($\square$).

and Christophorou [81]. In mixtures containing $60\% N_2$ with 5%-20%-40% $(c - C_4F_8)$ and the remainder SF_6, they found that the negative 50% breakdown values for a standard impulse increased slightly with the increase of $c - C_4F_8$ fraction, but that the positive 50% breakdown values were totally unaffected.

4.2.2 SF_6 mixtures with air as a buffer gas

The impulse breakdown voltage-pressure characteristics for the 1.27/5.2 cm coaxial cylinder gap obtained in mixtures comprising 60% air with a different percentage of electronegative gases are shown in Figures 4.19 and 4.20. As can be seen from the figures, the breakdown voltage increases nearly linearly with pressure for both positive and negative polarities up to about 400 kPa. As in the case of N_2 mixtures, the content of $(c - C_4F_8)$ has a very small influence on breakdown voltages of the mixtures. For negative polarity and positive polarity at pressures below 300 kPa, the influence is barely noticable. However, the effect appears to increase as the pressure exceeds 400 kPa under positive polarity (Fig.4.19). In these mixtures the discontinuity of the V-P curve observed in N_2 mixtures is hardly noticable.

4.2.3 SF_6 mixtures with CO_2 as a buffer gas

The corresponding breakdown voltage-pressure characteristics for CO_2 mixtures with $60\%CO_2 + 39\%SF_6 + 1\%(c - C_4F_8)$, $60\%CO_2 + 35\%SF_6 + 5\%(c - C_4F_8)$, and $40\%CO_2 + 59\%SF_6 + 1\%(c - C_4F_8)$ are shown in Figures

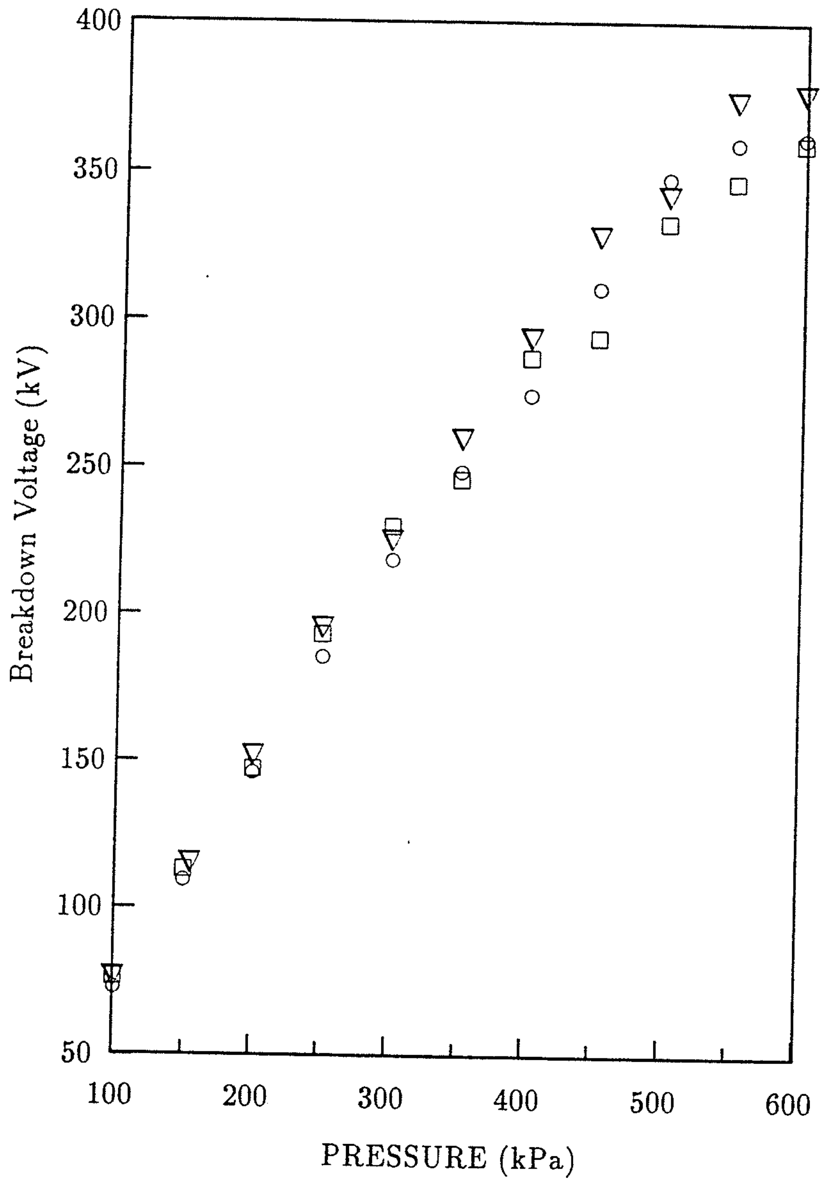

Figure 4.19: The impulse breakdown voltage *vs* total pressure in air mixtures for the coaxial cylinder gap under *positive* polarity voltages: $60\% air + 40\% SF_6$ (∇); $60\% air + 39\% SF_6 + 1\%(c - C_4F_8)$ ($\bigcirc$); $60\% air + 35\% SF_6 + 5\%(c - C_4F_8)$ ($\square$).

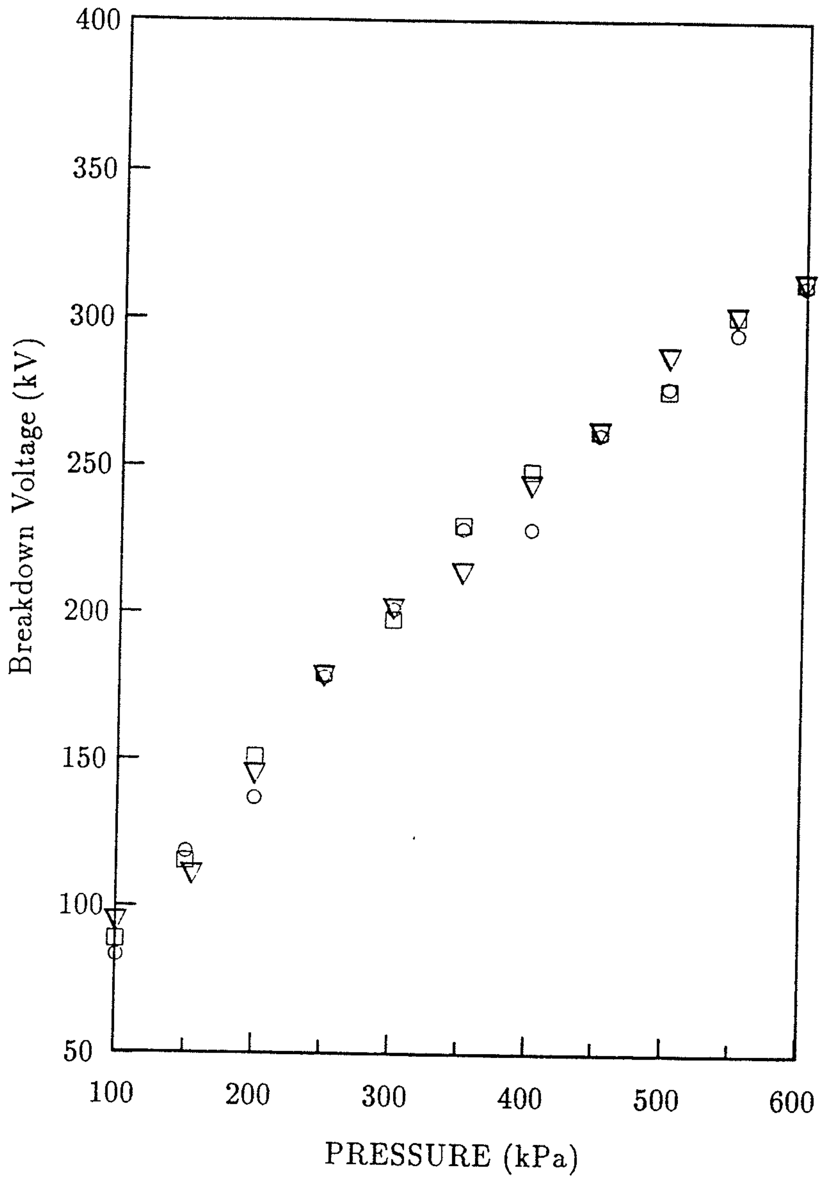

Figure 4.20: The impulse breakdown voltage *vs* total pressure in air mixtures for the coaxial cylinder gap under *negative* polarity voltages: $60\%air + 40\%SF_6$ (∇); $60\%air + 39\%SF_6 + 1\%(c - C_4F_8)$ ($\bigcirc$); $60\%air + 35\%SF_6 + 5\%(c - C_4F_8)$ ($\square$).

4.21 and 4.22 respectively for the 1.27/5.2 cm coaxial cylinder gap. In all cases, the breakdown voltage increases linearly with pressure over the entire pressure range studied. The change of $(c - C_4F_8)$ from 1% to 5% by volume in the mixture with the same percentage of electronegative gases did not improve the breakdown strength significantly but the increase of the total amount of electronegative gases from 40% to 60% increased the breakdown voltages under both positive and negative impulse applied voltages.

4.2.4 SF_6 mixtures with CO as a buffer gas

The SF_6/CO/$(c - C_4F_8)$ mixtures were investigated using the present electrode configuration since several reports [64,67,69] indicated that these mixtures were also a promising insulation candidate for practical application as far as the dielectric strength was concerned. The results are shown in Figures 4.23 and 4.24. The curves followed the same trend as those for other mixtures studied. However, in this case the saturation value is approached more gradually. Again, increasing the total percentage of electronegative gases increases the breakdown strength, but replacing a portion of SF_6 by $(c - C_4F_8)$ has no significant effect on the breakdown strength of the mixture.

4.2.5 Comparison of the breakdown-pressure characteristics for the mixtures

Figures 4.25 and 4.26 compare the breakdown voltage-pressure characteristics for SF_6 mixtures with 60% buffer gas + 1% $(c - C_4F_8)$ with those for

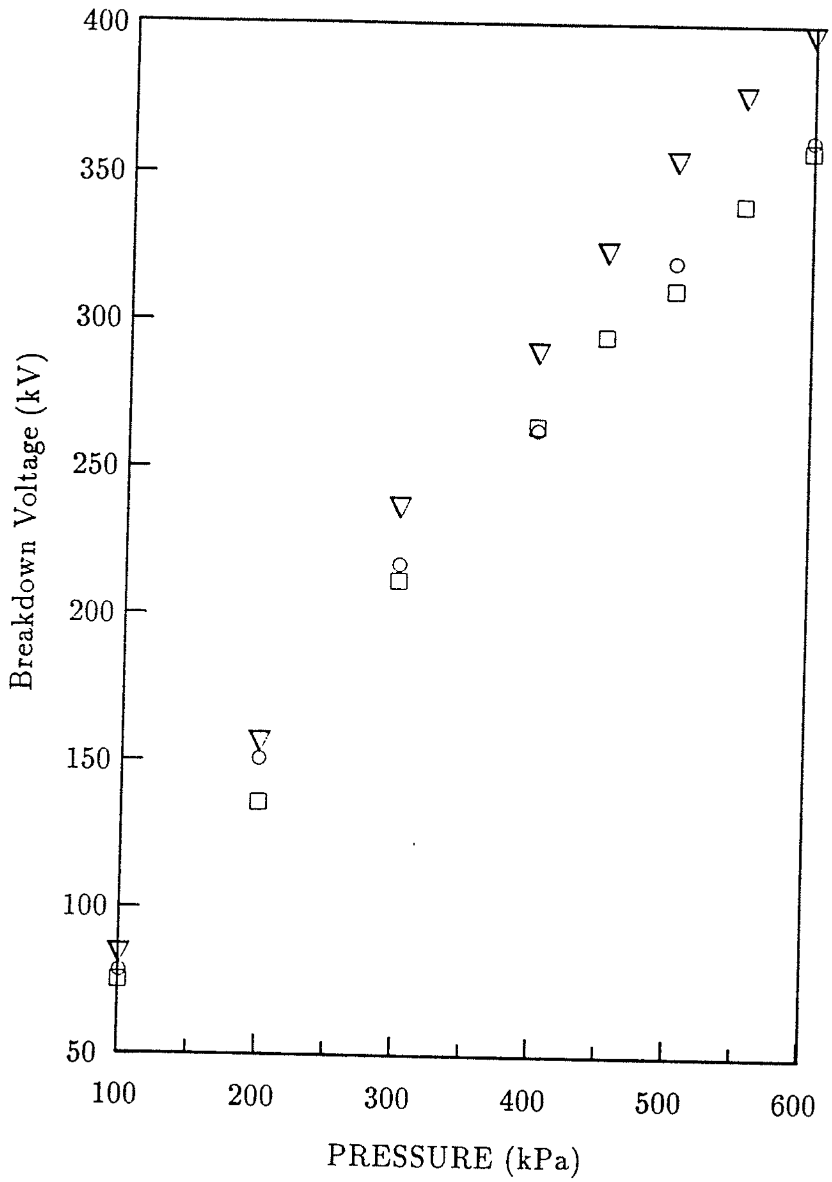

Figure 4.21: The impulse breakdown voltage *vs* total pressure in CO_2 mixtures for the coaxial cylinder gap under *positive* polarity voltages: $40\% CO_2 + 59\% SF_6 + 1\%(c - C_4F_8)$ (∇); $60\% CO_2 + 39\% SF_6 + 1\%(c - C_4F_8)$ ($\bigcirc$); $60\% CO_2 + 35\% SF_6 + 5\%(c - C_4F_8)$ ($\square$).

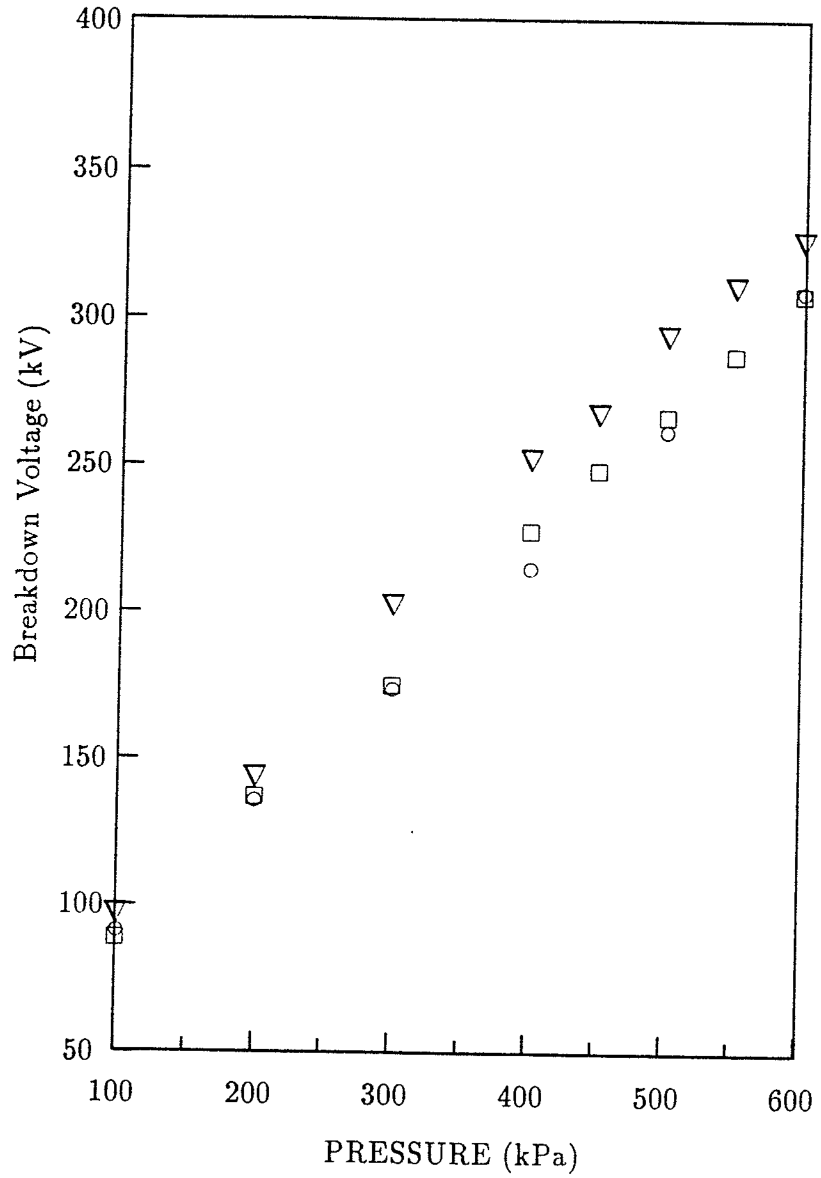

Figure 4.22: The impulse breakdown voltage *vs* total pressure in CO_2 mixtures for the coaxial cylinder gap under *negetive* polarity voltages: $40\%CO_2 + 59\%SF_6 + 1\%(c - C_4F_8)$ (∇); $60\%CO_2 + 39\%SF_6 + 1\%(c - C_4F_8)$ ($\bigcirc$); $60\%CO_2 + 35\%SF_6 + 5\%(c - C_4F_8)$ ($\square$).

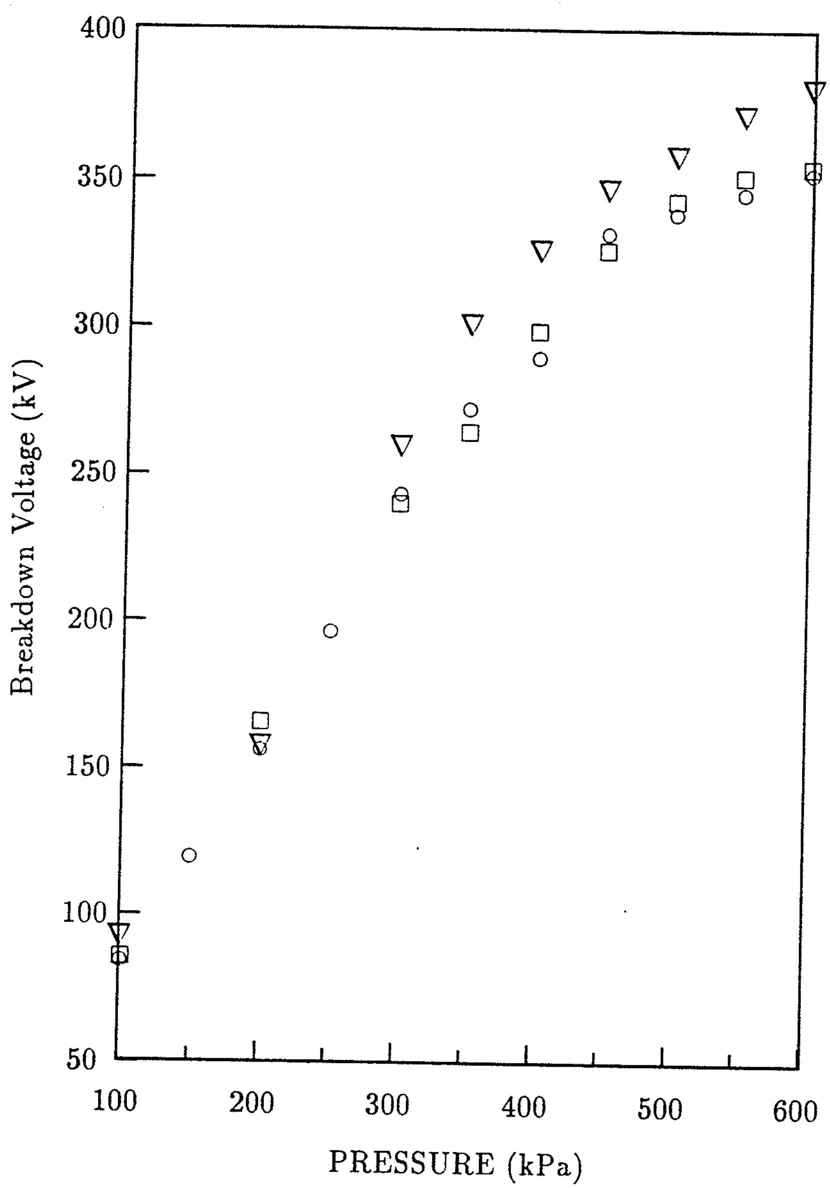

Figure 4.23: The impulse breakdown voltage *vs* total pressure in CO mixtures for the coaxial cylinder gap under *positive* polarity voltages: $40\%CO + 59\%SF_6 + 1\%(c - C_4F_8)$ (∇); $60\%CO + 39\%SF_6 + 1\%(c - C_4F_8)$ ($\bigcirc$); $60\%CO + 35\%SF_6 + 5\%(c - C_4F_8)$ ($\square$).

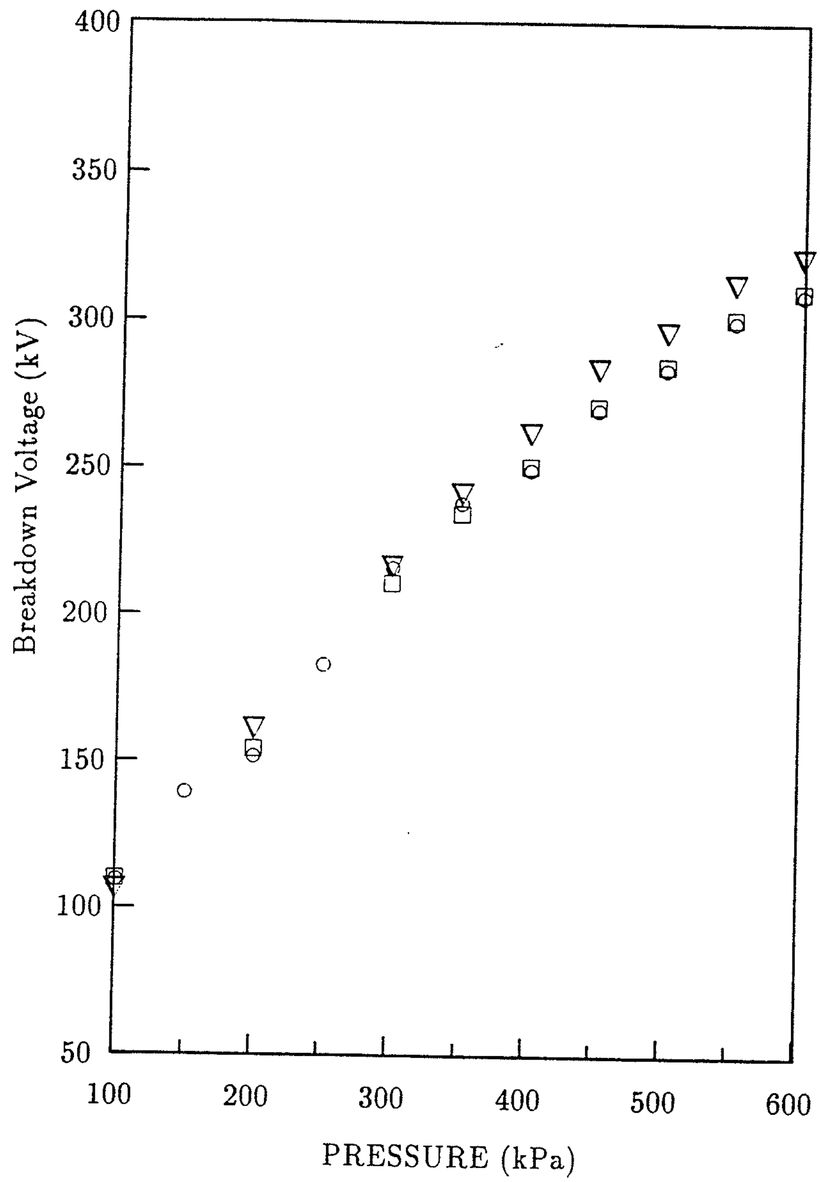

Figure 4.24: The impulse breakdown voltage *vs* total pressure in CO mixtures for the coaxial cylinder gap under *negative* polarity voltages: $40\%CO + 59\%SF_6 + 1\%(c - C_4F_8)$ (∇); $60\%CO + 39\%SF_6 + 1\%(c - C_4F_8)$ ($\bigcirc$); $60\%CO + 35\%SF_6 + 5\%(c - C_4F_8)$ ($\square$).

SF_6 under positive and negative polarities respectively. As is seen from the figures, the breakdown voltages for the CO mixture are highest for both polarities at pressures up to about 500 kPa. On the other hand the breakdown voltages for air mixture and N_2 mixture are nearly equal under negative polarity. The spread between breakdown values for different mixtures diminishes as the pressure increases, becoming insignificant at a pressure of 600 kPa.

The comparison of the breakdown voltage-pressure characteristics for SF_6 mixtures with 60% buffer gas + 5%$(c - C_4F_8)$ with those for SF_6 are shown in Figures 4.27 and 4.28. No significantly different trend from that found in SF_6 mixtures with 60% buffer gas + 1% $(c - C_4F_8)$ is observed.

Although the breakdown voltages for CO mixture are highest in the present experimental condition, from a practical point of view, N_2 or air mixtures may still be preferred since their corresponding strength are only a few percent lower than that of a mixture containing CO as a buffer gas.

4.3 Volt-time characteristics

Although impulse breakdown voltage-time characteristics are of fundamental importance to insulation coordination, the information on these characteristics of SF_6 mixtures is rather scanty, particularly for short time lags below 1 μs. Moreover, it was found that in a gas insulated substation (GIS) travelling waves with a very fast rise time of only a few ns can be generated

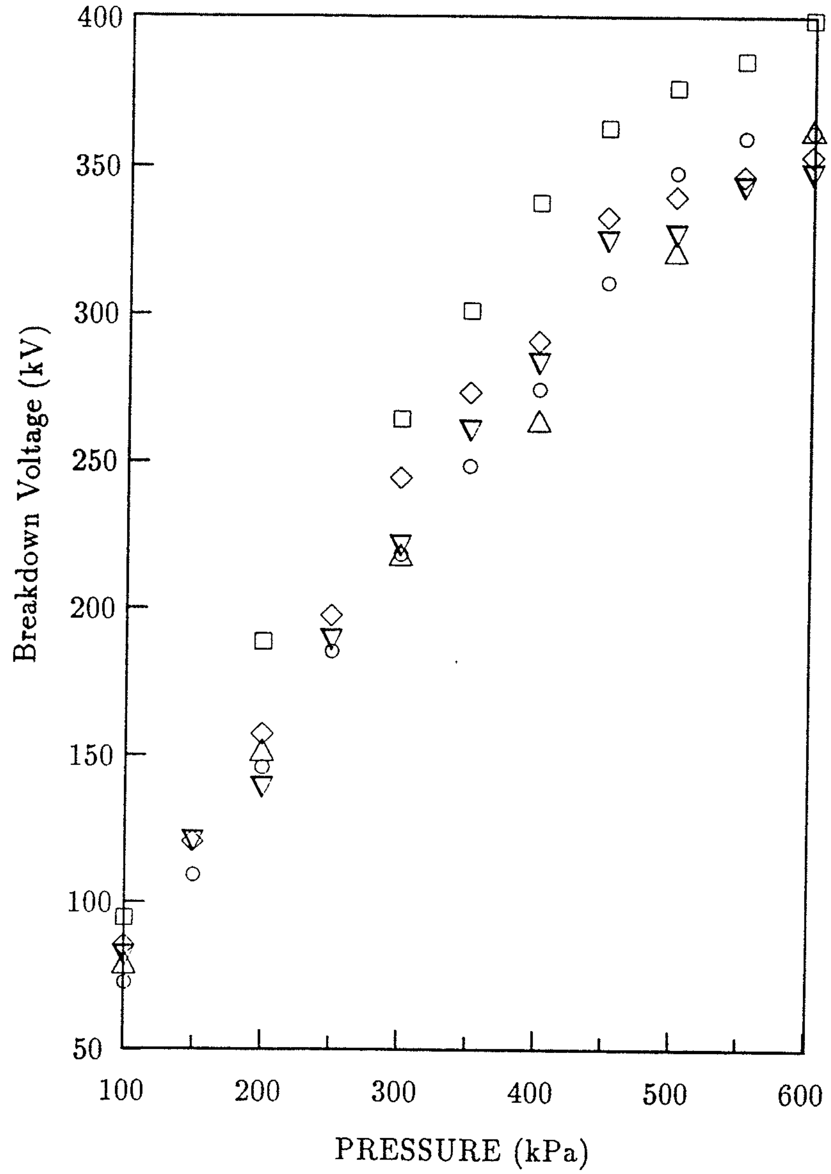

Figure 4.25: A comparison of the impulse breakdown voltage-pressure characteristics for mixtures containing $1\%(c - C_4F_8) + 39\%SF_6 + 60\%$ of buffer gas with that of pure SF_6, positive polarity: (□) pure SF_6, (○) 60%air, (▽) 60%N_2, (◇) 60%CO, (△) 60%CO_2.

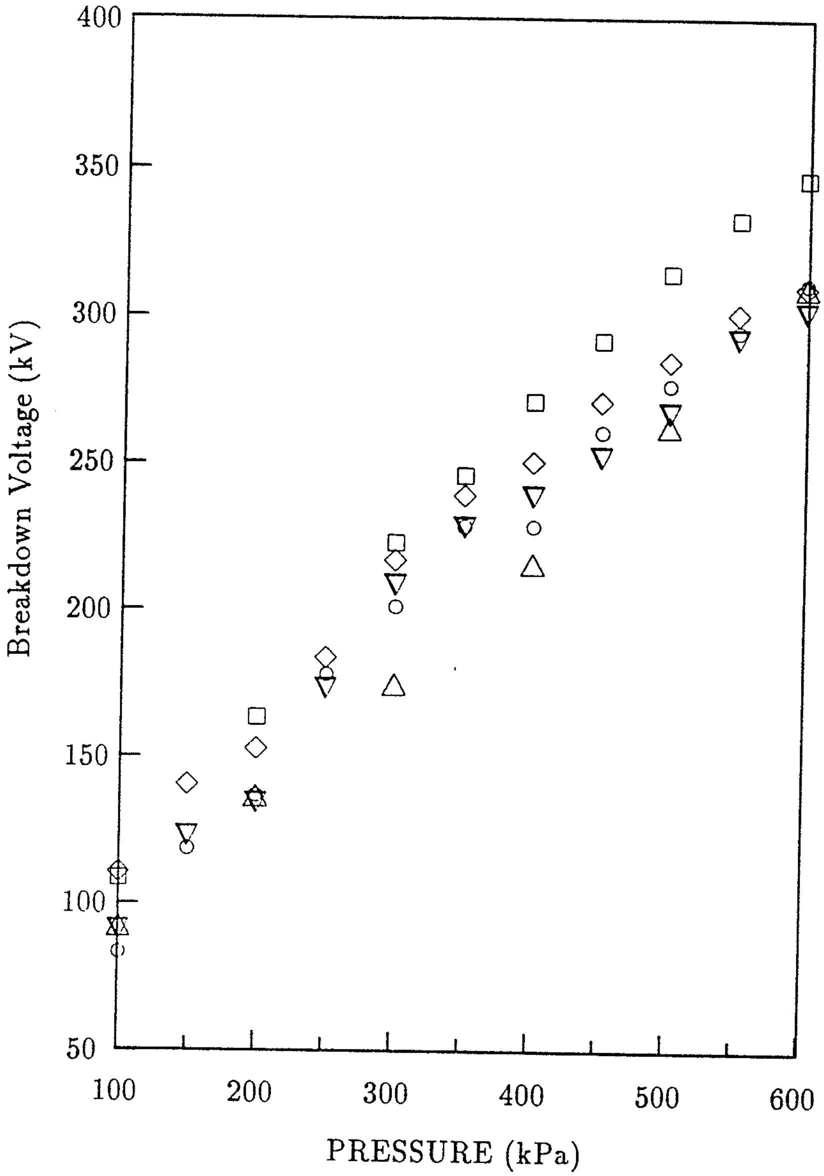

Figure 4.26: A comparison of the impulse breakdown voltage-pressure characteristics for mixtures containing $1\%(c - C_4F_8) + 39\%SF_6 + 60\%$ of buffer gas with that of pure SF_6, negative polarity: (□) pure SF_6, (○) 60%air, (▽) $60\%N_2$, (◇) 60%CO, (△) $60\%CO_2$.

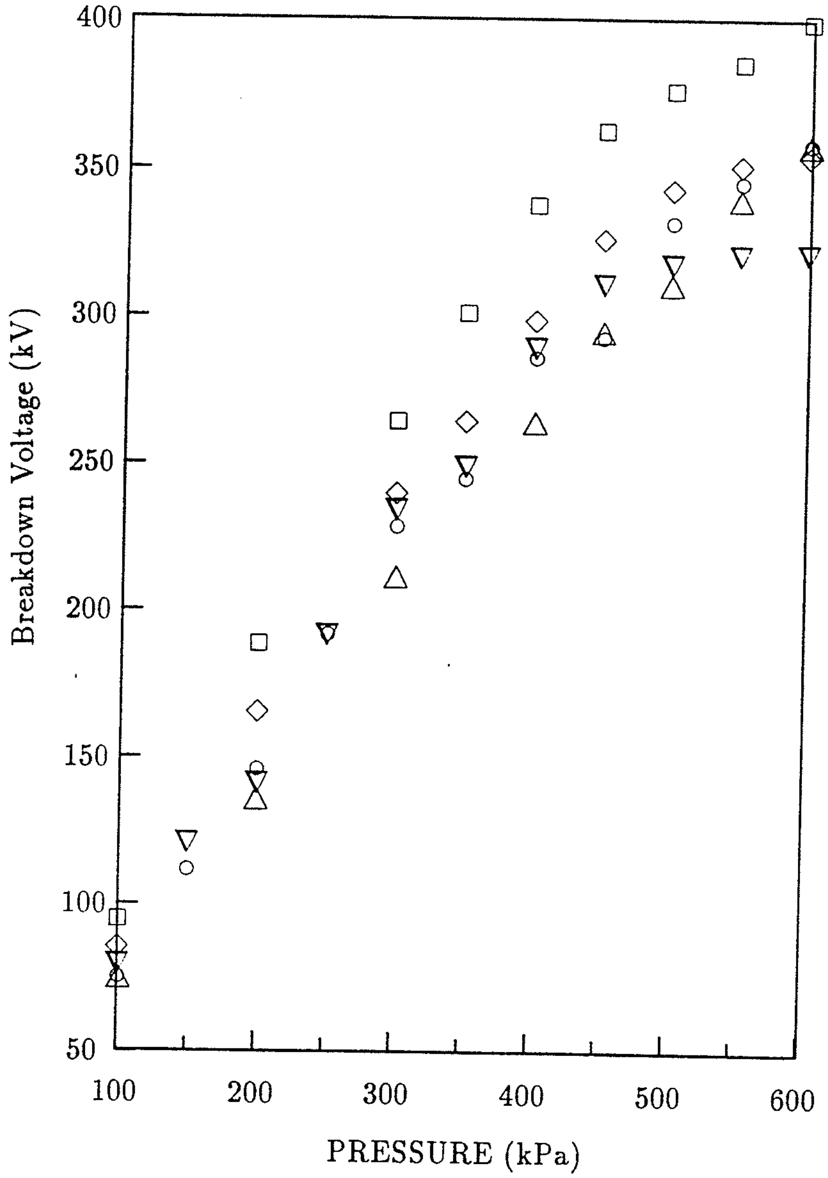

Figure 4.27: A comparison of the impulse breakdown voltage-pressure characteristics for mixtures containing 5%($c-C_4F_8$) + 35%SF_6 + 60% of buffer gas with that of pure SF_6, positive polarity: (□) pure SF_6, (○) 60%air, (▽) 60%N_2, (◇) 60%CO, (△) 60%CO_2.

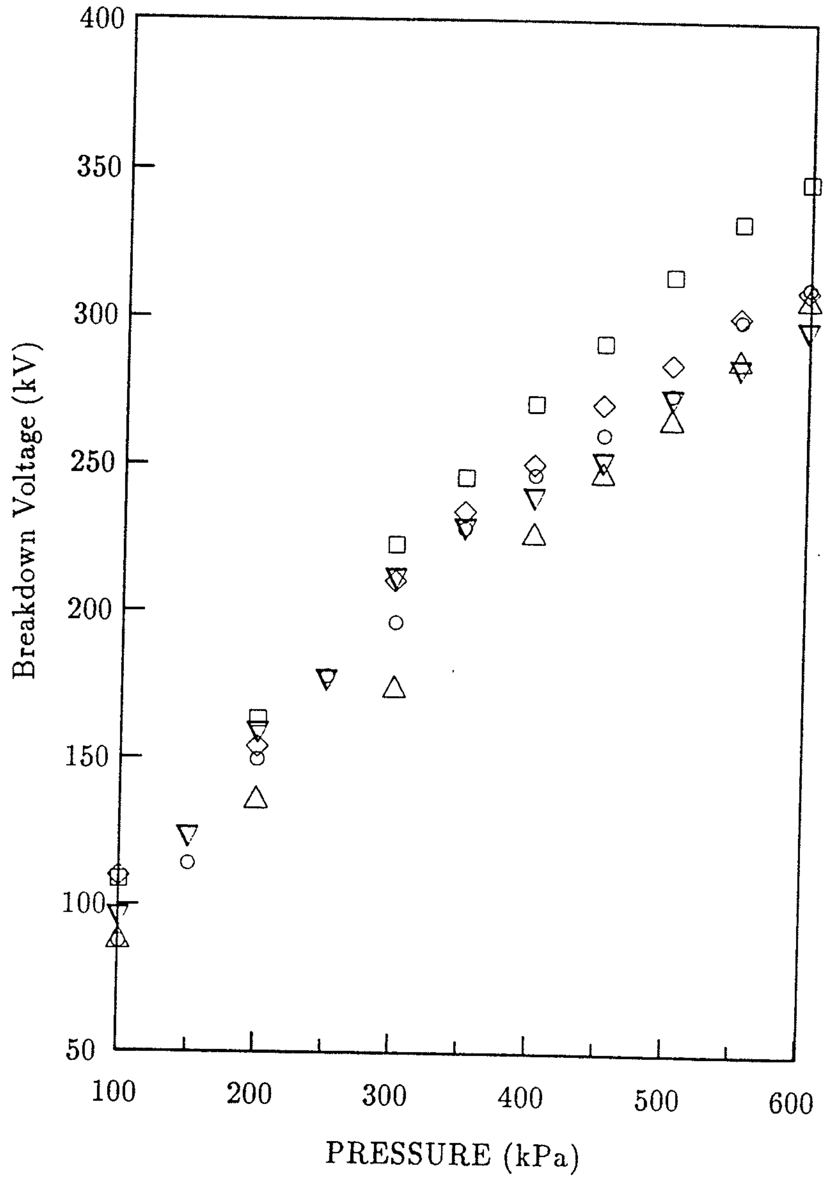

Figure 4.28: A comparison of the impulse breakdown voltage-pressure characteristics for mixtures containing 5%$(c - C_4F_8)$ + 35%SF_6 + 60% of buffer gas with that of pure SF_6, negative polarity: (□) pure SF_6, (○) 60%air, (▽) 60%N_2, (◇) 60%CO, (△) 60%CO_2.

by disconnector operation [84]. Hence, attention has been drawn to the investigation of impulse breakdown voltage-time characteristics of SF_6 and its mixtures for steep-fronted impulse voltages in divergent as well as in quasi-uniform field gaps. The main intent of this investigation was therefore to obtain experimental data on this aspect.

4.3.1 Volt-time characteristics of a coaxial cylinder gap in air and air mixture with 1% SF_6

Many researchers have studied the dielectric strength behavior of air mixtures with a small amount of SF_6 as an additive. Kurimoto [53] found that the addition of a small percentage (1%) of SF_6 to dry air produced a considerable increase in the breakdown value above that of pure SF_6 over a wide pressure range. Qiu and Kuffel [87] reported an impulse strength for a 30 mm point-sphere gas in a 1% SF_6/air mixture higher than that of pure SF_6 and an ac strength nearly the same as that for pure SF_6. Recently, Okabe and Kuffel [71] studied volt-time characteristics of a rod-sphere gap in 99% dry air + 1%SF_6 mixture under standard impulse voltages. They found that there is a pronounced decrease in the breakdown voltage for a steep rising impulse notably under negative polarity voltages. Naturally, it is desirable to know the volt-time characteristics of this mixture in coaxial cylinder gaps since this electrode arrangement is often found in practical apparatus. This work led to a paper published in IEEE Transaction on Electrical Insulation [85].

Figures 4.29 and 4.30 show the positive and negative volt-time characteristics respectively for the coaxial-cylinder gap in dry air and in $1\% SF_6$/air mixture at a total pressure of 500 kPa. As can be seen from Figure 4.29, the 50% breakdown values for dry air under positive polarity and the given pressure are approximately equal for all impulse wave shapes used. However, in $1\% SF_6$/air mixture the steep-fronted impulse caused a 50% value about 10% lower than the standard impulse and switching surge voltages. For standard impulses and shorter fronted surges the breakdown values increase with increasing overvoltage, whereas the breakdown values remain nearly constant with overvolted switching surge voltages. It is noteworthy that in both types of gases the characteristics for standard impulse and the steep-fronted surges do not correspond. The characteristics obtained under the steep-fronted impulses are significantly lower than those obtained under standard impulses in the time interval from 0.3 to 0.6 μs.

Under negative polarity, the 50% values for the standard switching surge voltages are considerablely lower than those obtained for other wave shapes studied.

It is interesting to note that under standard impulses, the breakdown values for dry air decrease with increasing overvoltage for steeply rising voltages. The effect is observed under both polarities. This is also noted in a $1\% SF_6$/air mixture under negative polarity.

In general, the negative breakdown values are less scattered than the corresponding positive ones. The lowest 50% breakdown values for dry air as well

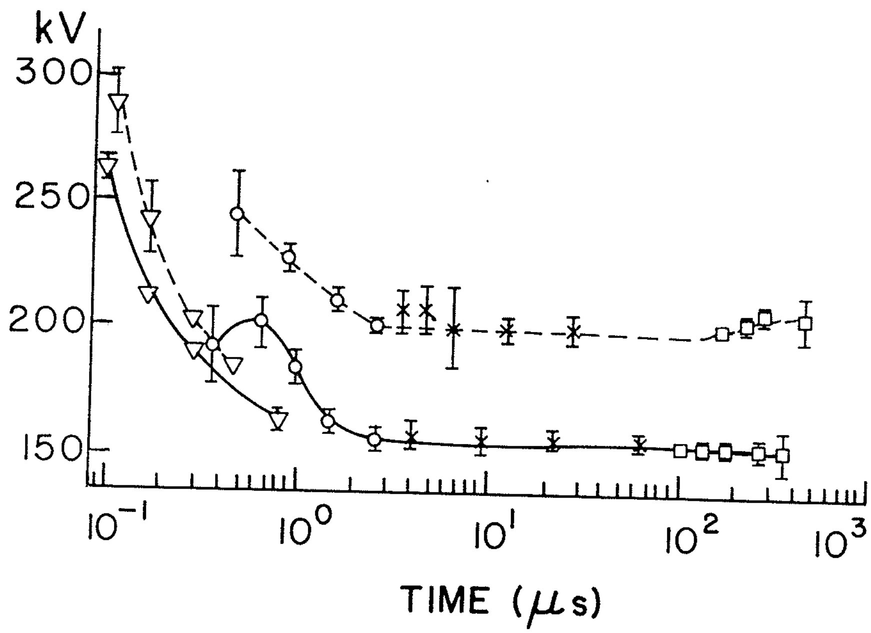

Figure 4.29: Volt-time characteristics of coaxial-cylinder gap in dry air and air/1%SF_6 mixture; pressure 500 kPa; positive polarity; (∇) 0.2/60 μs; (○) standard lightning impulse; (x) 15/1200 μs; (□) 275/2500 μs; — dry air; - - - air/1%SF_6.

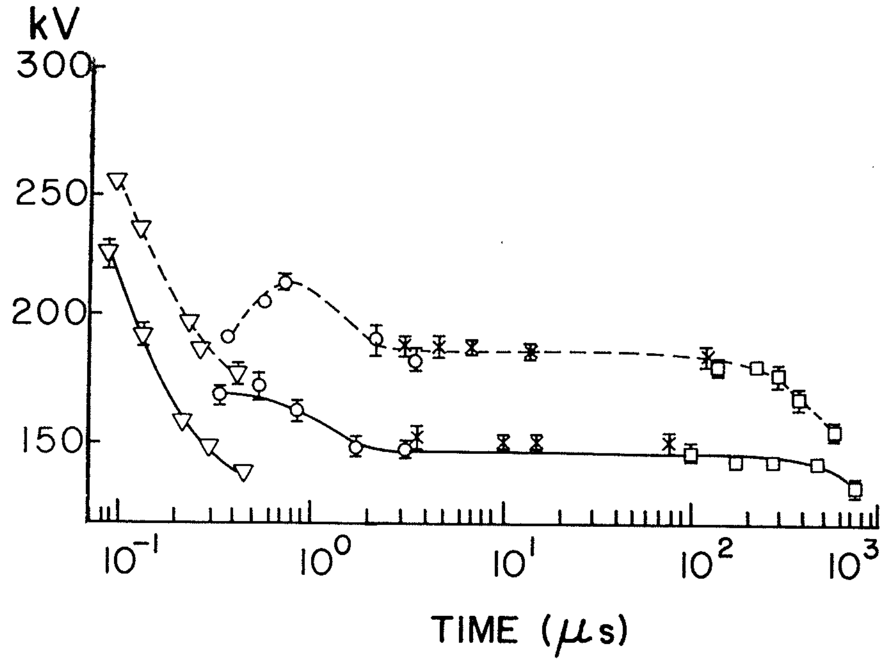

Figure 4.30: Volt-time characteristics of coaxial-cylinder gap in dry air and air/1%SF_6 mixture; pressure 500 kPa; negative polarity; (∇) 0.2/60 μs; (○) standard lightning impulse; (x) 15/1200 μs; (□) 275/2500 μs; — dry air; - - - air/1%SF_6.

as for the $1\% SF_6$/air mixture are obtained under negative standard switching surge voltages. In this case, the 50% breakdown value for a $1\% SF_6$/air mixture is only 10% higher than that for dry air. This indicates that the addition of $1\% SF_6$ to dry air causes little improvement in the dielectric strength under the present experimental conditions.

The volt-time curves recorded for a pressure of 300 kPa under both positive and negative polarity surges are presented in Figures 4.31 and 4.32 respectively. Although the curves follow a similar trend as those for 500 kPa, no reduction in breakdown voltages is observed under steep-fronted surges. The lowest 50% breakdown values for dry air occurs under a negative standard switching surge voltage (Fig.4.32). The breakdown strength of a $1\% SF_6$/air mixture remained approximately 25% higher than that for dry air for all impulse wave shapes except the very steep-fronted impulse where the difference is smaller. The latter impulse wave resulted in significantly lower breakdown values for both dry air and the air/SF_6 mixture.

The volt-time characteristics recorded at a pressure of 100 kPa under positive and negative polarity impulse voltages for dry air and $1\% SF_6$/air mixture are shown in Figures 4.33 and 4.34 respectively. Again, the curves follow the same trend as those for higher pressures. At this pressure, however, the addition of $1\% SF_6$ had little effect on the insulation strength of the dry air. Also the effect of steeply rising impulses upon the breakdown strength is less pronounced than the higher pressures.

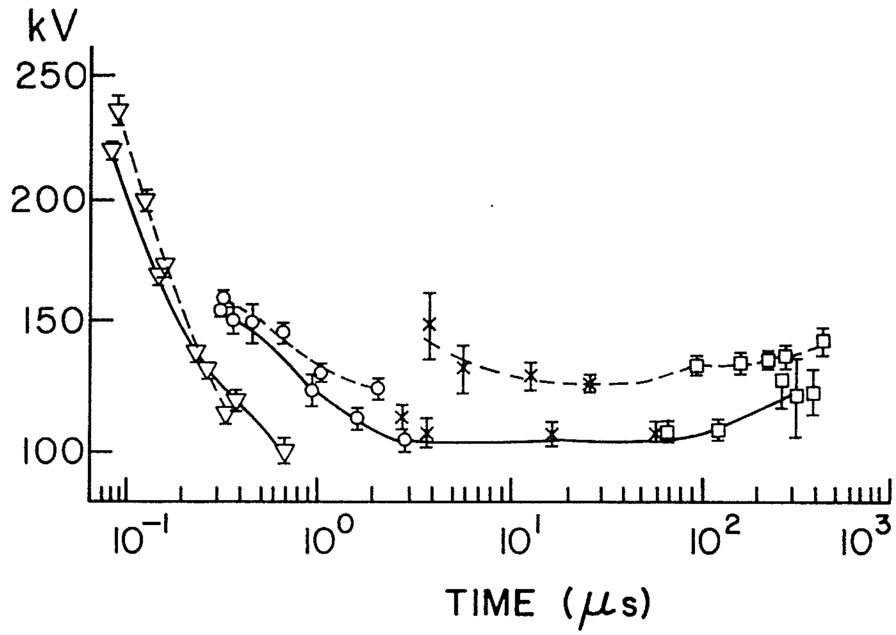

Figure 4.31: Volt-time characteristics of coaxial-cylinder gap in dry air and air/1%SF_6 mixture; pressure 300 kPa; positive polarity; (∇) 0.2/60 μs; (○) standard lightning impulse; (x) 15/1200 μs; (□) 275/2500 μs; — dry air; - - - air/1%SF_6.

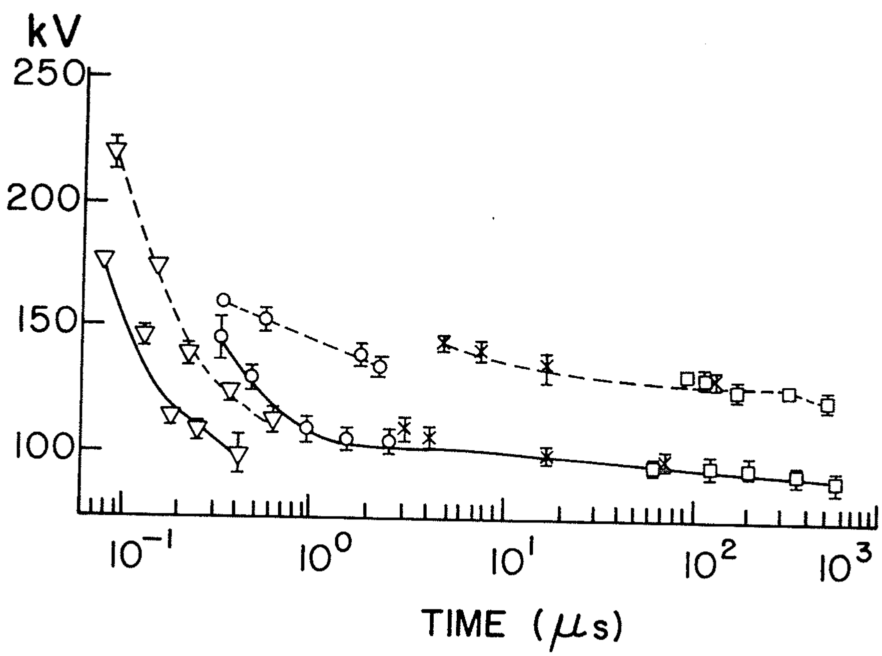

Figure 4.32: Volt-time characteristics of coaxial-cylinder gap in dry air and air/1%SF_6 mixture; pressure 300 kPa; negative polarity; (∇) 0.2/60 μs; (o) standard lightning impulse; (x) 15/1200 μs; (□) 275/2500 μs; — dry air; - - - air/1%SF_6.

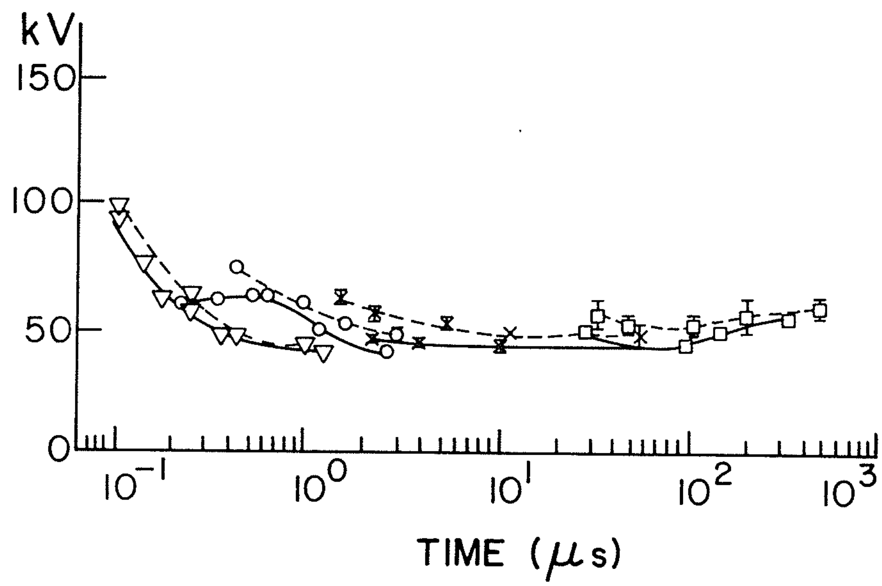

Figure 4.33: Volt-time characteristics of coaxial-cylinder gap in dry air and air/1%SF_6 mixture; pressure 100 kPa; positive polarity; (∇) 0.2/60 μs; (o) standard lightning impulse; (x) 15/1200 μs; (□) 275/2500 μs; — dry air; - - - air/1%SF_6.

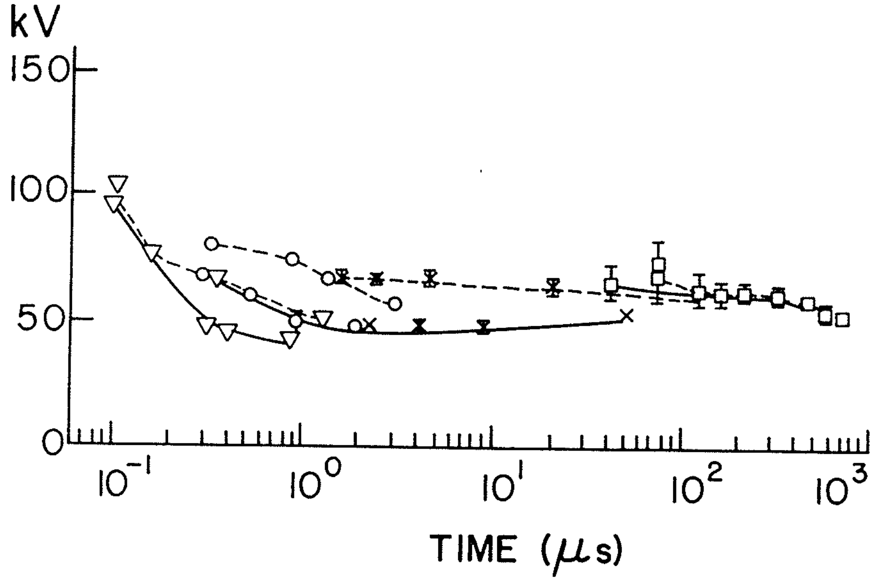

Figure 4.34: Volt-time characteristics of coaxial-cylinder gap in dry air and air/1%SF_6 mixture; pressure 100 kPa; negative polarity; (∇) 0.2/60 μs; (○) standard lightning impulse; (x) 15/1200 μs; (□) 275/2500 μs; — dry air; - - - air/1%SF_6.

4.3.2 Volt-time characteristics of a coaxial cylinder gap in SF_6 and SF_6 mixtures with N_2 or air as buffer gases

As mentioned in section 4.2.5, no particular benefit can be obtained from using CO or CO_2 as a buffer gas in a coaxial-cylinder electrode configuration. Therefore, the steep-fronted impulse measurements were focussed on SF_6 and its mixtures with N_2 or air as buffer gas. The results have been presented at an international sysposium on gaseous dielectrcs [86].

Volt-time characteristics for SF_6 under steep-fronted impulse applied voltages

The volt-time characteristics for pure SF_6 under positive and negative polarity steep-fronted impulses are shown in Figures 4.35 and 4.36 respectively. Under positive polarity, at pressures of 100 and 200 kPa, the breakdown voltage increases with decreasing time to breakdown as expected. However, at a pressure of 300 kPa anomalous behaviour was observed. The breakdown voltages increase with increase in breakdown time to about 0.3 μs and then decrease with further increase in breakdown time.

Under negative polarity the breakdown voltage decreases continuously with increase in breakdown time and the slope is generally steeper than that under positive polarity. Hence, while the negative breakdown voltages are lower than the corresponding positive ones under longer-fronted impulses, for

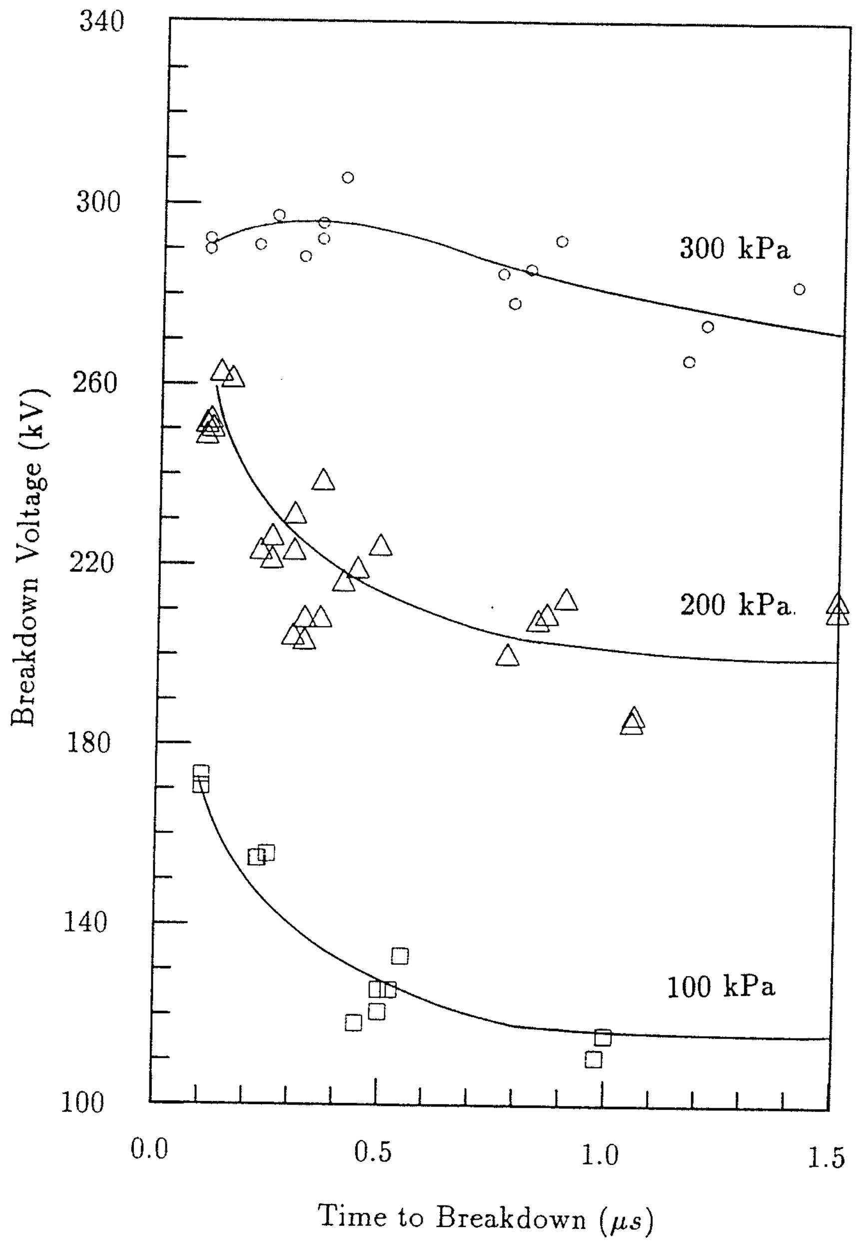

Figure 4.35: Positive impulse breakdown voltage-time characteristics for pure SF_6 in a 1.27/5.2 cm coaxial-cylinder gap: (○) 300 kPa, (△) 200 kPa, (□) 100 kPa.

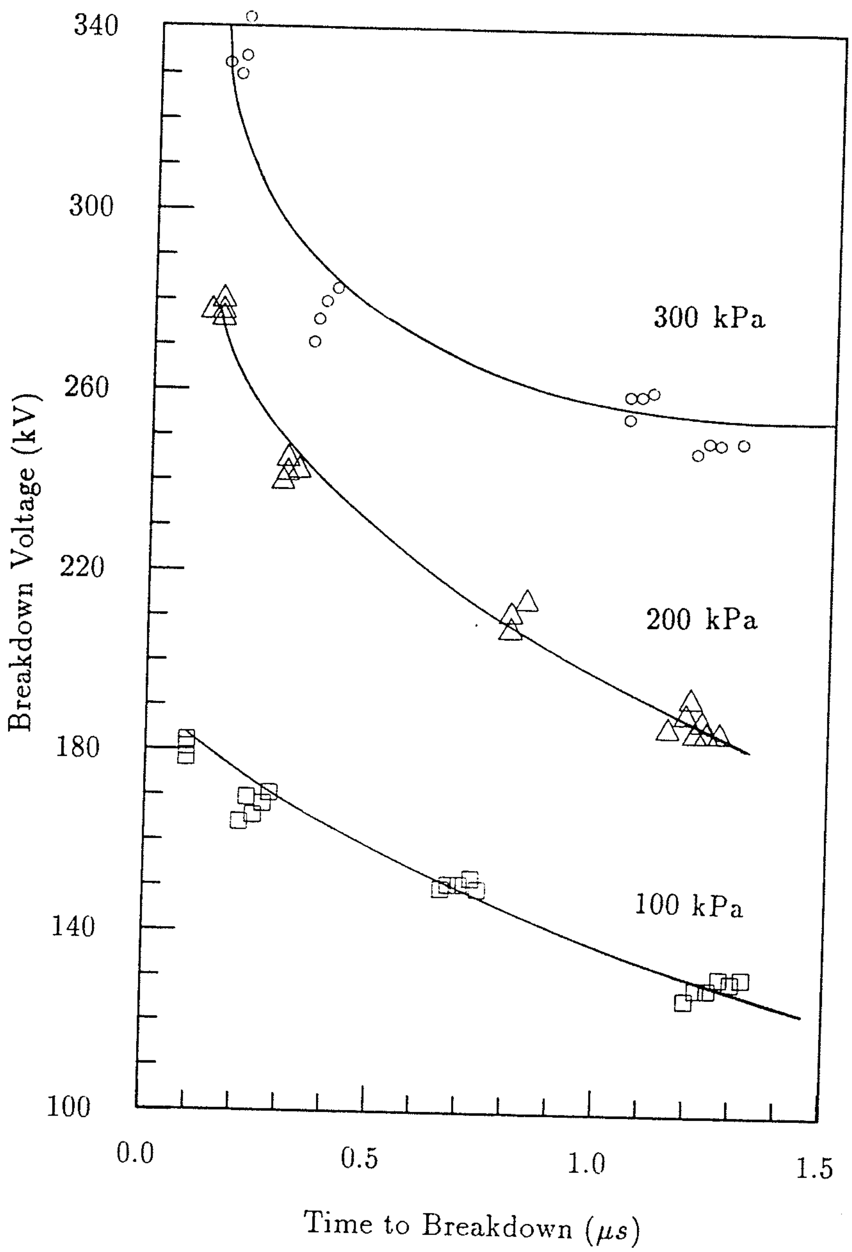

Figure 4.36: Negative impulse breakdown voltage-time characteristics for pure SF_6 in a 1.27/5.2 cm coaxial-cylinder gap: (○) 300 kPa, (△) 200 kPa, (□) 100 kPa.

shorter times to breakdown the negative breakdown values become higher. The scatter of the data is generally smaller under negative polarity than under a positive one.

Volt-time characteristics for SF_6 mixtures with N_2 as a buffer gas under steep-fronted impulse applied voltages

Figure 4.37 shows the breakdown voltage-time characteristics for gas mixtures containing 60% electronegative gases including SF_6 and $c-C_4F_8$ and 40% N_2 under positive impulse voltages. The corresponding characteristics for negative values are given in Figure 4.38.

As can be seen from Figure 4.37, the breakdown voltages under positive polarity at the shorter breakdown time do not rise sharply and the minimum breakdown values remain nearly constant down to 0.3 μs at 300 kPa. It is also seen that the replacement of 1% SF_6 by $c-C_4F_8$ gas did not affect the breakdown characteristics notably in this time range, as was found for 50% breakdown voltages for standard impulses described in section 4.2.1. However, the 1% ($c-C_4F_8$) additive seems to improve the breakdown strength for the shorter chopped impulse voltages. At a pressure of 200 kPa the results were similar to those at 300 kPa, while for 100 kPa the breakdown voltage rises gradually at shorter times to breakdown. Under negative polarity, the breakdown voltages rise at shorter times for the entire range studied and the scatter was smaller than the corresponding positive impulse voltages.

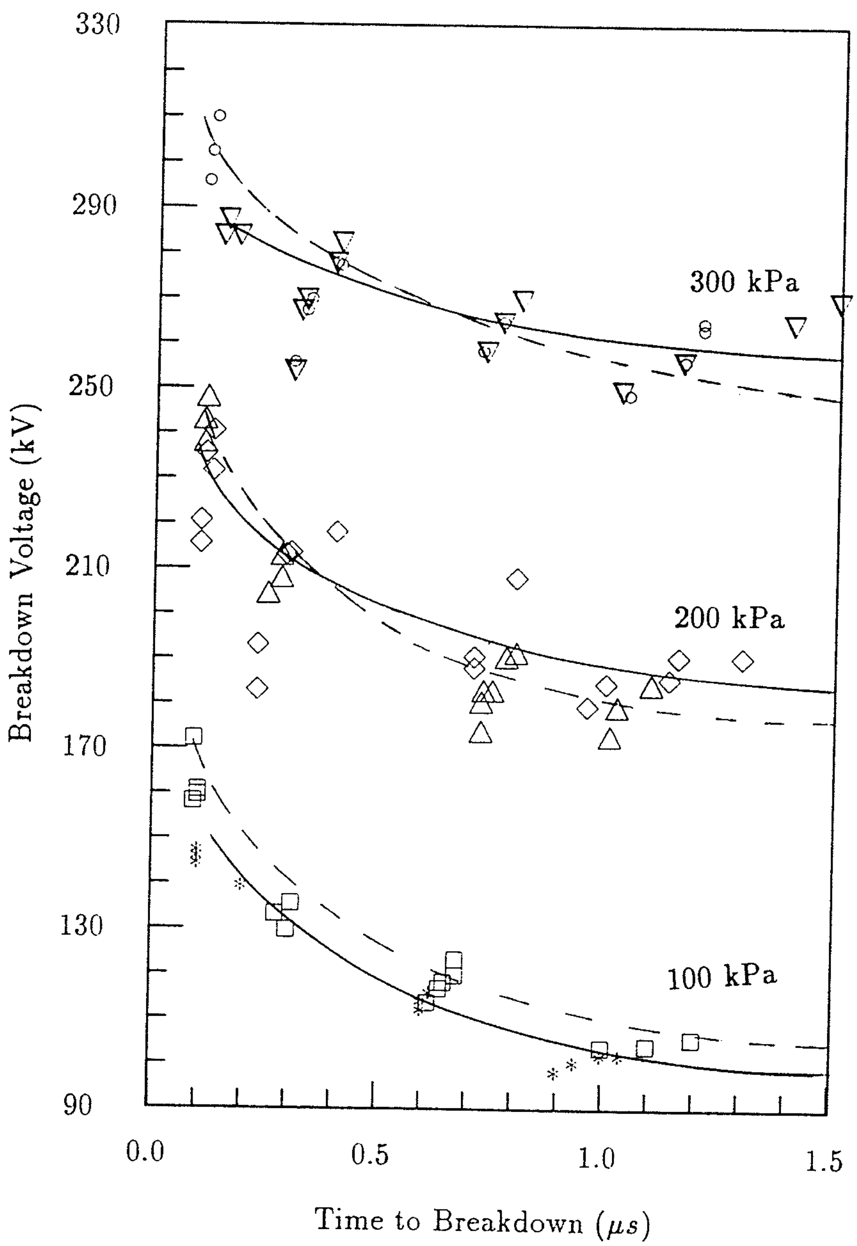

Figure 4.37: Positive impulse breakdown voltage-time characteristics for SF_6 mixtures in a 1.27/5.2 cm coaxial-cylinder gap: (1) (○, △, □) 59%SF_6 + 40%N_2 + 1%($c - C_4F_8$ (2) (▽, ◇, *) 60%SF_6 + 40%N_2, (○, ▽) 300 kPa, (△, ◇) 200 kPa, (□, *) 100 kPa.

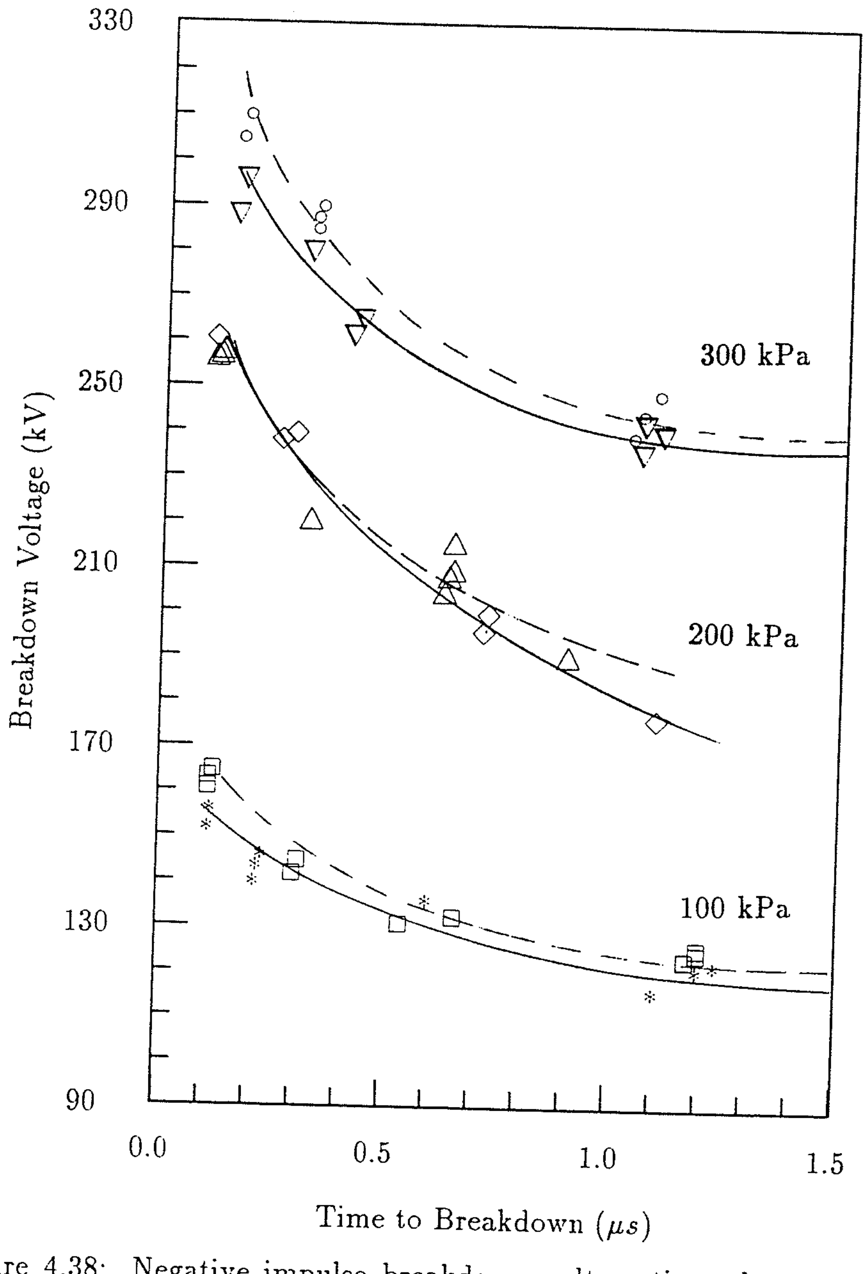

Figure 4.38: Negative impulse breakdown voltage-time characteristics for SF_6 mixtures in a 1.27/5.2 cm coaxial-cylinder gap: (1) (○, △, □) 59%SF_6 + 40%N_2 + 1%($c - C_4F_8$ (2) (▽, ◇, *) 60%SF_6 + 40%N_2, (○, ▽) 300 kPa, (△, ◇) 200 kPa, (□, *) 100 kPa.

For mixtures containing $40\%SF_6 + 60\%N_2$ and $39\%SF_6 + 1\%(c-C_4F_8)$ $+ 60\%N_2$, the measured results followed a similar trend (Figures 4.39 and 4.40.) with the breakdown values being correspondingly lower due to the smaller percentage of electronegative gas present.

Volt-time characteristics for SF_6 mixtures with air as a buffer gas under steep-fronted impulse applied voltages

The volt-time characteristics for air mixtures under both positive and negative polarities are shown in Figures 4.41 and 4.42. Under negative impulse applied voltages, the curves show the same trend as N_2 mixtures as discussed in the previous section. However, under positive polarity the volt-time characteristics increased steeply for the shorter time to breakdown with the sharpest increase noted for a pressure of 300 kPa. There was no anomalous behaviour noted in this mixture as observed in the mixture with low SF_6 content mentioned in section 4.3.1.

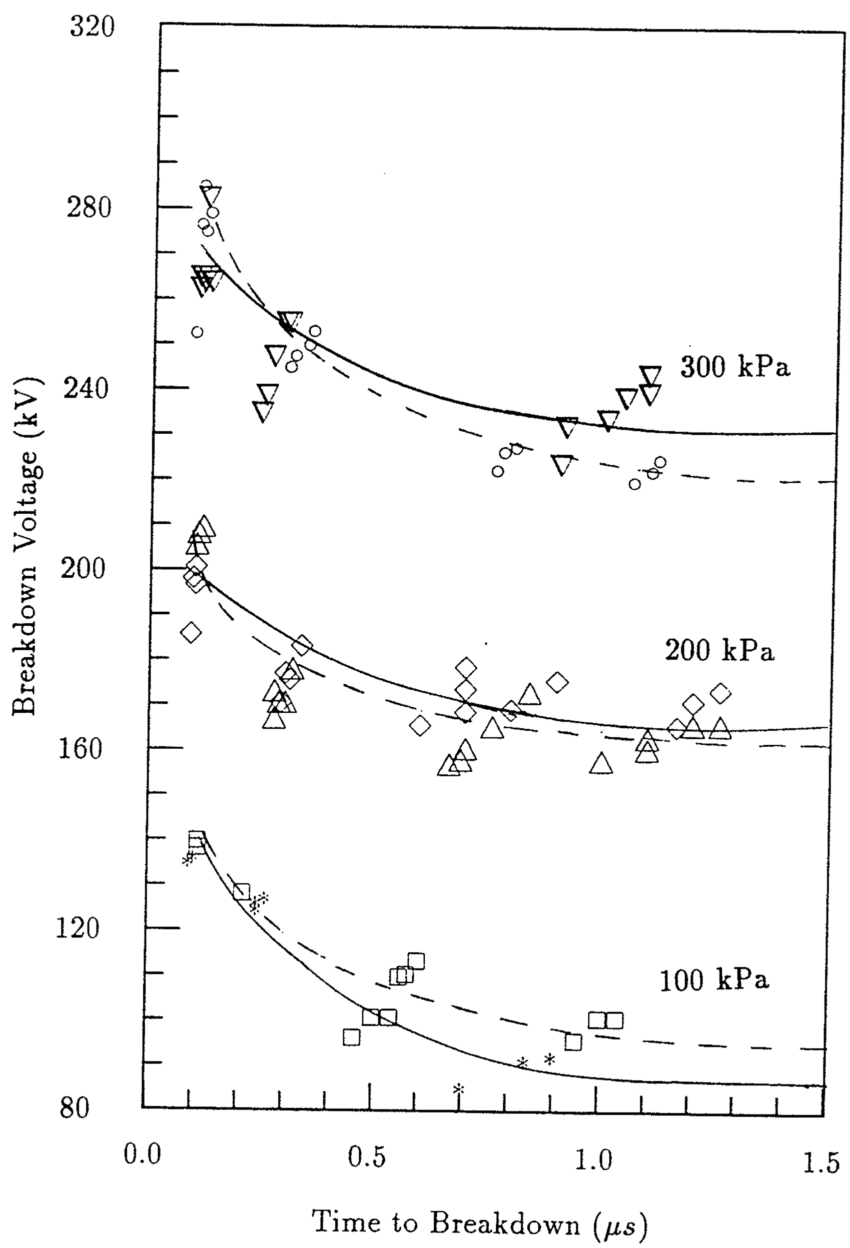

Figure 4.39: Positive impulse breakdown voltage-time characteristics for SF_6 mixtures in a 1.27/5.2 cm coaxial-cylinder gap: (1) (○, △, □) 39%SF_6 + 60%N_2 + 1%(c − C_4F_8 (2) (▽, ◇, *) 40%SF_6 + 60%N_2, (○, ▽) 300 kPa, (△, ◇) 200 kPa, (□, *) 100 kPa.

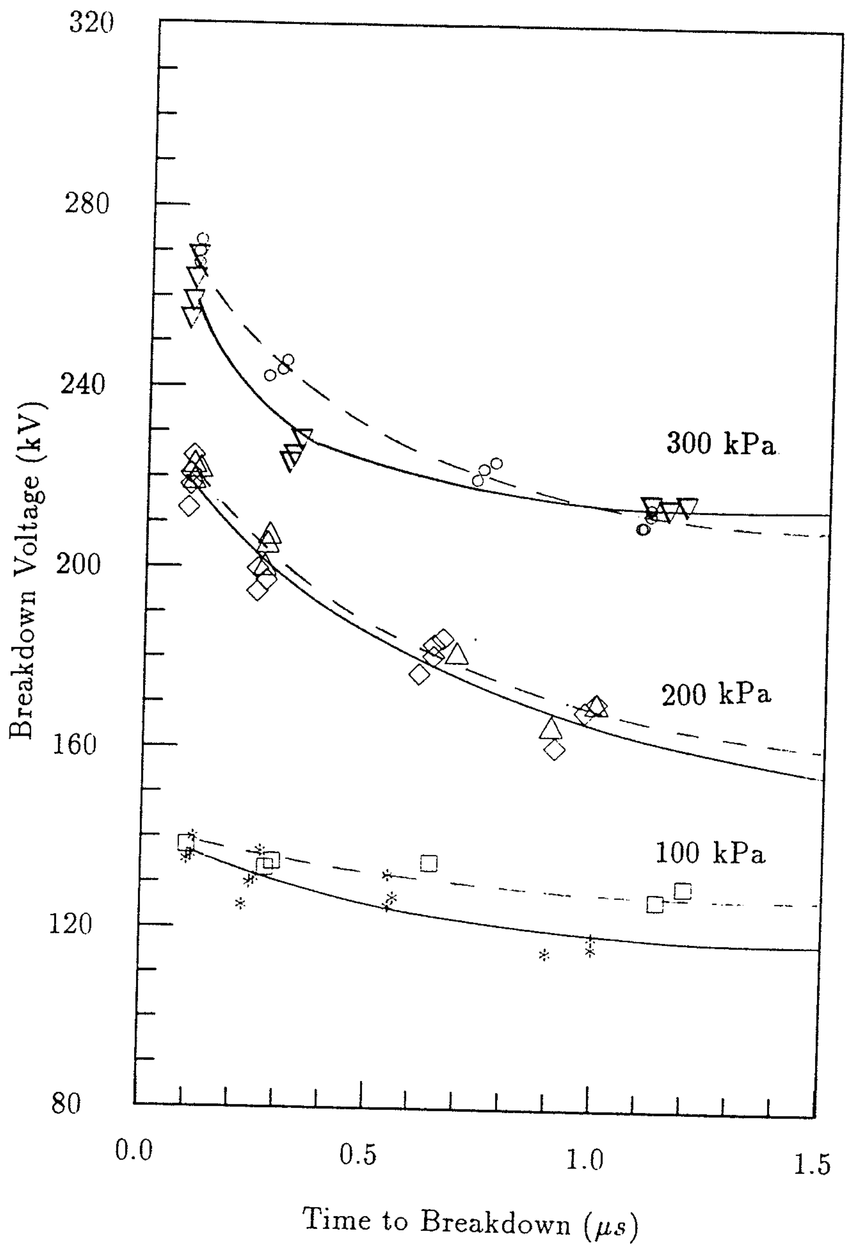

Figure 4.40: Negative impulse breakdown voltage-time characteristics for SF_6 mixtures in a 1.27/5.2 cm coaxial-cylinder gap: (1) (○, △, □) 39%SF_6 + 60%N_2 + 1%($c-C_4F_8$ (2) (▽, ◇, *) 40%SF_6 + 60%N_2, (○, ▽) 300 kPa, (△, ◇) 200 kPa, (□, *) 100 kPa.

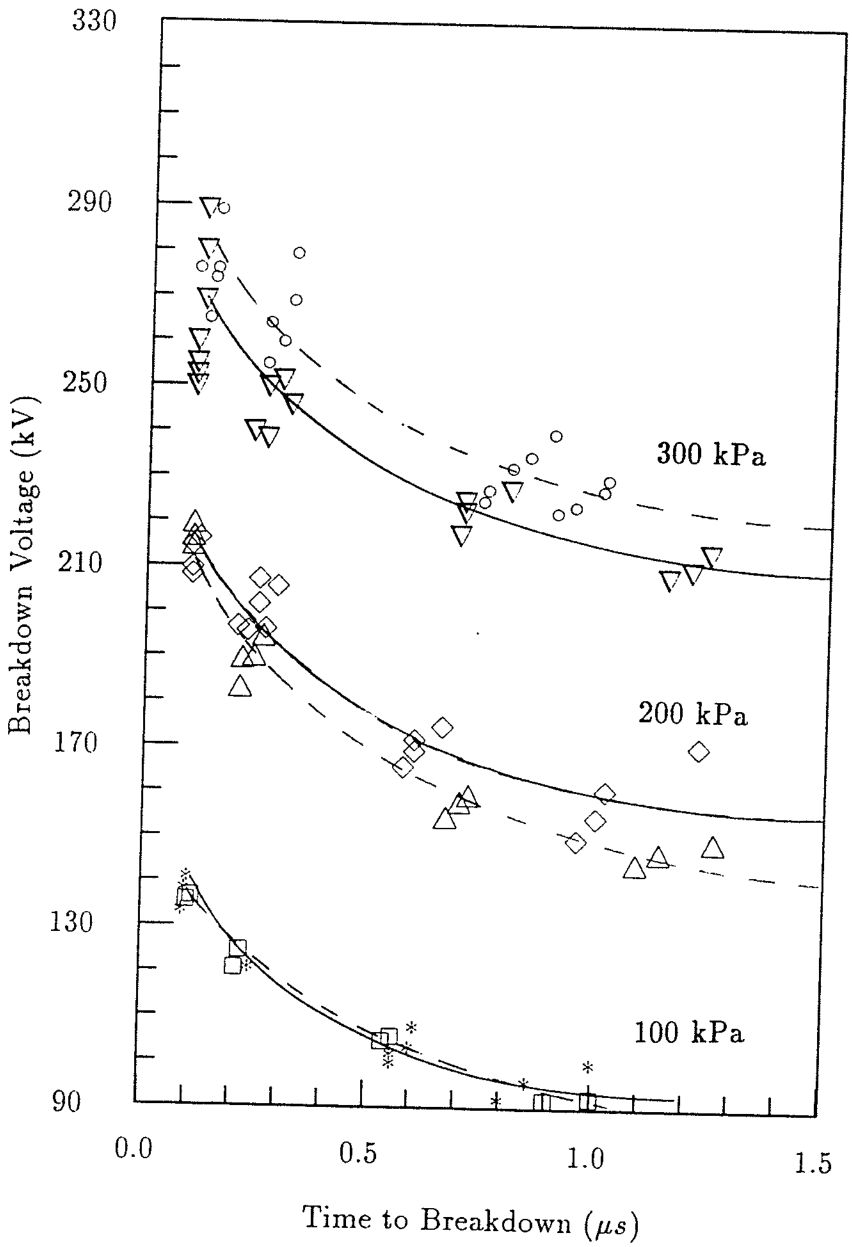

Figure 4.41: Positive impulse breakdown voltage-time characteristics for SF_6 mixtures in a 1.27/5.2 cm coaxial-cylinder gap: (1) (○, △, □) $39\%SF_6 + 60\%air + 1\%(c - C_4F_8$ (2) (▽, ◇, *) $40\%SF_6 + 60\%air$, (○, ▽) 300 kPa, (△, ◇) 200 kPa, (□, *) 100 kPa.

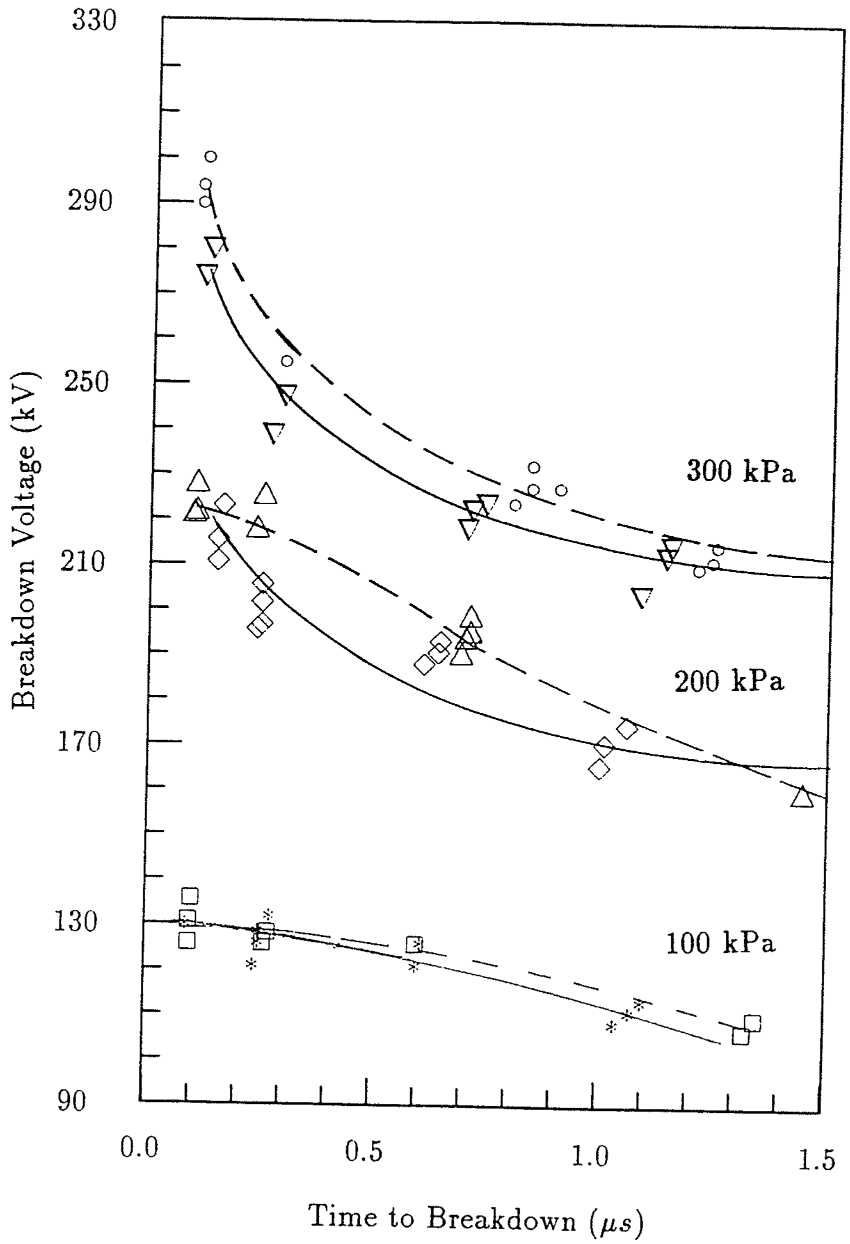

Figure 4.42: Negative impulse breakdown voltage-time characteristics for SF_6 mixtures in a 1.27/5.2 cm coaxial-cylinder gap: (1) (○, △, □) $39\% SF_6 + 60\% air + 1\% (c - C_4F_8$ (2) (▽, ◇, *) $40\% SF_6 + 60\% air$, (○, ▽) 300 kPa, (△, ◇) 200 kPa, (□, *) 100 kPa.

Chapter 5

Comparison of experimental and theoretical values of the voltage-time characteristics

The theoretical analysis of the v-t curves consists of two parts: (i) Prediction of dc breakdown voltages for a coaxial cylinder gap. (ii) Calculation of v-t characteristics for a coaxial cylinder gap under impulse applied voltages. Both parts are based on the streamer breakdown mechanism and are treated in sections 5.1 and 5.2 respectively.

In section 5.1, a formula to calculate the corona onset or direct breakdown voltage for coaxial cylinder gaps in SF_6 and its mixtures is derived according to the streamer criterion. The calculated values using the formula are then compared with the experimental results obtained in this investigation and from published articles. To reduce the apparent differences between the calculated values and the measured ones at higher pressures, an equivalent limiting value is introduced to modify the formula.

In section 5.2, the breakdown voltage for coaxial cylinder gaps in SF_6 and its mixtures under impulse applied voltages are calculated based again on the streamer criterion. However, since the applied voltage appears across the gap for only a very short time, statistical phenomena of the initiating electrons must be taken into account in this case. Based on the assumption that the main source of the initiating electrons is the negative ion detachment, formulae related to the phenomena are derived. The comparison is then made between the calculated and experimental values.

5.1 Applying the streamer theory for calculating the corona onset or breakdown voltages for coaxial cylinder gaps in SF_6 and its mixtures

The streamer breakdown mechanism assumes that when a single electron avalanche becomes unstable, the instability can result in the formation of fast moving cathode and anode directed streamers which form a highly conducting channel across the gap leading to breakdown. This theory involves ionization by electrons and high energy photons in the gas. The transition from an electron avalanche into a streamer is believed to occur when the field at the head of the avalanche is of the order of the externally applied field.

The criterion of this theory for the corona onset or direct breakdown to occur is satisfied when a critical number of ions (N_c) in an electron avalanche is reached. This may be expressed as [28,29]:

$$\int_0^{x_c} (\alpha - \eta)dx = \int_0^{x_c} \overline{\alpha} dx = K = \ln(N_c) \tag{5.1}$$

where α = the Townsend first ionization coefficient (cm^{-1}), η = the electron attachment coefficient (cm^{-1}), $\overline{\alpha} = \alpha - \eta$= the effective ionization coefficient (cm^{-1}), x_c = the critical avalanche length,

Both coefficients (α and η) depend on the field strength E and/or the pressure P. However it has been shown that for SF_6 and it mixtures with N_2, CO_2 or air as a buffer gas, the effective ionization coefficient $\overline{\alpha}$ can be approximated by [30]

$$\frac{\overline{\alpha}}{P} = k[\frac{E(x)}{P} - (\frac{E}{P})_{lim}] = k(\frac{E(x)}{P} - M) \tag{5.2}$$

where M is the limiting value of the parameter of $E(x)/p$ and is a constant for a given mixture. k is a constant for a given mixture.

Both M and k depend on the content of SF_6 in the mixture and are given in Table 3. Substituting eqn.(5.2) into eqn.(5.1) yields:

$$\int_0^{x_c} E(x)dx - P \cdot x_c \cdot M = \frac{K}{k} \tag{5.3}$$

For a coaxial cylinder gap equation (5.3) becomes:

$$\int_{R_i}^{R_c} E(r)dr - P \cdot (R_c - R_i) \cdot M = \frac{K}{k} \tag{5.4}$$

where R_c is the distance from the axis of the cylinder gap to the point in the gap where $\overline{\alpha}$=0 and R_i is the radius of the inner electrode. That is

$E(R_c)/p = M$. Neglecting the effects of space charges, the electric field stress in a coaxial cylinder gap can be expressed as:

$$E(r) = \frac{U}{r \ln \frac{R_o}{R_i}} = \frac{U}{rN} \tag{5.5}$$

Hence, R_c is given by

$$R_c = \frac{U}{P \cdot M \cdot N} \tag{5.6}$$

Substituting eqns.(5.5) and (5.6) into eqn.(5.4), the breakdown criterion expression becomes:

$$\frac{U}{N} \ln \frac{U}{R_i \cdot P \cdot M \cdot N} - P \cdot M \cdot (\frac{U}{P \cdot M \cdot N} - R_i) = \frac{K}{k} \tag{5.7}$$

The solution to eqn.(5.7) is:

$$U = R_i \cdot P \cdot M \cdot N \cdot e \cdot x \tag{5.8}$$

where x is defined by:

$$x \cdot \ln x + e^{-1} - A = 0 \quad with \quad A = \frac{K}{R_i \cdot P \cdot M \cdot e \cdot k} \tag{5.9}$$

The values of x depending on A are given in Table 4.

Table 3: Variations of k (kV^{-1}) and M $(kV \cdot cm^{-1} \cdot kPa^{-1})$ with SF_6 content z.

z	$SF_6 - N_2$		$SF_6 - air$		$SF_6 - CO_2$	
	M	k	M	k	M	k
1.0	0.8775	27	0.8775	27	0.8775	27
0.9	0.8554	25.9	0.8504	26.4	0.8432	26.0
0.8	0.8314	24.8	0.8215	25.6	0.8040	25.1
0.7	0.8049	23.7	0.7904	24.8	0.7668	24.2
0.6	0.7755	22.4	0.7564	23.7	0.7242	23.2
0.5	0.7424	21.2	0.7186	22.5	0.6780	22.2
0.4	0.7042	19.8	0.6756	21.1	0.6276	21.5
0.3	0.6589	18.2	0.6250	19.4	0.5712	20.4
0.2	0.6021	16.0	0.5620	16.9	0.5055	19.0
0.1	0.5210	12.6	0.4742	13.6	0.4205	16.3
0.05	0.4392	10.0	0.3749	11.7	0.3587	12.9

Table 4: Variations of x with A.

A	0.001	0.002	0.003	0.004	0.005	0.006	0.007	0.008	0.009
x	0.398	0.407	0.415	0.423	0.430	0.438	0.443	0.448	0.453

A	0.010	0.020	0.030	0.040	0.050	0.060	0.070	0.080	0.090
x	0.458	0.500	0.530	0.555	0.580	0.600	0.620	0.635	0.650

A	0.10	0.20	0.30	0.40	0.50	0.60	0.70	0.80	0.90
x	0.670	0.814	0.930	1.035	1.1295	1.212	1.293	1.370	1.445

Calculation shows that the term of $U/(R_i \cdot P \cdot M \cdot N)$ in eqn.(5.7) is very close to unity for electrode configurations used in practice [88]. Therefore the term of $\ln(U/(R_i \cdot P \cdot M \cdot N)$ can be expanded for an analytical solution of eqn.(5.7):

$$\frac{U}{N} \ln \frac{U}{R_i \cdot P \cdot M \cdot N} - P \cdot M \cdot (\frac{U}{P \cdot M \cdot N} - R_i) = \frac{K}{k} \tag{5.10}$$

$$\frac{U}{N}\left(\frac{U}{R_i \cdot P \cdot M \cdot N} - 1\right) - P \cdot M \cdot \left(\frac{U}{P \cdot M \cdot N} - R_i\right) = \frac{K}{k} \tag{5.11}$$

$$U = R_i \cdot P \cdot M \cdot N \cdot \left(1 + \sqrt{\frac{K}{k \cdot R_i \cdot P \cdot M}}\right) \tag{5.12}$$

Figures 5.1 to 5.4 show the comparison between the calculated values and the experimental ones for the present coaxial cylinder gap. Data found in literature are included [27]. As can be seen from the figures the calculated values agree reasonably with the corresponding measured ones at pressure up to 200-300 kPa depending on the electrode geometry and gas used. At higher pressures, however, particularly for pure SF_6, the calculated values deviate from the measured ones. The difference is even larger when the inner electrode is negative. This indicates that either mechanisms other than streamer mechanism take place in the gas or the properties of the gas or gas mixtures have been changed due to increasing space charge density and reduced diffusion at higher pressures since the deviation from the measured values was also observed in a uniform field. The surface conditions of the inner electrode may also play an important role in the breakdown voltages under negative polarity voltages. However, if we assume that the streamer mechanism is still the prevalent mechanism at higher pressures within the range of practical applications, an equivalent limiting value of the parameter $E(r)/p$ can be used for the calculation to minimize the difference. This assumption means that for SF_6 and its mixtures the effective ionization coefficient can

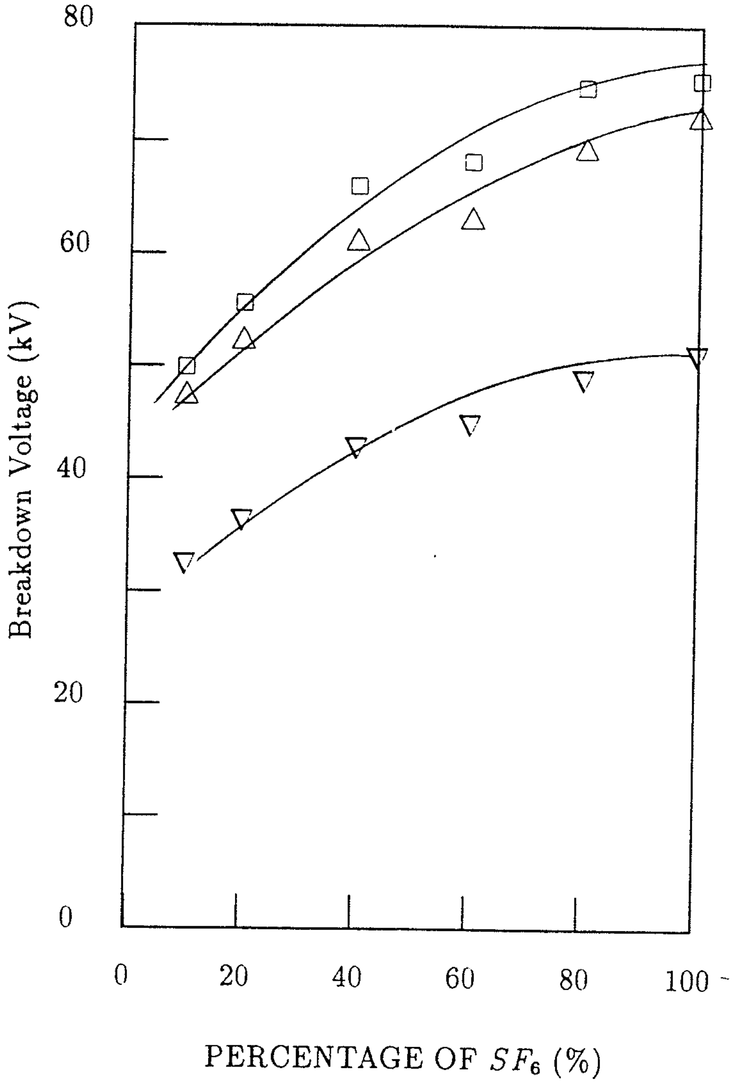

Figure 5.1: Positive *dc* breakdown voltage for $SF_6/N2$ mixture *vs* % of SF_6 for different inner electrodes: outer electrode radius 2.0 *cm*; inner electrode radii: (□) 0.75 *cm*, (△) 0.4 *cm*, (▽) 1.4 *cm*. (—) calculated at 102 kPa [27]

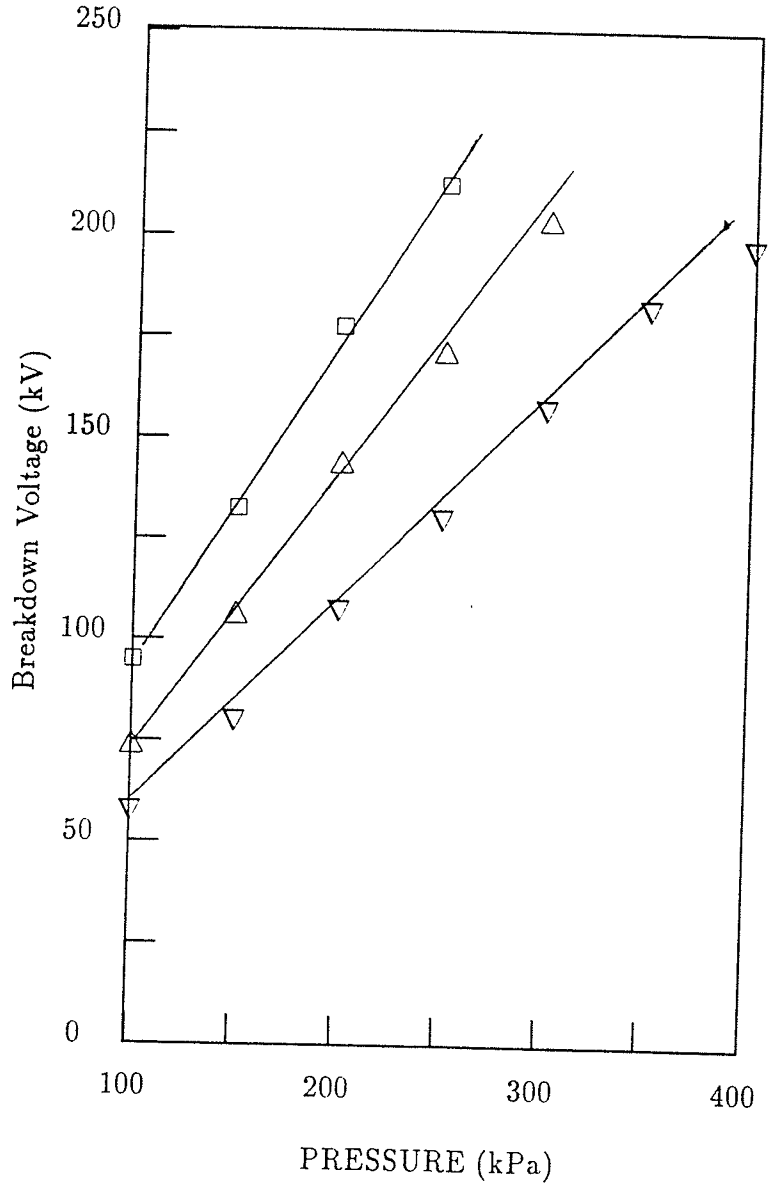

Figure 5.2: Positive *dc* breakdown voltage-pressure relationship for a 1.27/5.2 *cm* coaxial cylinder gap in air/SF_6 mixtures: (□) 100% SF_6; (△) 40%SF_6 + 60%air; (∇) 10%SF_6 + 90%air. (—) calculated.

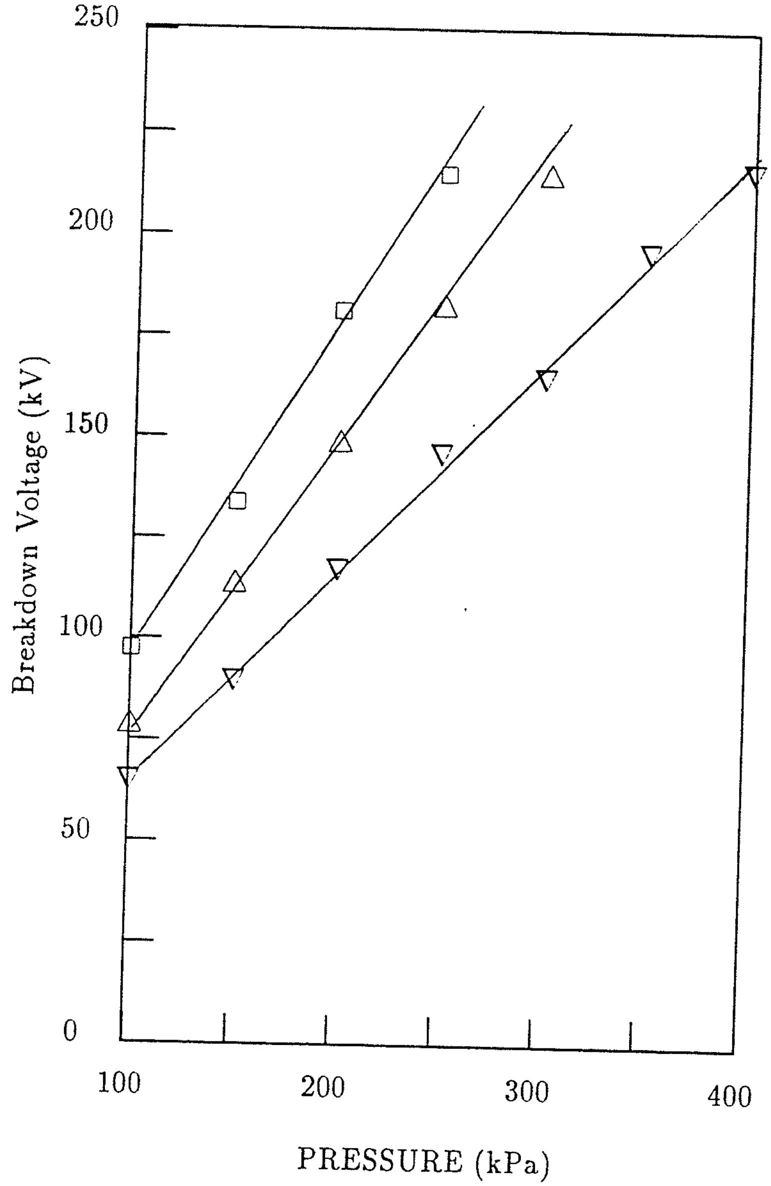

Figure 5.3: Positive *dc* breakdown voltage-pressure relationship for a 1.27/5.2 *cm* coaxial cylinder gap in N_2/SF_6 mixtures: (□) 100% SF_6; (△) 40%SF_6 + 60%N_2; (▽) 10%SF_6 + 90%N_2. (—) calculated.

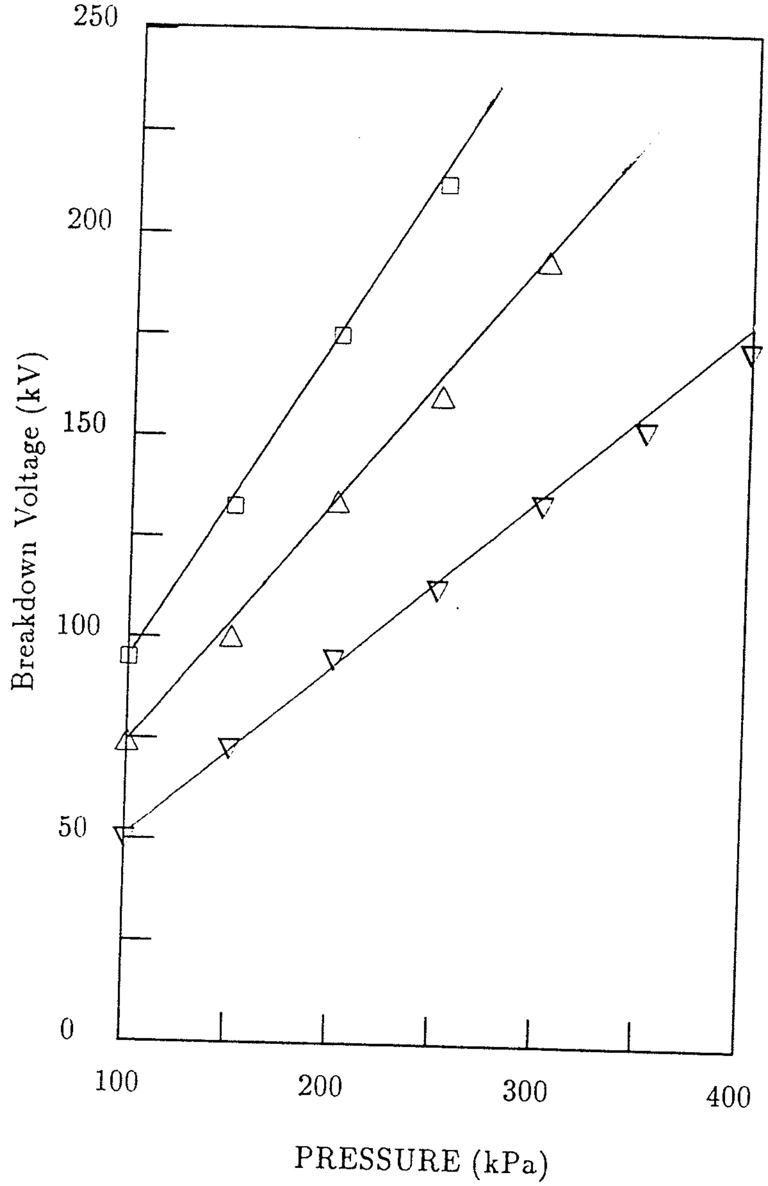

Figure 5.4: Positive *dc* breakdown voltage-pressure relationship for a 1.27/5.2 *cm* coaxial cylinder gap in CO_2/SF_6 mixtures: (□) 100% SF_6; (△) 40%SF_6 + 60%CO_2; (▽) 10%SF_6 + 90%CO_2. (—) calculated.

be approximated by:

$$\frac{\overline{\alpha}}{P} = k[\frac{E(r)}{P} - (\frac{E}{P})_{eq \cdot lim}]$$
$$= k[\frac{E(r)}{P} - M_{eq}] \tag{5.13}$$

where the value of k is assumed to be a constant independent of pressure and $(E/p)_{eq.lim}$ is the equivalent limiting value of $E(r)/p$ depending on both pressure and gap length. It is easy to understand that if M in the above equations is replaced by M_{eq}, the equations are still valid. Therefore the breakdown criterion of eqn.(5.7) can be rewritten as

$$\frac{U}{N} \ln \frac{U}{R_i \cdot P \cdot M_{eq} \cdot N} - P \cdot M_{eq} \cdot (\frac{U}{P \cdot M_{eq} \cdot N} - R_i) = \frac{K}{k} \tag{5.14}$$

The equivalent limiting values can be determined by solving eqn.(5.14) if the breakdown voltages for a given gap are known.

The equivalent limiting values of $E(r)/p$ for a coaxial cylinder gap in SF_6 and SF_6/N_2 mixtures were measured under negative polarity using an optimized electrode configuration which for a coaxcial cylinder is $\frac{r_o}{r_i} = e$, which is also the system used in practice. The results are shown in Figures 5.5 and 5.6 for pressures up to 300 kPa which is the limit of the apparatus available in the lab. The coaxial cylinder gap was 5.2/1.86 cm outer and inner diameters respectively. As can be seen from figure 5.5 the value for pure SF_6 decrease sharply when the gas pressure reaches about 250 kPa, while the value for $50\%SF_6/50\%N_2$ decreased nearly linearly in the pressure range measured (Fig.5.6).

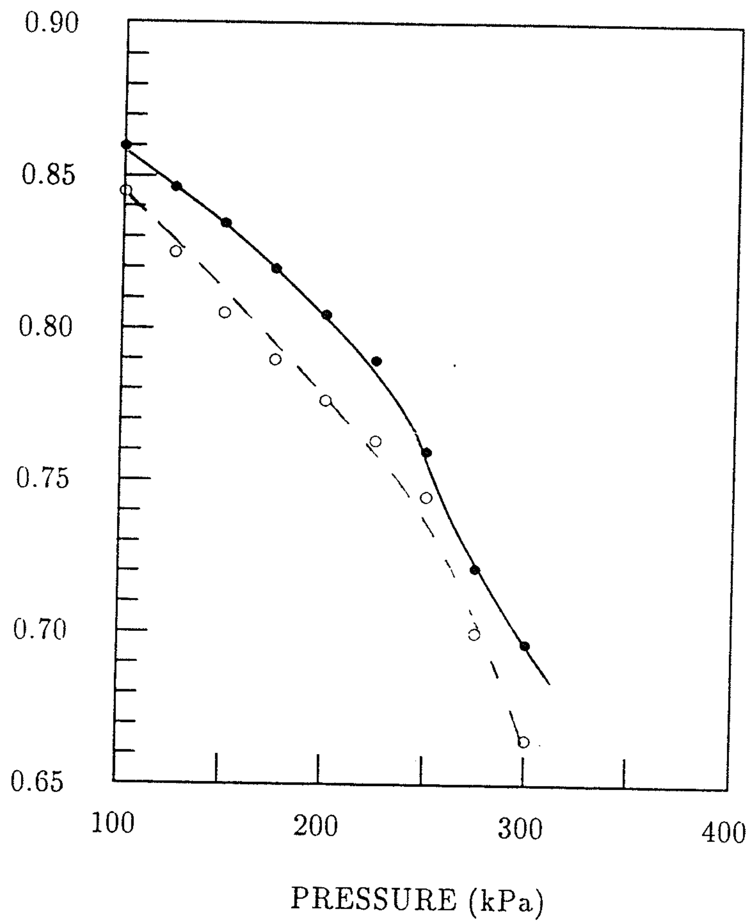

Figure 5.5: Equivalent limiting values of the parameter $E(r)/p$ measured by a 1.86/5.2 *cm* coaxial cylinder gap, (•) average values, (○) minimum of 5 measurements.

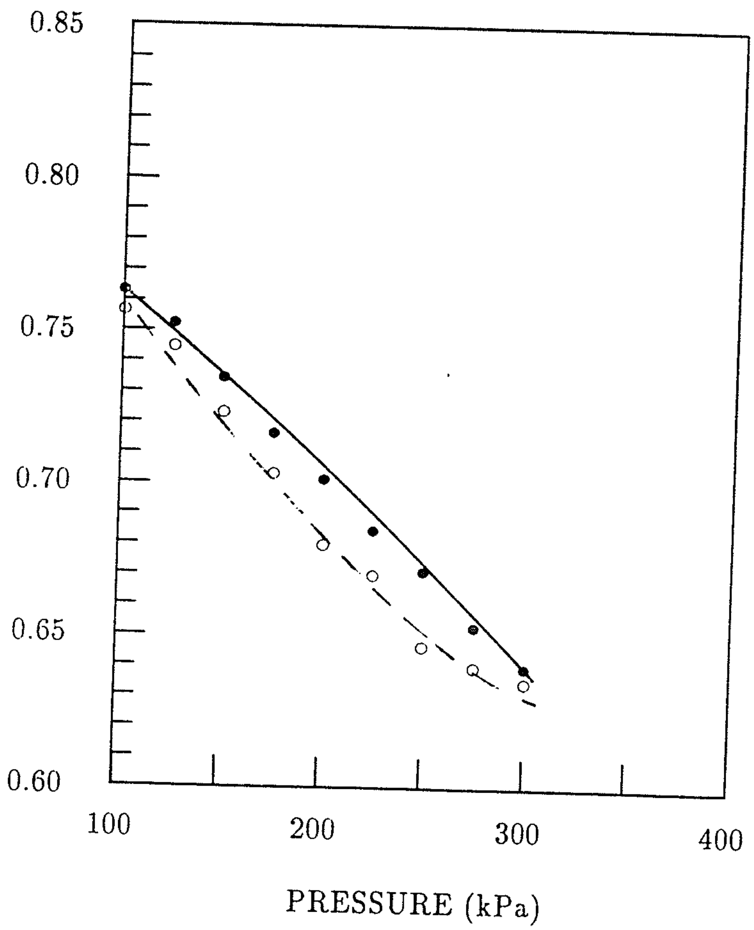

Figure 5.6: Equivalent limiting values of the parameter $E(r)/p$ for $50\% SF_6$-$50\% N_2$ measured by a 1.86/5.2 *cm* coaxial cylinder gap, (•) average values, (○) minimum of 5 measurements.

On the other hand, considering eqn.(5.12), one can assume that

$$U = R_i \cdot P \cdot M_{eq} \cdot N \tag{5.15}$$

without causing significant error since in most cases the second term in the parentheses is only a few percent. Substituting eqn.(5.15) into eqn.(5.5), one obtains

$$E(R_i) = P \cdot M_{eq} \tag{5.16}$$

Equation (5.16) implies that the breakdown voltages for a coaxial cylinder gap in SF_6 and its mixtures are, to a large extent, determined by the field intensity on the surface of the inner electrode which is a function of pressure.

It is interesting to observe that the measured breakdown field intensities on the surface of the inner electrode of the cylinder gas nearly coincide with the average breakdown field intensities for the uniform field gaps [89] shown in Figure 5.7. The average field intensity as a function of pressure obtained for uniform field gaps is, therefore, used for the estimation of breakdown voltages of SF_6 in coaxial cylinder gaps for pressures higher than those used for obtaining the equivalent limiting factors. Figures 5.8 to 5.10 show the calculated values together with the measured ones found in the literature [90, 99]. Considering the large scatter of the measured data, especially for larger electrode configurations, and the conditioning-related low breakdown values for the first few voltage applications, the calculated values are in reasonable agreement with the measured ones.

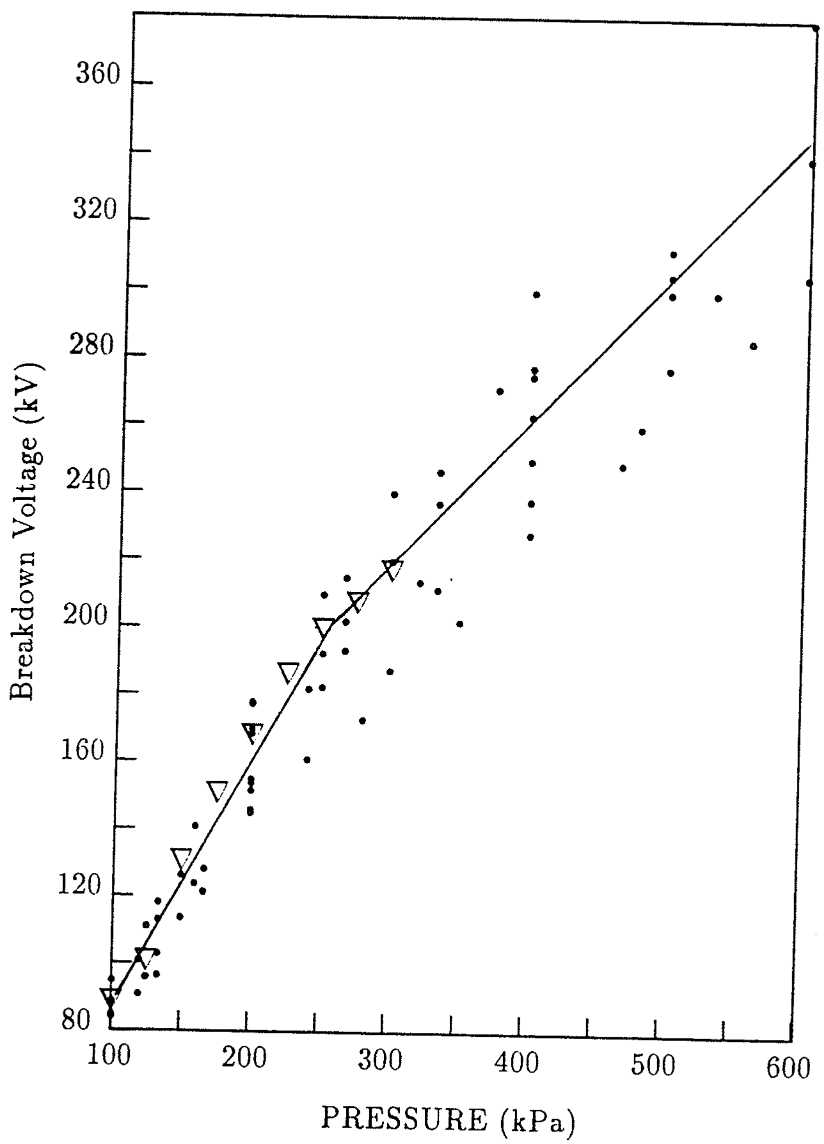

Figure 5.7: The average breakdown field intensity for gaps in SF_6 gas under *ac* or negative *dc* applied voltages: (•) measured with uniform gap under *ac* applied voltages [89], (∇) (inner electrode) measured with a 1.86/5.2 *cm* coaxial cylinder gap under negtive *dc* applied voltages.

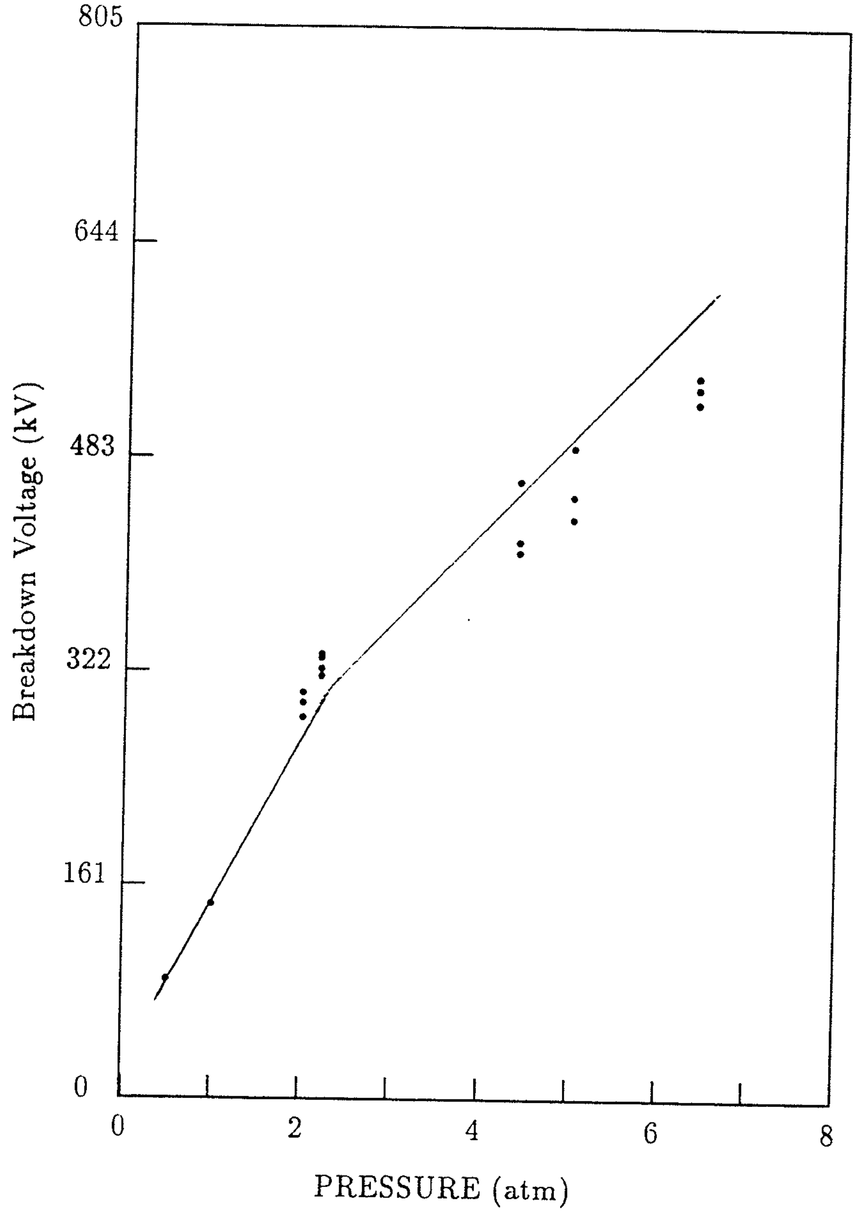

Figure 5.8: Breakdown voltage-pressure relationship for a 1.0/25 *cm* coaxial cylinder gap in SF_6 gas under negtive *dc* applied voltages: (•) measured [90], (—) calculated.

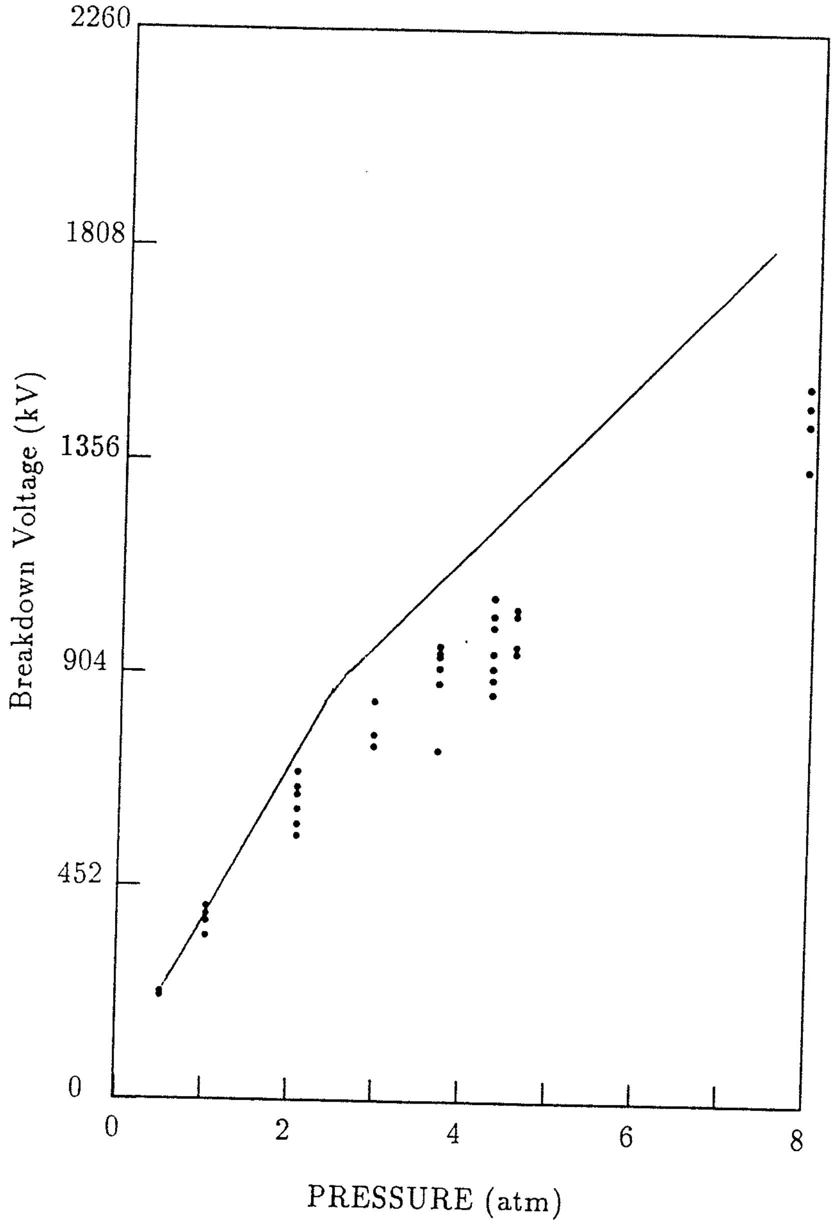

Figure 5.9: Breakdown voltage-pressure relationship for a 7.6/25 *cm* coaxial cylinder gap in SF_6 gas under negtive *dc* applied voltages: (•) measured [90], (—) calculated.

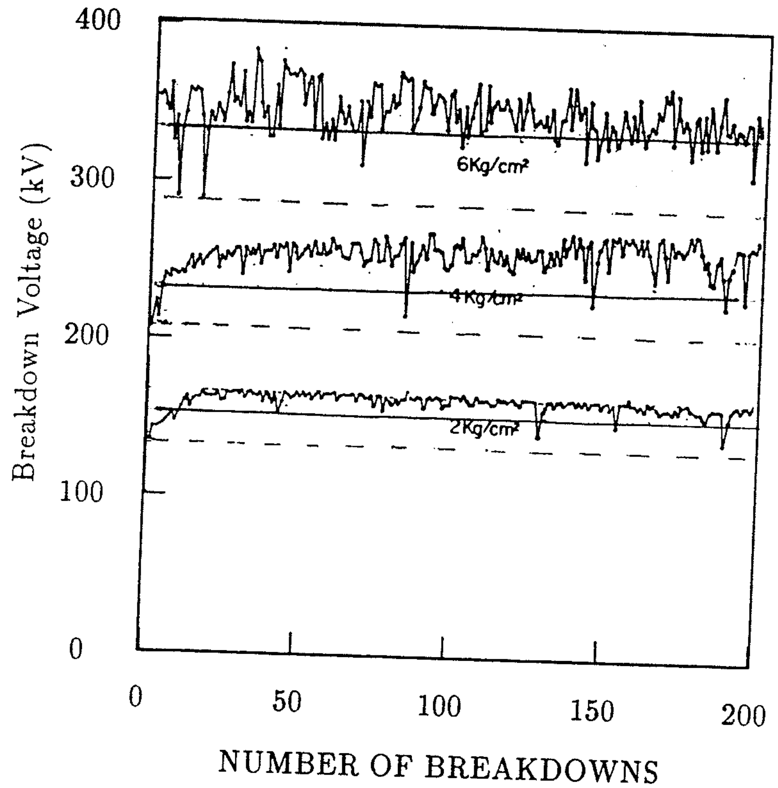

Figure 5.10: AC breakdown voltages (peak) for SF_6 in a 13.2/15.2 cm coaxial-cylinder gap: (1) measured (•) [99]; (2) calculated: (—) average, (- - -) minimum.

5.2 Numerical evaluation of the breakdown voltage-time characteristics

The calculation of the volt-time characteristics for impulse applied voltages is based on the statistical behaviour of the gas or gas mixtures under impulse voltages.

To develop an electron avalanche, an initiating electron must be provided. An initiating electron may come from cosmic radiation, negative ion detachment or other sources such as field emission and photo ionization. However, because of the electronegative nature of SF_6 and its mixtures, not all electrons in the gap can develop a critical avalanche leading to a breakdown of the gap. This can be easily understood if the processes of ionization and attachment within an electron avalanche are considered. Assuming that the electric field intensity in the gas is E_o, for this field intensity $\alpha = \eta$, where α, η are the ionization and electron attachment coefficients respectively, the probabilities of ionization and attachment of an initiating electron are equal. Therefore, there is a 50% probability that the avalanche stops at the beginning and a 50% probability that another electron is generated by collision. Similarly, there is 50% probability of releasing a secondary electron by collision. The result is that the probability of the two electrons being attached to form negative ions is 25%. Hence, the probability that the electron avalanche stops after it travels a distance of two mean free paths is 62.5%. On average, for uniform field where the breakdown field strength is very close to the limiting value at which $\alpha = \eta$, about 3 initiating electrons are needed to initiate an avalanche leading to a breakdown.

For nonuniform field gaps, according to the streamer criterion, the probability of an electron leading to a breakdown of a given gap can be expressed by: [91]

$$p_o = \frac{\{\int_0^s \alpha exp[-\int_0^x (\alpha - \eta) d\xi] dx\}^{n_k - 1}}{\{1 + \int_0^s \eta exp[-\int_0^x (\alpha - \eta) d\xi] dx\}^{n_k}} \qquad (5.17)$$

where s is the distance that the initiating electron has travelled in the direction of the electric field and n_k is the number of electrons needed in the avalanche head leading to a breakdown of the gas or gas mixture in the gap. The equation can be approximated by:

$$p_0 = \begin{cases} 1 - \frac{\eta}{\alpha} & \alpha \geq \eta \\ 0 & \alpha < \eta \\ 0 & s < l_f \end{cases} \qquad (5.18)$$

$$\int_0^{l_f} (\alpha - \eta) dx = \ln n_k$$

Since SF_6 gas and its mixtures are electronegative, most electrons will be attached to form negative ions. Therefore, it is reasonable to assume that the initiating electrons come from negative ion detachment. Hence, the number of electrons in the gas will be a function of negative ion population and the rate of electron detachment.

Assuming that the negative ion density in the gas in the time instant t is $n(t)$ and the rate of electron detachment is B, then the electrons detached from negative ions in a given small volume dv in the gap in the time interval from t to $(t + dt)$ are $(n(t) \cdot dv \cdot B \cdot dt)$. At the same time, assuming that the increment of negative ions in the given volume due to electron attachment processes is equal to the negative ions generated by the electrons detached from the negative ions in that volume, travelling a very small distance dx in the direction of electric field, then the increment of negative ion in the given volume is given, according to Townsend mechanism, by:

$$\triangle n_- = \frac{n_0\eta}{\alpha-\eta}[e^{(\alpha-\eta)dx}-1] = \frac{n(t)\cdot dv\cdot B\cdot dt\cdot\eta}{\alpha-\eta}[e^{(\alpha-\eta)dx}-1] \qquad (5.19)$$

$$\triangle n_- = n(t)\cdot dv\cdot B\cdot dt\cdot\eta\cdot dx \qquad (5.20)$$

The total increment of negative ions in that volume is then determined by

$$\triangle n_T = n(t)\cdot dv\cdot B\cdot dt\cdot\eta\cdot dx - n(t)\cdot dv\cdot B\cdot dt \qquad (5.21)$$

Expressing eqn.(5.21) in terms of ion density, we obtain:

$$dn(t) = n(t)\cdot B\cdot dt\cdot\eta\cdot dx - n(t)\cdot B\cdot dt \qquad (5.22)$$

It can be seen that the first term of the equation is a higher order infinitesimal as compared with the second term and hence can be neglected. Then eqn.(5.22) becomes

$$dn(t) = -n(t)\cdot B\cdot dt \quad or \quad \frac{dn(t)}{n(t)} = -B\,dt \qquad (5.23)$$

Integrating,

$$n(t) = Ce^{-Bt} \qquad (5.24)$$

Let $t = t_o$, $n(t) = N_o$, where t_o is the time instant at which the applied voltage reaches the onset level and N_o is the number of negative ions per unit volume in the gap.

$$n(t) = N_o e^{-B(t-to)} \tag{5.25}$$

It is clearly seen that the negative ions in the gap exponentially decrease with time based on the above assumptions.

For a cylindrical layer of thickness dr and volume dv in a coaxial cylinder gap the probability of generating an electron leading to breakdown in the time interval from t to $(t + dt)$ is given by:

$$F(r_i, t) = 1 - (1 - p_0)^{B \cdot n(t) \cdot dv_i \cdot dt} \tag{5.26}$$

and the probability of generating an electron leading to a breakdown in the critical volume at this time interval can be expressed as:

$$p_c = 1 - \prod_{i=1}^{j} [1 - F(r_i, t)] = 1 - \prod_{i=1}^{j} (1 - p_0)^{B \cdot n(t) \cdot dv_i \cdot dt} \tag{5.27}$$

where j is the number of cylindrical layer of the critical volume of the gap.

Then the probability of breakdown in the time interval becomes:

$$dp = (1 - P) \cdot p_c \tag{5.28}$$

where P is the breakdown probability with statistical time lag $t - t_o < t_s$ and P is therefore determined by:

$$P = \int_{t_o}^{t} dp \tag{5.29}$$

The evaluation of eqn.(5.29) involves the estimation of parameters of N_o and B respectively. Hence, the calculation can be done only by initially arbitrarily assigning values to them due to the lack of information. The calculation was done by first setting $n(t) = N_o$ in equation (5.27) and choosing parameter $B \cdot N_o$ using the experimental data with low breakdown probability, since the time instants for these breakdowns are very close to the onset value t_o. Then, the equation was re-evaluated by changing the parameter B while maintaining $B \cdot N_o$ to fix the 95% breakdown probability data assuming all breakdown data are enveloped by the 95% breakdown probability curve. Figures 5.11 to 5.16 give the comparison between experimental results and computed values. Table 5 gives the parameters used for the calculation.

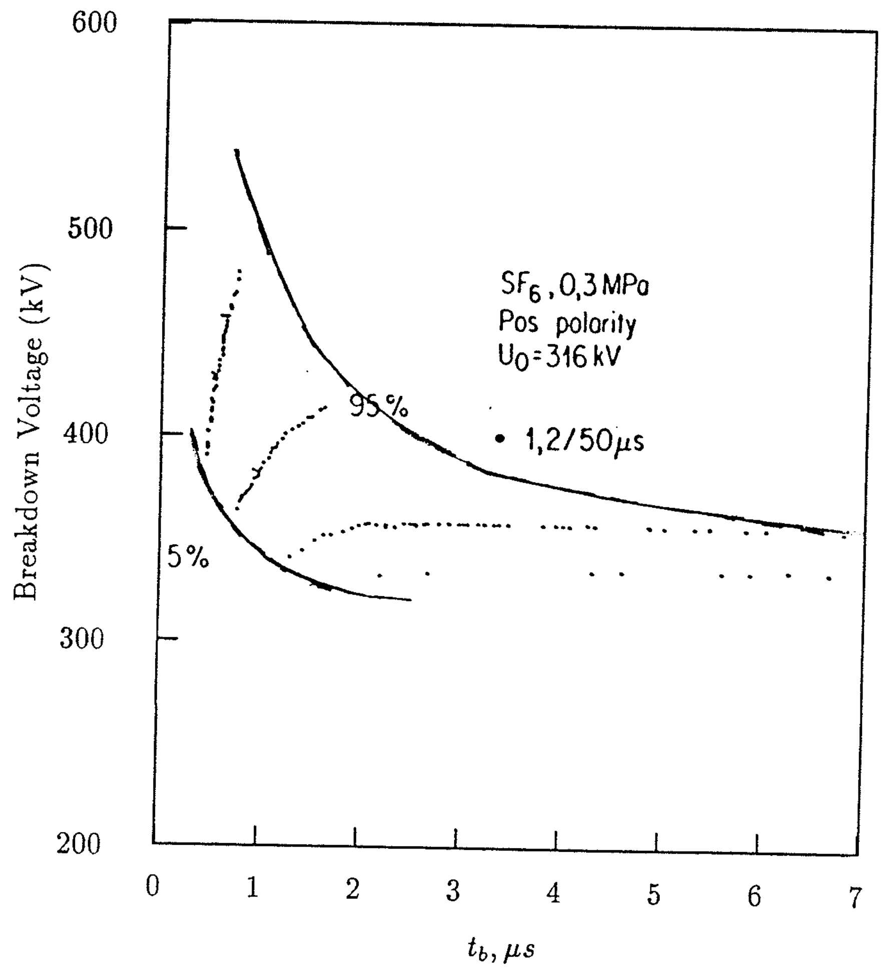

Figure 5.11: Positive impulse breakdown voltage-time characteristics for pure SF_6 in a 2.54/7.0 cm coaxial-cylinder gap: (1) measured (•) 300 kPa [70]; (2) (—) calculated.

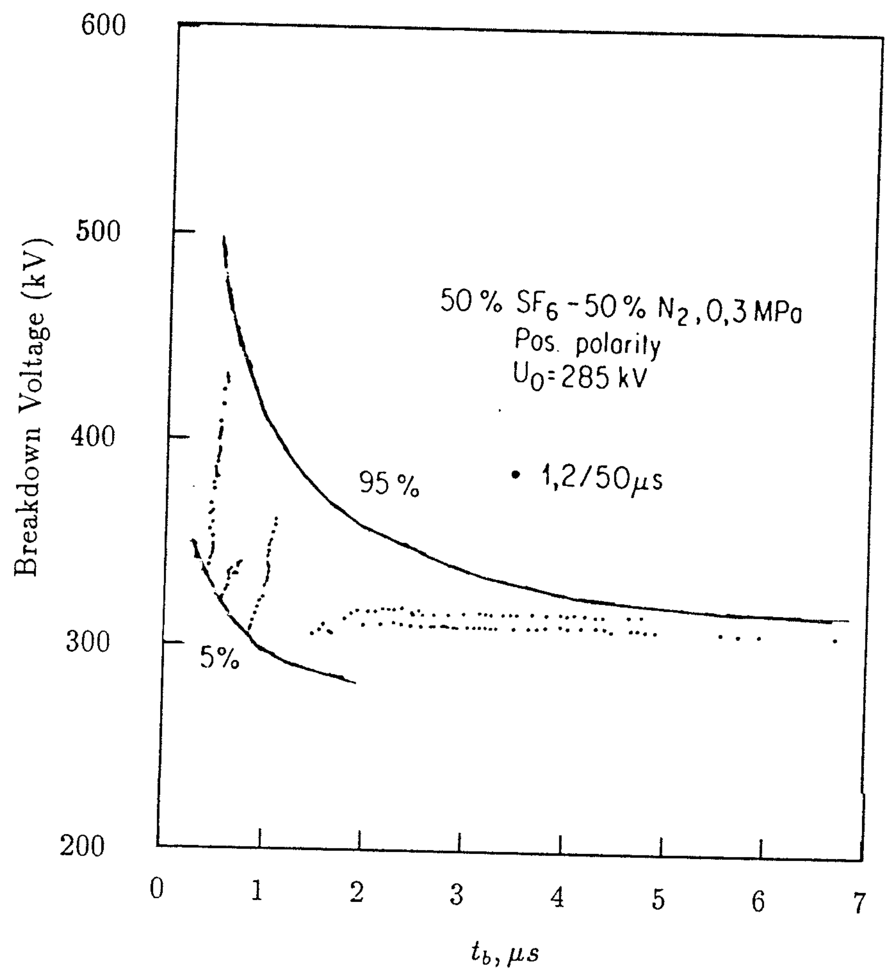

Figure 5.12: Positive impulse breakdown voltage-time characteristics for $50\% SF_6 - 50\% N_2$ in a 2.54/7.0 cm coaxial-cylinder gap: (1) measured (•) 300 kPa [70]; (2) (—) calculated.

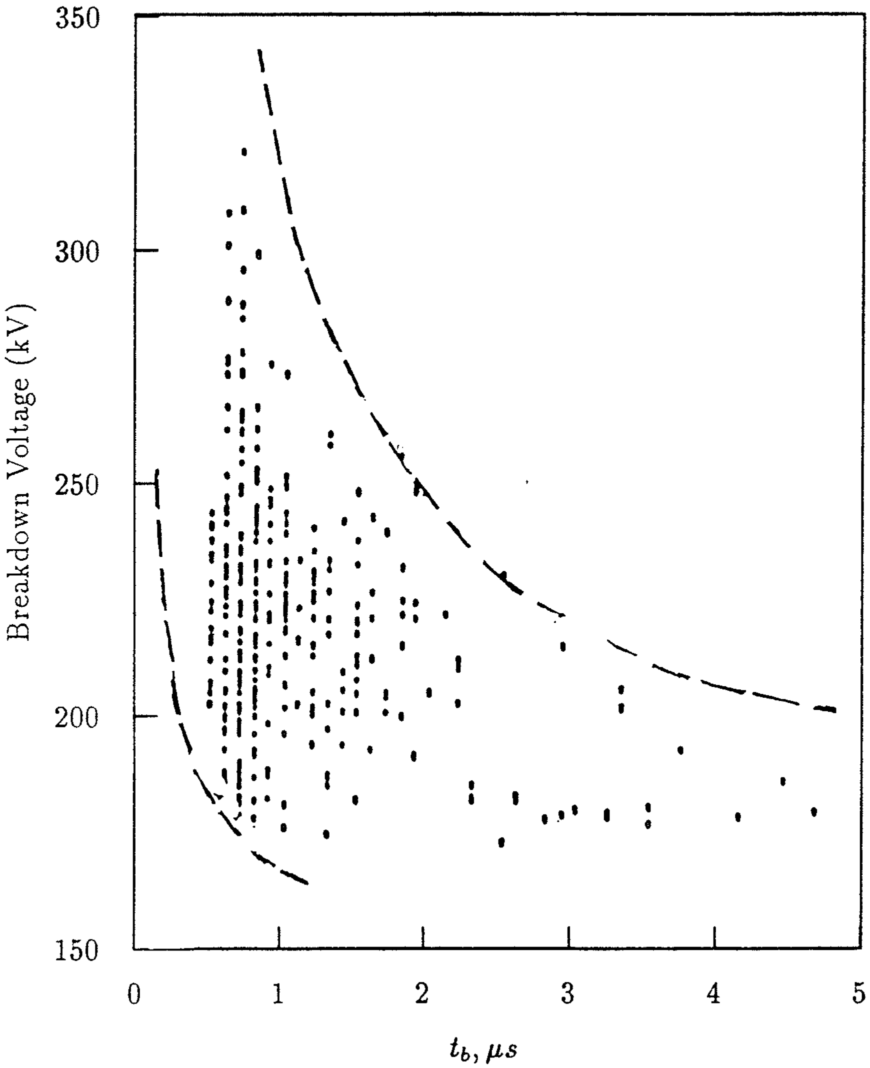

Figure 5.13: Positive impulse breakdown voltage-time characteristics for $10\% SF_6 - 90\% N_2$ in a 0.5/6.9 cm coaxial-cylinder gap: (1) measured (•) 400 kPa [97]; (2) (—) calculated.

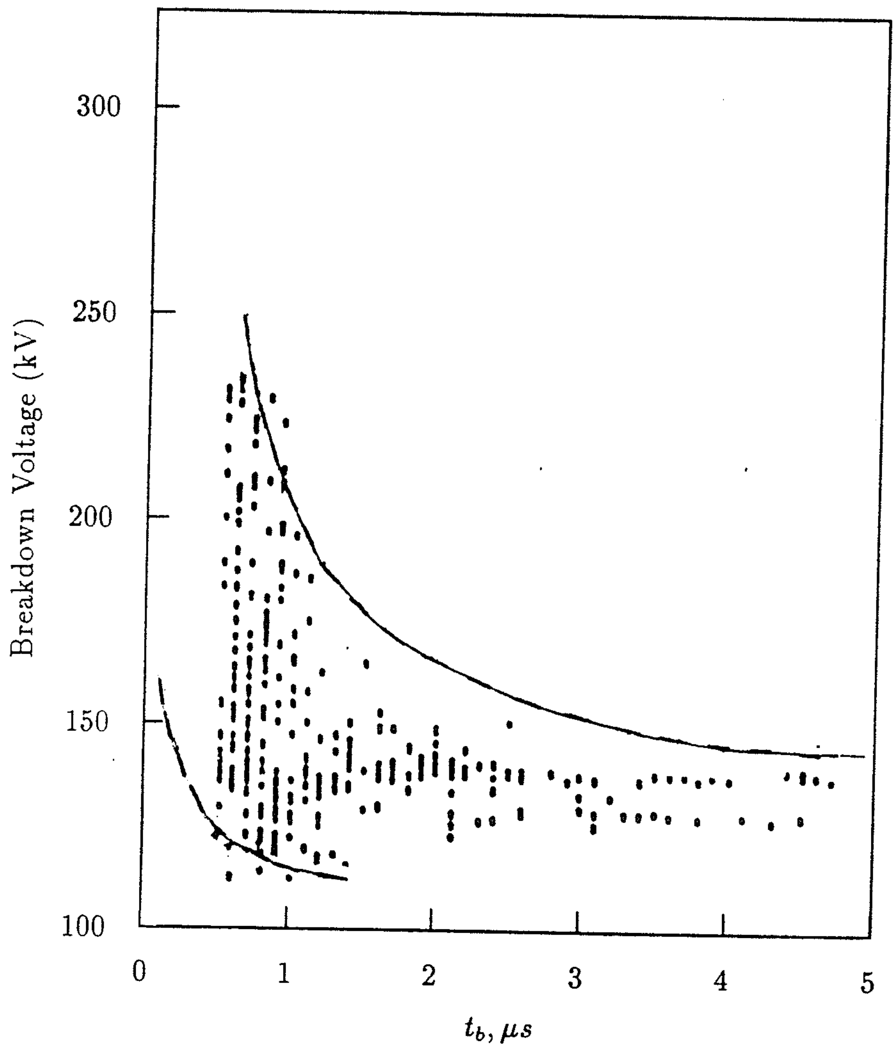

Figure 5.14: Positive impulse breakdown voltage-time characteristics for $10\%SF_6 - 90\%N_2$ in a 0.5/6.9 cm coaxial-cylinder gap: (1) measured (•) 250 kPa [97]; (2) (—) calculated.

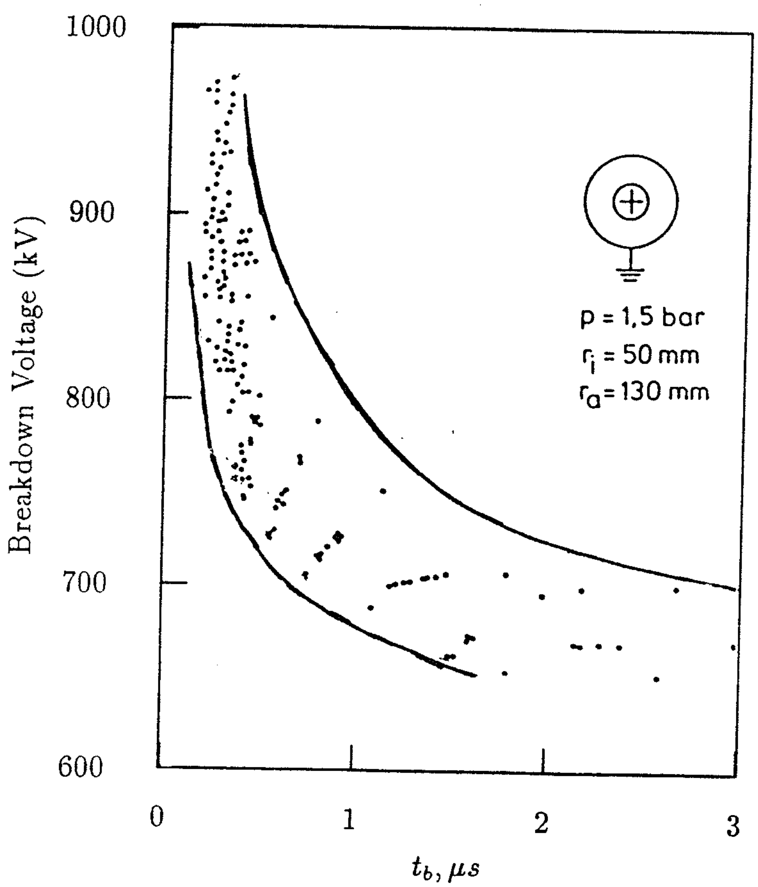

Figure 5.15: Positive impulse breakdown voltage-time characteristics for SF_6 in a 10/26 cm coaxial-cylinder gap: (1) measured (•) 150 kPa [98]; (2) (—) calculated.

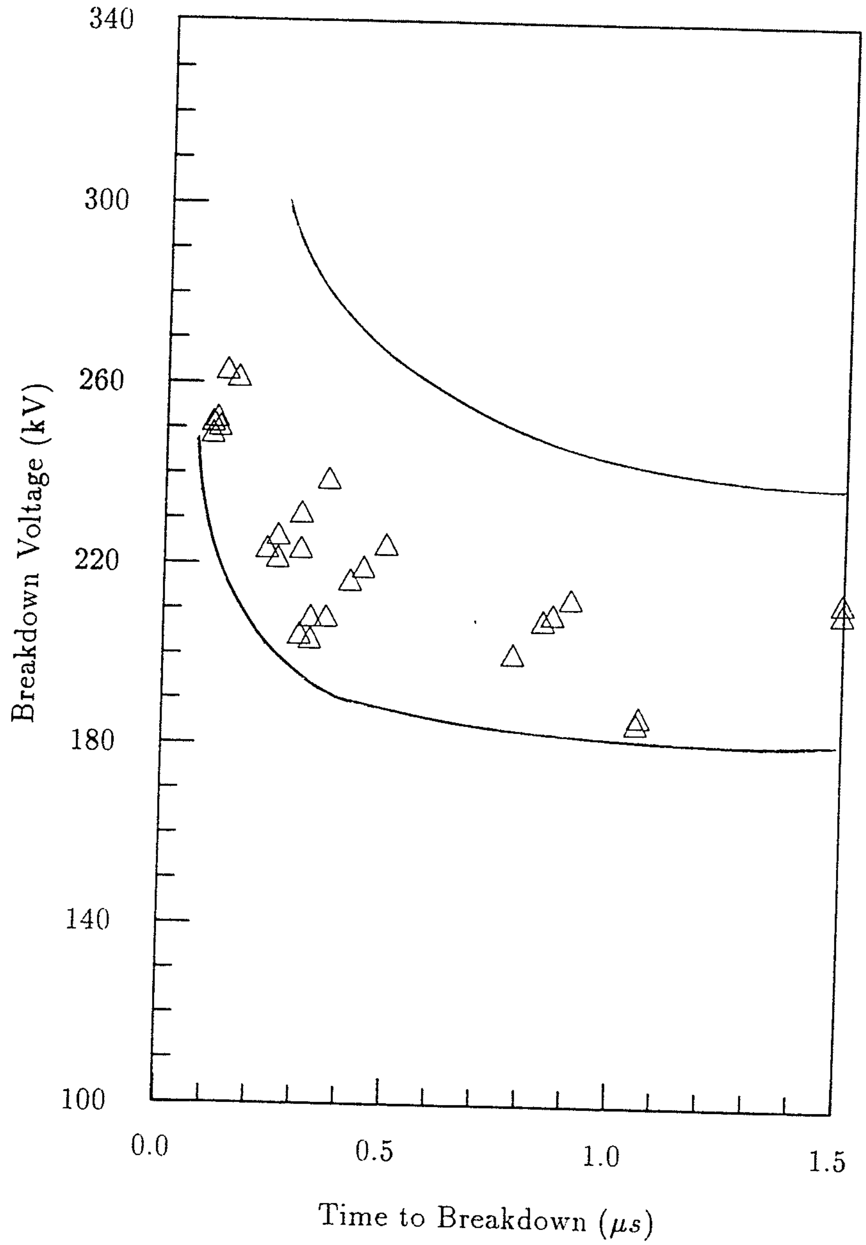

Figure 5.16: Positive impulse breakdown voltage-time characteristics for pure SF_6 in a 1.27/5.2 cm coaxial-cylinder gap: (1) measured (△) 200 kPa, (2) (—) calculated.

Table 5: Parameters used for calculation of Voltage-Time characteristics.

	GAP (cm)	Pressure (kPa)	B	N_o	$B \cdot N_o$	*Reference Figure*
SF_6	2.54/7.0	300	0.6	0.1	0.06	5.11
$50\%SF_6 - 50\%N_2$	2.54/7.0	300	0.8	0.1	0.08	5.12
$10\%SF_6 - 90\%N_2$	0.5/6.9	400	0.5	0.2	0.10	5.13
$10\%SF_6 - 90\%N_2$	0.5/6.9	250	0.9	0.2	0.18	5.14
SF_6	10/26	150	0.25	0.08	0.02	5.15
SF_6	1.27/5.2	200	0.9	0.4	0.36	5.16

As can be seen from Table 5, the parameters are functions of gas pressure, composition of the mixture and electrode configuration and do not seem to follow any rule. It should be mentioned that both B and N_o could not be decided precisely because individually neither B nor N_o is very sensitive and because neither the 5% nor 95% curves could be determined precisely due to the lack of data. The negative ion population as a function of pressure might be due to the higher molecular density at higher pressure. However, the order-of-magnitude difference could not be understood at the present time although locally and temporarally varying natural radiation may be a factor [91]. Moreover, the different surface electrode conditions and the roughening effect on the electrode surface by accumulated sparks might also be influencing factors.

Chapter 6

Discussion of results

In this chapter experimental results will be interpreted and discussed.

6.1 The validity of analog compensation for resistor divider without grading rings

The analog compensation is satisfactory for reconstructing the voltage waves distorted by the shielded resistor divider and hence can be used for steep-fronted impulse voltage measurements as described in section 4.1. It is not known yet if this method can also be used for a resistor divider without grading rings. Theoretically, the removal of the grading is equivalent to setting C_1 to zero and increasing the value of C_2 in the equivalent circuit (Fig.4.1). This indicates that the method might still be valid in this case. To check this, the two toroid rings of the divider were removed, and the compensation network was readjusted accordingly. Figures 6.1 (a) and (b) shows the oscillograms of the unit step response of the uncompensated and compensated measuring systems respectively using the resistor divider without grading rings. The response time for the compensated divider is about 15.5 ns.

It should be pointed out that the value of R_o affects the analog compensation profoundly, even although equation (4.1) did not give any hint that the value would have any effect on the compensation. Fig. 6.2 shows the oscillograms of the step response of the compensation with different values of R_o under otherwise similar conditions. As can be seen from the figure, the decrease of the value of R_o enhances the compensation while an increase of the value suppresses the compensation. Therefore, the compensation network should be adjusted to suit the conditions for a particular measurement.

6.2 The effect of $c - C_4F_8$ on the impulse breakdown characteristics of SF_6 mixtures with N_2 and air as buffer gases

Christophorou and co-workers [63] reported that for highly divergent fields such as a point-plane gap, the addition of a small amount of $c - C_4F_8$ to a $SF_6 + N_2$ mixture caused a large increase in the negative breakdown strength and a small reduction in the positive one. This can be easily explained from the knowledge of electron ionization and electron attachment cross sections of the constituent gases in the mixture since $c - C_4F_8$ not only has a larger electron attachment cross section than SF_6 in a higher electron energy range,

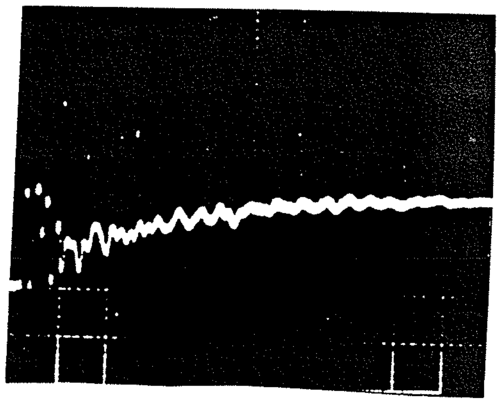

(a)

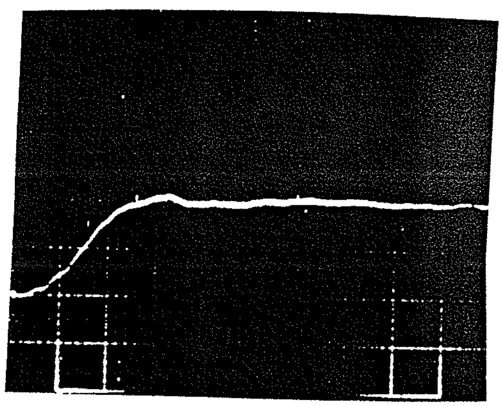

(b)

Figure 6.1: Step response of the resistor divider without shielding toroids: (a) before compensation, $50ns/div.$; (b) after compensation $20ns/div.$.

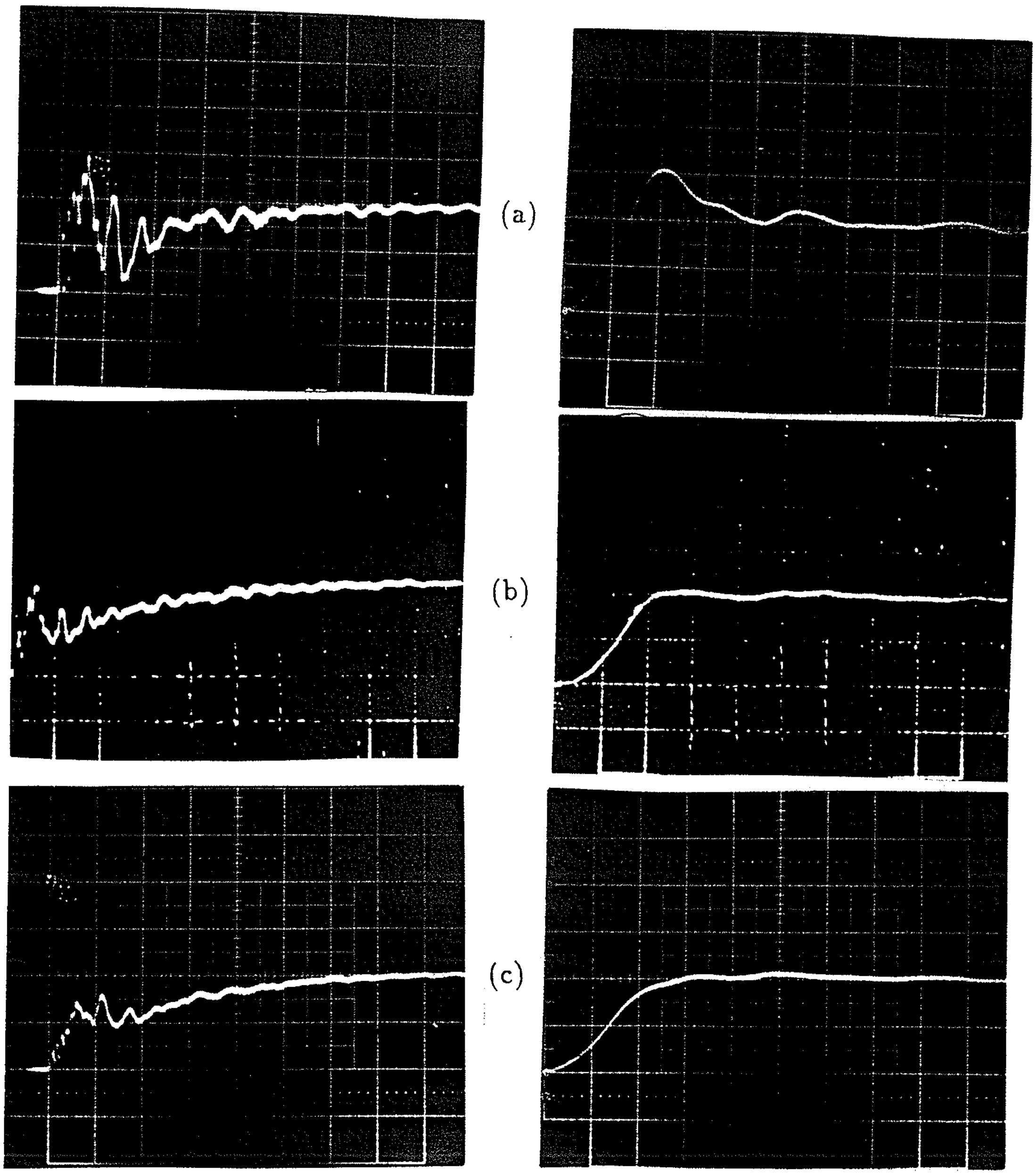

Figure 6.2: Effect of low voltage arm resistance R_o of the divider on step response of the compensated measuring system, $20ns/div.$: (a) R_o=26.85 Ω, (b) R_o=76.1 Ω, (c) R_o=454.5 Ω.

but also has a lower ionization onset than either pure SF_6 or N_2. Hence, in a point-plane gap under negative polarity, the addition of $c-C_4F_8$ to $SF_6 + N_2$ mixture leads to an increase of positive space charges in the region further in the gap. Thus, the positive space charges enhance the field strength near the cathode tip and augment corona discharge which modifies the sharpness of the cathode when the applied voltage reaches corona onset voltage. Moreover, in the above conditions the negative space charge modifies the field in the highly stressed region, causing a more even field distribution. The net effect of the space charges on the breakdown strength is that it increases the negative breakdown voltage. Under positive polarity, however, the population of electrons is significant only in highly stressed regions. In these regions the attachment cross section is small even for $c - C_4F_8$ gas. Therefore, the addition of $c - C_4F_8$ to a $SF_6 + N_2$ mixture cannot affect the breakdown characteristics of the mixture significantly.

The argument given above may apply only at pressures below the critical pressure and gaps with high nonuniformity factor, i.e. in the corona-stabilized breakdown region. With the coaxial cylinder gap used in this experiment, the nonuniformity factor is small and the electrode used were smooth and were conditioned by being subjected to some hundreds of sparkovers before the experiment. In addition, the pressures used were above the critical range. Therefore the breakdown strength is not affected significantly by increasing $c - C_4F_8$

6.3 The effect of the "sweeping action" on breakdown voltage-time characteristics

As was shown in section 4.3.1, for $1\% SF_6$/air mixture, the steep-fronted impulse caused not only a 50% breakdown value about 10% lower than the standard impulse and switching surge voltages, but also a significantly lower breakdown value than that obtained under a standard impulse in the time interval from 300 to 600 ns at a pressure of 500 kPa. This phenomenon may be of importance when the gas mixture used in this study is considered for insulation of a power system apparatus which may, at times, be subjected to fast rising overvoltages. While the anomalous phenomenon was not observed in SF_6/air mixture with higher percentage of SF_6 (40%) in the same electrode configuration, it appeared on the volt-time curve for pure SF_6 in other steep-fronted impulse voltage measurements under positive polarity. The anomalous breakdown was also observed in Naidu's experiment in a $10\% SF_6/90\% N_2$ mixture under a positive standard impulse at a pressure of 250 kPa [97]. It is obvious that factors controlling this phenomenon are very complicated and are not yet completely understood.

The qualitative explanation for the phenomenon is related to the so called "sweeping action", which explains the sweeping effect of the applied electric field associated with different impulse voltage shapes on the electrons or negative ions in the gap in question. Under slowly rising impulse voltages, most electrons or negative ions are swept out of the critical region or out of the gap before the applied voltage reaches the inception level, thus causing an increase of the statistical time lag and increasing the average breakdown voltage. Under steeply rising impulses, the applied voltage may reach the inception level before the electrons are removed from the critical region, leading to a reduction of the average breakdown voltage.

The sweeping effect was first used to explain the decrease in the impulse ratio for a small sphere-sphere gap in air with increasing front steepness of the impulse applied voltages [92]. Recently, Qiu [93] reported low impulse ratios for enclosed gaps under steep-fronted impulses. The reported difference between standard impulses and steep-fronted ones was even larger than the earlier data reported by Meek. The "sweeping action" explanation is also consistent with the observed decrease in scatter reported in Qiu's paper. More recently, Nelson and others [94] indicated that the dielectric strength of the gap in SF_6 is consistently lower when subjected to a steep-rising impulse. They suggested that in the case of a steep rising impulse the initiation process which depends on both the size and the establishment of the critical initiation volume becomes very important. For the steep-rising impulse of 5/800 ns used in their investigation, the volume corresponding to the pulse peak would be established almost immediately upon application of the pulse. In this situation residual negative ions in the critical volume would undergo collisional detachment to supplement the electron population and would initiate the breakdown. On the other hand, for a slower-rising pulse of 0.8/1750

μs the critical volume was established gradually. In this case, the applied impulse might act as a sweeping voltage in a similar way to the prestressed sweeping field. This would deplete the critical volume of negative ions before the stress reaches a level sufficient to make the detachment coefficient significant. In this way, initiation at a given time lag becomes less probable unless large stresses are used.

The anomalous phenomenon in SF_6 at higher pressure and shorter time might be pressure dependent, since it was not observed at pressures of 100 and 200 kPa. This may be related to the different spark formation for different pressures and the pressure dependance of negative ion mobility which is smaller for higher pressure. The phenomenon might also be polarity dependent. Under a negative impulse the negative ions are swept from the high field region to the low field region. Since the critical layer is small compared with the total gap length for a coaxial cylinder gap, even the fastest rising voltage used in this experiment might still be able to sweep most of the negative ions out of the high field region before collisional detachment becomes significant. Hence, the initiatory electrons will depend on the rate of production of free electron in the critical volume by other sources. It is reasonable to assume the appearance of the first initiating electron produced this way to be constant since the critical volume in the coaxial cylinder gap used was quite large. Therefore, the breakdown time lag is mainly dependent on the formative time lag which in turn is determined by the equal voltage-time criterion [95]. This explains the continuous rise of the negative impulse breakdown voltage at shorter times to breakdown under present experimental conditions.

To further investigate this phenomenon in the other extreme of a SF_6/N_2 mixture, pure N_2 gas was tested under otherwise the same experimental conditions as those used for pure SF_6. The results are included in figures 6.3 and 6.4. In this case, with the negative ions absent, only free electrons created by cosmic ray and other source are available. The free electrons might play a similar role as negative ions in the "sweeping effect". Since an electron moves faster than a negative ion and the formative time lags are shorter for N_2 than for SF_6 [96], it is easy to understand the larger scatter of the data as compared with SF_6 under positive polarity and the continuous rise of the breakdown voltages at shorter time to breakdown with small increasing rate as shown in the figures.

Although several attempts have been made, a quantitative explanation of the phenomenon is not available at this stage. Volt-time characteristics of SF_6 and SF_6/N_2 for coaxial cylinder gaps under standard impulse voltages were studied by Eteiba and Rizk in 1982 [70]. Based on the results of several earlier investigations they attempted to calculate the volt-time characteristics numerically taking into account the statistical nature of both the statistical time lag and formative time lag. Although the values calculated by the proposed method agree well with the experimental data, the method has little

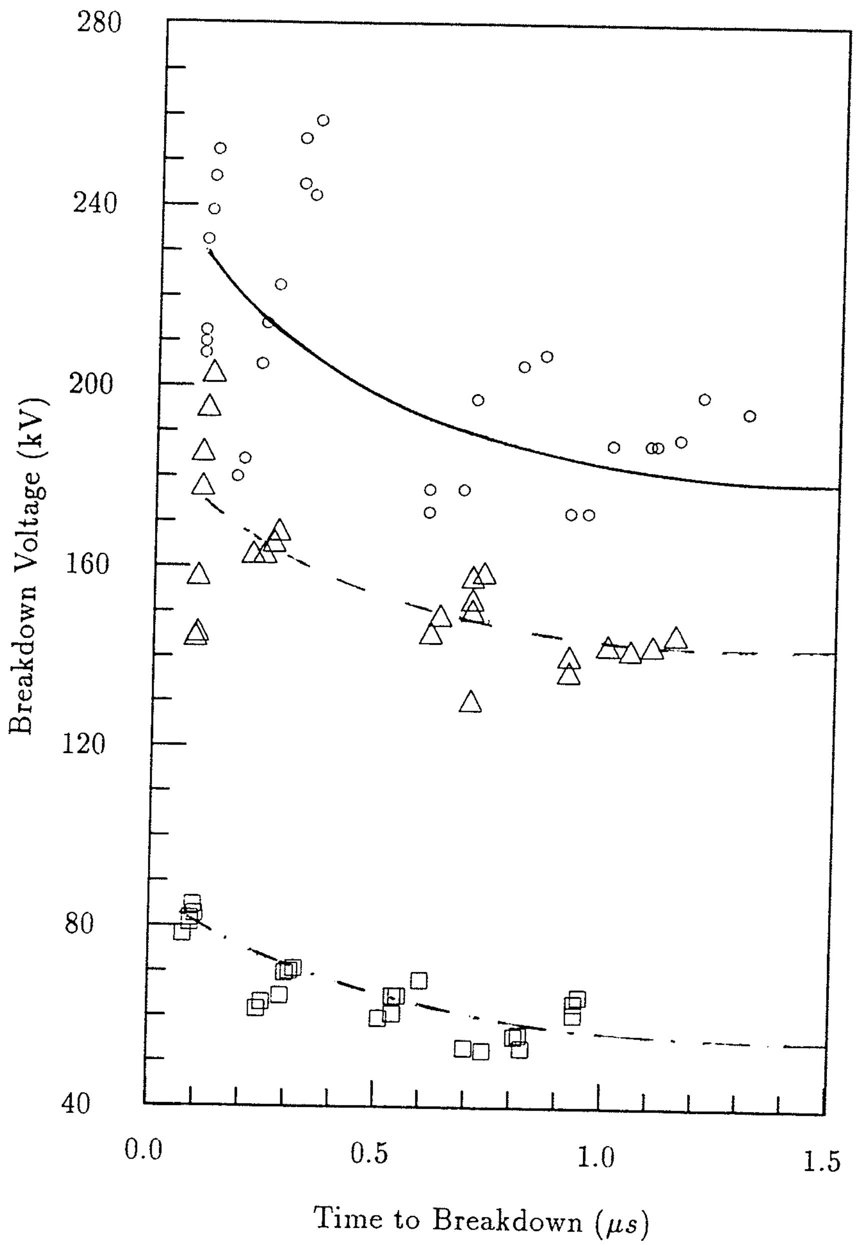

Figure 6.3: Positive impulse breakdown voltage-time characteristics for pure N_2 in a 1.27/5.2 cm coaxial-cylinder gap: (1) (○) 500 kPa; (2) (△) 300 kPa; (3) (□) 100 kPa.

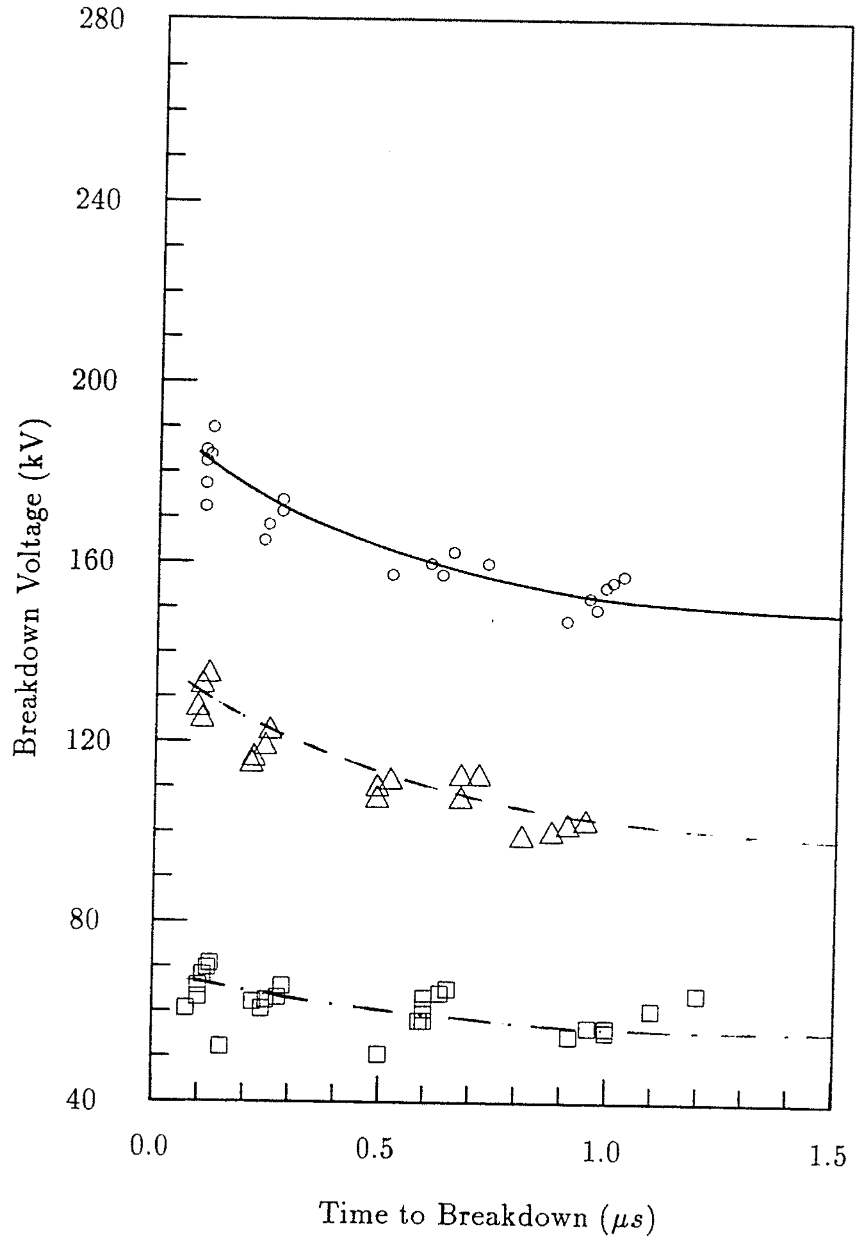

Figure 6.4: Negative impulse breakdown voltage-time characteristics for pure N_2 in a 1.27/5.2 cm coaxial-cylinder gap: (1) (○) 500 kPa; (2) (△) 300 kPa; (3) (□) 100 kPa.

practical application since the parameter n_o , defined as the rate of production of free electrons per unit volume and time, can only be determinated from the same set of experimental data. Later Boeck and Kindersberger [91] reported that in case of a coaxial cylinder arrangement the value of n_o was almost constant according to Dreger's results. However, the order of magnitude difference for n_o that has to be assigned for the calculations in order to fit the experimental results casts some doubt on their conclusion.

Assuming n_o is a function of overvoltage ratio, Naidu and others [97] calculated the volt-time characteristics for a $SF_6 + N_2$ mixture. Although there was a good agreement between the experimental results and calculated values, the method has a similar shortcoming since the functional relationship between n_o and overvoltage ratio was unpredictable.

Besides the difficulties mentioned above, their approach has another drawback which is related to the assumption they used to calculate the probability dp for the creation of an effective primary electron which would be able to start a critical avalanche in the gas volume $v(t)$ and the differential time interval dt. According to their definition the probability dp is given by

$$dp = n_o \cdot V_w(t) \cdot dt = n_o(\int_{v(t)} p_o dv)dt$$

It is seen that from the above expressions that for a given n_o and dt, dp could be equal to or greater than unity if $V_w(t)$ is large enough. This is physically impossible.

As mentioned in section 5.2, this approach to the problem also failed to establish a firm relationship between the parameters B and N_o and electrode configurations. However, the drawback mentioned above is overcome by using eqn.(5.28) in section 5.2 to compute dp. The uncertain relationship perhaps indicates that either the parameters used in the calculation are not constant or factors other than the negative ions play a vital role in the breakdown process of a gas dielectic.

6.4 Conclusions and suggestions for further research

The breakdown voltage characteristics for SF_6 and SF_6 mixtures with N_2 CO, CO_2 and dry air as buffer gases were studied both experimentally and theoretically in a coaxial cylinder gap in the pressure range from 100 to 600 kPa under *dc* and impulse voltages. The impulse voltages ranged from a switching surge impulse to a steep-fronted impulse with a front duration as low as 0.2 μs. Both full and chopped waves were used in the experiment. The investigation was focussed on the breakdown voltage-time characteristics of the gas or gaseous mixtures under steep-fronted impulses chopped on the wave-front with time to chop down to 100ns. The influence of adding small amount of $c - C_4F_8$ to the mixtures to form ternary mixtures was also studied under the same experimental conditions. Theoretical treatment by applying the streamer criterion was developed with some assumptions. The experimental results were then compared with the theoretical values.

To have a reliable measuring system for the steep-fronted impulse measurement, the technique of using an analog compensating network to compensate a resistor divider measuring system was proposed and developed. Problems related to the steep-fronted impulse measurements were examined and solved.

From the discussion given in previous chapters the following conclusions can be drawn:

An analog circuit can be used for compensation of a resistor divider measuring system for H.V. impulse measurements. The measuring system can be used for measurements of both full and chopped steep-fronted impulses. The method is significant when a resistor divider with high resistance and high voltage rating is desirable, since it has been proved that the method can also be used to compensate a resistor divider without shielding.

The study of impulse breakdown voltage-pressure characteristics showed that the replacement of a small amount of SF_6 by $c-C_4F_8$ in mitures of SF_6 with one of the buffer gases such as N_2, CO_2, CO, or dry air did not significantly change the breakdown characteristics of the corresponding binary mixture, unlike the characteristics for a highly non-uniform field. The breakdown voltage-pressure characteristics for both SF_6/N_2 and $SF_6/N_2/c-C_4F_8$ under negative standard impulses exhibited an apparent discontinuity at a pressure of about 300 kPa. Although a SF_6 mixture with CO as a buffer gas has a slightly higher standard impulse breakdown strength than that with N_2 as a buffer gas, other properties of N_2, especially its inertness, make it the preferred buffer gas for industrial applications. Since a coaxial cylinder gap was found to be insensitive to a small replacement of SF_6 by $c-C_4F_8$ and the addition of $c-C_4F_8$ could improve the insulation strength of the SF_6/N_2 mixture in a non-uniform field, the addition of a $c-C_4F_8$ to the SF_6/N_2 mixture is considered to be beneficial for surface roughness and particle-contamination control in a coaxial cylinder electrode system. However, the

$c - C_4F_8$ content should not exceed 5% so that the other properties of the mixture such as condensation temperature do not deteriorate.

The voltage-time characteristics study revealed that there were anomalous breakdowns taking place when a particular gas or gaseous mixture was subjected to a steep-fronted impulse voltage under certain experimental conditions. The phenomenon could be qualitatively explained by considering the so called "sweeping action" on free electrons or negative ions in the gap. The occurrence of the phenomenon depends on the nature of the gas or gaseous mixture, the polarity of the applied impulse voltages and/or the gaseous pressure.

The breakdown voltages for SF_6 mixtures with N_2, CO_2 and dry air in coaxial cylinder gaps can be calculated using the formula derived from the streamer criterion. The agreement between the experimental results and calculated values is good for pressures up to 250 kPa. The agreement could be improved if a modified formula is used for the calculation of breakdown voltages at higher pressures. The breakdown strength of SF_6 or its mixtures with N_2, CO_2 and dry air in a coaxial cylinder gap was shown to be determined, to a large extent, by the field intensity at the inner electrode surface.

Many attempts have been made to formulate theoretically the voltage-time characteristics including the one described in this thesis but it is not possible at this stage since the parameters used in the calculation were from experimental results. Moreover, none of the published methods can establish a firm relationship between the parameters used for the computation and the experimental conditions such as pressure or gaseous composition. Therefore, it is considered that the main approach to obtain reliable data in this field remains experimental and a breakthrough in the theoretical area is required before reliable data can be obtained by calculation alone.

To make the calculation of voltage-time characteristics possible, fundamental research on the processes of negative ion detachment is needed to estimate quantitatively the detachment coefficient and to understand factors affecting the detachment process.

As mentioned earlier, the anomalous breakdown seems to be controlled by many factors. Therefore, tests of the gas or mixtures at higher pressures than used in this experiment are needed to obtain data for insulation coordination at the higher pressures. Furthermore, the characteristics for the mixtures under oscillating steep-fronted impulses still need to be studied. Finally, the effect of replacement of a small portion of SF_6 by $c - C_4F_8$ in SF_6/N_2 mixtures on the surface flashover characteristics under *ac* and *dc* applied voltages should also be investigated. The investigation should focus on long term effects after the system is subjected to some sparkovers.

References

[1] V.N.Maller and M.S.Naidu *Advances in High Voltage Insulation and Arc Interruption in SF_6 and Vacuum.* Pergamon Press, 1981.

[2] G.Camilli and J.J.Chapman, *"Gaseous Insulation for High Voltage Apparatus"*. Trans. AIEE, Vol.66, pp.1463-1470, 1947.

[3] J.Sudzuki, *Inst. Elect. Engrs. Japan* 61, pp.636, 1941.

[4] H.C.Doepken, *"Compressed-gas Insulation in Large Coaxial Systems"*. IEEE Trans. PAS-88, No.4, pp.364-369, 1969.

[5] H.C.Diessner and J.G.Trump, *"Free Conducting Particles in a Coaxial Compressed Gas Insulated System"* IEEE Trans. PAS-89, No.8, pp.1970-1976, 1970.

[6] A.H.Cookson, O.Farish and G.M.L.Somermann, *"Effect of Conducting Particles on AC Corona Breakdown in Compressed SF_6"*. IEEE Trans. PAS-91, pp.1329-1338, 1972.

[7] A.H.Cookson and O.Farish, *"Motion of Spherical Metal Particles and AC Breakdown in Compressed SF_6"*. Annual Report Conf. on Elect. Insul. and Dielect. Phenomena, 1971. Office of Publications, National Academy of Sciences.

[8] A.H.Cookson and O.Farish, *Particle Initiated Breakdown in Compressed SF_6"*. Annual Report Conf. on Elect. Insul. and Dielect. Phenomena, 1970. Office of Publications, National Academy of Sciences.

[9] L.G.Christophorou, D.R.James and R.Y.Pai, *Applied Atomic Collision Physics*. Vol.5, pp.87-167, 1982.

[10] S.R.Hunter and L.G.Christophorou, *"Pressure-dependent Electron Attachment and Breakdown Strength of Unitary Gases and Synergism of Binary Gas Mixtures: A Relationship"*. Journal of Applied Physics. 57(9), pp.4377-4385, 1985.

[11] J.D.Cobine, *"Some Electrical and Thermal Characteristics of Helium and Sulphur-Hexafluoride Mixtures"*. Trans. of AIEE, Vol.74, part I, pp.318-321, July. 1955.

[12] J.L.Moruzzi and J.D.Craggs, *"Ionization and Attachment and Breakdown Measurement in Mixtures of SF_6 with Helium, Argon and Hydrogen"*. Proc. of 12 Interna. Conf. on Phenomena in Ionized Gases. pp.225 Eindhoven, The Netherlands, 1975

[13] O.Farish, S.J.Dale and A.M.Sletten, *"Impulse Breakdown of Positive Rod-Plane Gaps in Hydrogen-SF_6 Mixtures"*. IEEE Trans. PAS-95 No.5 pp.1639-1647, 1976.

[14] O.Farish, S.J.Dale and A.M.Sletten, *"Impulse Breakdown of Negative Rod-Plane Gaps in Hydrogen-SF_6 Mixtures"*. IEEE Trans. PAS-97 No.1 pp.118-124, 1978.

[15] A.H.Cookson and R.E.Wooton, *"AC Corona and Breakdown Characteristics for Rod Gaps in Compressed Hydrogen,SF_6 and Hydrogen-SF_6 mixtures"*. IEEE Trans.PAS-97,No.2, pp.415-423, 1978.

[16] J.Dutton, F.M.Harris and D.B. Hughes, *"The Dielectric Strength of N_2O/SF_6 and N_2/O_2 Mixtures"*. Proc. of 3rd Interna. Conf. on Gas Discharges, IEE. Conf. Publ. No.118, pp.95-99 1974.

[17] J.Dutton, F.M.Harris and D.B. Hughes, *"Electrical Breakdown of N_2O, SF_6 and N_2O/SF_6 Mixtures"*. Proc. IEE, Vol.121, No.3, pp.223-226, 1974.

[18] A.H.Sharbaugh and P.K.Waton, *"Breakdown Strengths of Perfluorocarbon Vapor (Fe-75) and Mixtures of The Vapor with SF_6"*. IEEE Trans. on PAS, Vol.83, No.2, 1964 pp.131-136.

[19] L.J.Berbreich, C.N.Works and E.W.Lindsay, *"Electric Breakdown of Perfluorocarbon Vapors and Their Mixtures with Nitrogen"*. Trans. of AIEE, Vol.74, part I, Nov. 1955, pp.660-666.

[20] G.Camilli, T.W.Liao and R.E.Plump, *"The Dielectric Behavior of Some Fluorogases and Their mixtures"*. Trans. of AIEE, Vol. 74, part I,Nov. 1955, pp.637-642.

[21] E.Gockenbach, *"The Dielectric Strength of Some Freons and Their Mixtures with Nitrogen and Sulfur-Hexafluoride"*. Proc. Intern. Symp. on Gaseous Dielectrics, Knoxville, Tenn.,U.S.A. 1978, pp.355-357.

[22] L.G.Christophorou, *"Atomic and Molecular Radiation Physics"*. New York, Wiley-Interscience, 1971.

[23] D.W.Bouldin, D.R.James, M.O.Pace and L.G.Christophorou, *"A Current Assessment of The Potential of Dielectric Gas Mixtures for Industrial Application"*. Gaseous Dielectrics IV, L.G.Christophorou (Ed.), Pergamon Press, New York pp.204-212.

[24] C.C.Chan, M.O.Pace and L.G.Christophorou, *"DC Breakdown Strength of Some Mulitticomponent Gas Mixtures in Concentric Cylinder Geometries"*. Gaseous Dielectrics II, L.G.Christophorou (Ed.), Pergamon Press, New York pp.149-159.

[25] E.H.Cohen *"The Electric Strength of Highly Compressed Gases"*. Proc. IEE, Vol.103 Part A pp.57-68 1956.

[26] M.O.Pace, L.G.Christophorou, D.R.James, R.Y.Pai, R.A.Mathis and D.W.Bouldin *"Improved Unitary and Multicomponent Gaseous Insulators"*. IEEE Trans. Electr. Insul. Vol EI-13, No.1 pp.31-36 Feb. 1978.

[27] N.H.Malik and A.H.Qureshi, *"Calculation of Discharge Inception Voltages in SF_6-N_2 Mixtures"*. IEEE Trans. Electr. Insul. Vol EI-14, No.2 pp.70-76 April 1979.

[28] A.Petersen *"Calculation of Spark Breakdown or Corona Starting Voltages in Nonuniform Fields"*. IEEE Trans. PAS-86 No.2 pp200-206, 1967.

[29] A.Petersen *"Criteria for Spark Breakdown in Sulfur Hexafluoride"*. IEEE Trans. PAS-89 No.8 pp2043-2048 1970.

[30] N.H.Malik and A.H.Qureshi, *"Breakdown Gradients in SF_6-N_2, SF_6-air and SF_6-CO_2 Mixtures"*. IEEE Trans. on Elect. Insul., Vol.EI-15 No.5 pp.413-418 October 1980.

[31] R.Hazel and E.Kuffel *"Static Field Anode Corona Characteristics in Sulphur Hexafluoride"*. IEEE Trans. on PAS-95, pp.178-186,1976.

[32] N.H.Malik, A.H.Qureshi and G.D.Theophilus, *"Static Field Breakdown of SF_6-N_2 Mixtures in Rod-Plane Gaps"*. IEEE Trans. Electr. Insul. Vol EI-14, No.2 pp.61-69 April 1979.

[33] O.Farish, *"Corona-Controlled Breakdown in SF_6 and SF_6 Mixtures"*. Proc. of 16th Conf. on Ionization Phenomena in Gases, Dusseldorf, Aug. 1983.

[34] P.R.Howard, *"Insulation Properties of Compressed Electronegative Gases"*. Proc. IEE, Vol.104 Part A pp.123-138, 1957.

[35] T.R.Ford, *"Some Experiment on Positive Point-to-Plane Corona and Spark Breakdown of Compressed Gases"*. Proc. IEE. Vol.100, part II No.78 pp.585-590 1953.

[36] N.H.Malik, *"DC Voltage Breakdown of SF_6-air and SF_6-CO_2 Mixtures in Rod-Plane Gaps"*. IEEE Trans. Electr. Insul. Vol EI-18, No.6 pp.629-636 Dec. 1983.

[37] C.Korasli and O.Farish, *"Corona and Breakdown in Coaxial-Electrode Geometry in SF_6 and SF_6/N_2 Mixtures"*. Gaseous Dielectrics III, L.G.Christophorou (Ed.), pp.77-85 1982. Pergamon Press.

[38] N.H.Malik, A.H.Qureshi and G.D.Theophilus, *"Breakdown and Pre-breakdown Phenomenon in SF_6-N_2 Gas Mixtures"*. Proc.VIII Interna Symp. on Discharges and Elect. Insul. in Vacuum, Albuquerque New Mexico pp.F7.1-F7.14 1978.

[39] N.H.Malik, A.H.Qureshi G.D.Theophilus and M.R.Raghuveer, *"Pre-breakdown Phenomenon in SF_6-N_2 Mixture at Various Pressures"*. Proc. 1978 Interna. Symp. on Elect. Insul. IEEE Conf. Publ. pp.140-145 1978.

[40] M.Ermel, *"Das N_2-SF_6-Gasemisch als Isoliermittel der Hochspannungstechnik"*. ETZ-A,BD.96, H.5, pp.231-235, 1975.

[41] N.H.Malik and A.H.Qureshi, *"A Review of Electrical Breakdown in Mixtures of SF_6 and Other Gases"*. IEEE Trans. Electr. Insul. Vol EI-14, No.1 pp.1-13 Feb. 1979.

[42] A.H.Cookson and B.O.Pederson, *"High Voltage Performance of Mixtures of SF_6 with N_2, Air, CO_2 in Compressed Insulated Equipment"*. Proc, 5th Interna. Conf. on Gas Discharges pp.161-164, 1978.

[43] O.E.Ibrabim and O.Farish *"Impulse Breakdown and Prebreakdown Corona Processes in SF_6/N_2 Mixtures"*. Proc. of 2nd. Inter Symp Gaseous Dielectric, New York, pp.83-92, 1980. Gaseous Dielectrics II, Pergamon Press.

[44] O.Farish, I.D.Chalmers and P.Vidaud *"SF_6 Mixtures with Enhanced Corona Stabilisation"*. Proc. of 7th Inter. Conf. on Gas Discharges and Their applications, London, pp.223-226, 1982. Peter Peregrinus Ltd.

[45] D.J.Skipper and P.I.McNeall, *"Impulse-strength Measurement on Compressed-gas Insulation for Extra-high-voltage Power Cables"*. Proc.IEE. Vol.112, No.1 Jan. 1965.

[46] K.Itaka and G.Ikeda, *"Dielectric Characteristics of Compressed Gas Insulated Cables"*. IEEE Trans. PAS-89, No.8 pp.1986-1994, 1970.

[47] H.M.Ryan, S.J.Dale, D.J.Tedford and A.Kurimoto, *"Factors Affecting The Insulation Strength of SF_6 Filled System"*. CIGRE Paper 15-02 1976.

[48] T.Watanabe and T.Takuma, *"The Breakdown and Discharge Extension of Long Gaps in N_2-SF_6 and air-SF_6 Mixtures"*. J. of Applied Physics, Vol.48, NO.8, pp.3281-3287, 1977.

[49] E.Kuffel and A.Yializis, *"Impulse Breakdown of Positive and Negative Rod-Plane Gaps in SF_6-N_2 Mixtures"*. IEEE Trans. PAS-97, NO.6 pp.2359-2366, 1978.

[50] A.Yializis, N.H.Malik, A.H.Qureshi and E.Kuffel. *"Impulse Breakdown and Corona Characteristics for Rod-Plane Gaps in Mixtures of SF_6 and Nitrogen with Less Than 1% of SF_6 Content"*. IEEE Trans. PAS-98, NO.5 pp.1832-1840, 1979.

[51] O.Farish, O.E.Ibrahim and C.Korasli, *"Corona Stabilization and Breakdown in SF_6 and SF_6/N_2 Mixtures"*. Proc. of 5th Int. Conf. on Gas Discharges, Liverpool IEE pp.320-323, 1978.

[52] H.Rodrigo and P.A.Chatterton, *"Measurement of Impulse Positive Point Predischarge Growth in 50%$SF_6$50%N_2 Gas Mixtures"*. Proc. of 7th Interna. Conf. on Gas Discharges and Their Application pp.207-210, 1982.

[53] A.Kurimoto, *"Prebreakdown Phenomena in Long Nonuniform Field Gaps in SF_6/N_2 and SF_6/air Mixtures"*. Proc. of 7th Interna. Conf. on Gas Discharges and Their Application pp.211-214, 1982. Peter Peregrinus Ltd.

[54] N.H.Malik, Y.Safar and A.H.Qureshi *"Impulse Corona in Negative Rod-Plane Gaps Filled with SF_6-gas Mixtures"*. Proc. of 7th Interna. Conf. on Gas Discharges and Their Application pp.247-251, 1982.Peter Peregrinus Ltd.

[55] J.K.Nelson, P.A.Chatterton and N.H.Blomquist, *"Corona Stabilization in SF_6/N_2 Mixtures Under Impulse Conditions"*. Gaseous Dielectrics III, L.G.Christophorou (Ed.), pp.68-76 1982. Pergamon Press.

[56] A.Fatheddin, M.O.pace, L.G.Christophorou and R.Y.Pai, *"Impulse Breakdown in SF_6, SF_6/N_2 and SF_6/N_2/Perfluorocarbon"*. Gaseous

Dielectrics III, L.G.Christophorou (Ed.), pp.183-190 1982. Pergamon Press.

[57] A.Rein and J.Kulsetas, *"Impulse Breakdown of SF_6/N_2 Insulation. Influence of Electrode Covering. Polarity Effect"*. Gaseous Dielectrics III, L.G.Christophorou (Ed.), pp.315-321 1982. Pergamon Press.

[58] Y.A.Safar, N.H.Malik and A.H.Qureshi, *"Impulse Breakdown Behavior of Rod-Plane Gaps in SF_6-N_2, SF_6-air, SF_6-CO_2 Mixtures"*. IEEE Trans. on Elect. Insul. Vol. EI-17 No.5 pp.411-450 Oct.1982.

[59] P.T.Medeiros, S.R.Naidu and K.D.Srivastava, *"Lightning Impulse Breakdown Of Rod-Plane Gaps in SF_6-N_2 SF_6-N_2 Mixtures"*. Proc. of 4th Int. Symp. on High Voltage Engineering, Paper 33.03, Athens 1983.

[60] H.Rodrigo and P.A.Chatteron, *"A Study of The Critical Pressure in SF_6/N_2 Mixtures for Positive Point Plane Systems with Impulse Voltages"*. IEEE Trans. on Elect. Insul. Vol. EI-19 No.1 pp.53-62, Feb.1984.

[61] P.A.Chatterton and H.Rodrigo, *"Photomultiplier and Field Probe Studies of Positive Point Plane Discharge Development in SF_6/N_2 Mixtures"*. IEEE Trans. on Elect. Insul. Vol. EI-19 No.1 pp.63-74, Feb.1984.

[62] D.R.James, L.G.Christophorou, R.Y.Pai, M.O.Pace, R.A.Mathis and D.W.Bouldin, *"Breakdown Voltages of Some New Unitary and Multicomponent Gas Mixtures"*. Annual Report Conf. on Elect.Insul. and Di-

elect. Phenomena, pp.409-420. 1977. Office of Publications, National Academy of Sciences.

[63] L.G.Christophorou, D.R.James, I.Sauers, M.O.Pace, R.Y.Pai and A.Fatheddin, *"Ternary Gas Dielectrics"*. Gaseous Dielectrics III, L.G.Christophorou (Ed.), pp.151-165 1982. Pergamon Press.

[64] Y.Qiu and E.Kuffel *"High Dielectric Strength Gas Mixtures Comprising Sulphur Hexafluoride, Carbon Monoxide and Octafluorocyclobutane"*. Gaseous Dielectrics III, L.G.Christophorou (Ed.), pp.166-173 1982. Pergamon Press.

[65] A.Fatheddin, M.O.Pace, L.G.Christophorou and R.Y.Pai, *"Impulse Breakdown in SF_6, SF_6/N_2 and SF_6/N_2/Perfluorocarbon"*. Gaseous Dielectrics III, L.G.Christophorou (Ed.), pp.183-190 1982. Pergamon Press.

[66] L.G.Christophorou, I.Sauers, D.R.James, H.Rodrigo, M.O.Pace J.G.Carter and S.R.Hunter, *"Recent Advances in Gaseous Dielectrics at Oak Ridge National Laboratory"*. IEEE Trans. on Elect. Insul. Vol.EI-19 NO.6, pp.550-566, 1984.

[67] Y.Qiu, E.Kuffel, *"Dielectric Strength of Gas Mixtures Comprising SF_6, CO, $c-C_4F_8$ and SF_6, N_2, $c-C_4F_8$"*. IEEE Trans. PAS-102, No.5 pp.1445-1451 May 1983.

[68] R.Y.Pai, L.G.Christophorou, I.Sauers and A.Fatheddin, "*Measurement of Properties of Perfluorocarbon/SF_6 Mixtures Relevant to Applications*". Int. Conf. on Gas Discharges and Their Application,IEE Publ. No.189 (part 2) pp.232-235 1980.

[69] H.M.Rosenstock, K.Draxl, B.W.Steiner and J.T.Herron *J.Phys. and Chem. Ref. Data* 6, suppl 1, 1977.

[70] F.A.M.Rizk and M.B.Eteiba, "*Impulse Breakdown Voltage-Time Curves of SF_6 and SF_6-N_2 Coaxial-Cylinder Gaps*". IEEE Trans. PAS-101, No.12 Dec. 1982.

[71] S.Okabe and E.Kuffel, "*Volt-Time Characteristics of Rod-Sphere Gaps in Mixtures Comprising SF_6, $c-C_4F_8$, CO and Dry Air, SF_6*". Conf. Record of The 1984 IEEE Inter. Symp.on Elect. Insul. pp.143-146.

[72] T.Harada, T.Kawamura, Y.Akutsu, K.Kimura and T.Aizawa, "*Development of a High Quality Resistive Divider for Impulse Measurement*". IEEE Trans. PAS-90. pp.2247-2250 1971.

[73] T.Harada, T.Kawamura, K.Kishi, Y.A.Oshima, N.Ohira, K.Takigami, Y.Horiko, "*A High Quality Voltage Divider Using Optoelectronics for Impulse Voltage Measurement*". IEEE Trans. PAS-90, No.2, pp.494-500, 1972.

[74] Jiang, Guo-Xiong, Huang, De-Xiang, *"The Compensation of the Measuring Error of Impulse Resistive Voltage Divider on Its Low Voltage Side"*. 4th Inter. Symp. on H.V. Eng.,Athens,Greece, Sept. 1983, Paper 65.03.

[75] S.E. Kiersztyn, *"Numerical Correction of H.V. Impulse Deformed by the Measuring System"*. IEEE Trans. PAS-99, No.5, pp.1984-1995, 1980.

[76] R.Malewski, T.R.McComb and M.M.C.Collins, *"An Evaluation of Digital Recording Equipment and Numerical Correction Techniques in Impulse Measurement"*. NBS Special-Publication 628, Canada.

[77] R.Malewski and A.Dechamplain, *"Digital Impulse Recorder For High-Voltage Laboratories"*. IEEE Trans. on PAS- 1981.

[78] F.C. Creed, *"The Measurement of Impulse Voltage Chopped on The Front"*. CIGRE, 1958, Rep. No.320.

[79] IEEE Std 4-1978, pp.80-83.

[80] Z.Li and E.Kuffel, *"Impulse Voltage Breakdown Characteristics of Ternary Gas Mixtures in a Coaxial Cylinder Gap."* IEEE Trans. on Elect. Insul. vol. EI-22 No. 4 August, 1987.

[81] R.Y.Pai and L.G.Christophorou, *"Impulse Breakdown of* $c-C_4F_8/SF_6$ *and* $c-C_4F_8/SF_6/N_2$ *Mixtures."* Gaseous Dielectrics II, L.G.Christophorou (Ed.), Pergamon Press, New York pp.190-199.

[82] M.O.Pace, J.L.Adcock and L.G.Christophorou, *"Particle Contamnation in Gas-Insulated Systems: New Control Method"*. Gaseous Dielectrics IV, L.G.Christophorou (Ed.), Pergamon Press, New York pp.377-386.

[83] **K.B.Miners, M.J.Mastroianni, P.N.Sheldon and D.P.Wilson,** ***"Dew Points of SF_6/N_2 Gas Mixtures".*** **Gaseous Dielectrics III, L.G.Christophorou (Ed.), Pergamon Press, New York pp.509-516.**

[84] N.Fujimoto, H.A.Stuckless and S.A.Boggs, *"Calculation of Disconnector Induced Overvoltages in Gas-Insulated Substation"*. In L.G.Christophorou and M.O.Pace (Ed), Gaseous Dielectrics IV, Pergamon Press, pp.473-481, 1984.

[85] Z.Li, R.Kuffel, and E.Kuffel, *"Volt-time Characteristics in Air, SF_6/Air Mixture, and N_2 for Coaxial Cylinder and Rod-sphere Gaps."* IEEE Trans. on Elect. Insul. vol. EI-21 No. 2 April 1987.

[86] Z.Li and E.Kuffel, *"Breakdown Voltage-time Characteristics in SF_6 and SF_6 Mixtures for a Coaxial Cylinder Gap."* Gaseous Dielectrics V, L.G.Christophorou (Ed.), pp. 452-457 1987. Pergamon Press.

[87] Y.Qiu and E.Kuffel, *"The Breakdown Strengths of Gas Mixture Containing a Small Amount of Electronegative Gas in Non-uniform Field Gaps"*. Seventh Inter. Conf. on Gas Discharges and Their Applications, pp.215-218, 1982. Peter Peregrinus Ltd.

[88] Z.Li and E.Kuffel *"A New Approach to Calculate the Positive Corona Onset or Breakdown Voltages for Coaxial Cylinder Gaps"*. Conference Record of the 1985 Intern. Conf. on Properties and Applications of Dielectic Insulations, Xian, China. June 24-29, 1985.

[89] T.W.Dakin, G.Oppermann, J.Vigreux, G.Wind and H.Winkelnkemper, G.Luxa, *"Breakdown of Gases in Uniform Fields"*. Electra,No.32 pp.61-68, 1974.

[90] I.M.Bortnik and C.M.Cooke, *"Electrical Breakdown and the Similarity Law in SF_6 at Extra-High Voltages"*. IEEE Trans. PAS-91 pp.2196-2203 1972.

[91] W.Boeck and J.Kindersberger, *"Destination of the Statistcal Time Lag in SF_6"*. 4th Inter. Symp. on High Voltage Engineering, paper 31.06, Athens 1983.

[92] J.K.Meek, *"The Influence of Irradiation on the Measurement of Impulse Voltage with Sphere Gaps"*. IEE Journal, Vol. 93, Pt. II, p.97, 1946.

[93] Y.Qiu, *"Impulse Breakdown Characteristics of Enclosed Sphere Gaps"*. 4th Inter. Symp. on High Voltage Engineering, paper 33.o7, Athens 1983.

[94] J.K.Nelson, B.Railing and J.Sollia Mcdacedo, *Divergent Field Behaviour of SF_6 Subjected to Steep Fronted Surges"*. Conference Record of 1986 IEEE Inter. Symp. on Electr. Insul., Washington, D.C. pp.151-154 1986.

[95] T.Yamagiwa and Ozawa, *"Generalization of Equal Voltage-Time Area Criterion for Estimation Voltage-Time Characteristics of Various Arrangement in SF_6 Gas"*. Conference Record of the 1985 Intern. Conf. on Properties and Applications of Dielectic Insulations, Xian, China. pp.764-767 June 24-29, 1985.

[96] M.Giesselman, W.Pfeiffer and J.Wolf, *"Voltage-Time Characteristics in SF_6 and SF_6-N_2 Mixtures"*. Conf. Record of The 1986 IEEE Inter. Symp. on Elect. Insul. pp.155-158 1986.

[97] S.R.Naidu, Paulo de Tarso Mederos and K.D. Srivastava, *"Volt-Time Curves for A Coaxial Cylinder Gap in SF_6-N_2 Mixtures"*. IEEE Trans. on Elec. Insul. Vol. EI-22 No. 6, pp.755-762, 1987.

[98] W.Knorr, K.Moller and K.J.Diederich, *"Voltage-Time Characteristics of Slightly nonuniform Arrangement in SF_6 Using Linearly Rising and Oscillating Lightning Impulse Voltages"*. CIGRE, Volume 1, paper 15-05, 1980.

[99] T.Nitta, N.Yamada and Y.Fujiwara, *"Area Effect of Electrical Breakdown in Compressed SF_6"*. IEEE Trans on PAS-93, pp.623-629, 1974.